INTERACTIONS BETWEEN GALAXIES AND A HOT MEDIUM IN RICH CLUSTERS

Thesis by

Stephen Matthew Kent

In Partial Fulfillment of the Requirements

for the Degree of

Doctor of Philosophy

California Institute of Technology

Pasadena, California

1980

(Submitted 1979 November 29)

"If you push something hard enough, it <u>will</u> fall over."

Fudd's First Law of Opposition

ACKNOWLEDGEMENTS

It is with deep pleasure that I offer my thanks to the many individuals who provided the help and encouragement over the years that made this thesis possible.

My advisor Wal Sargent provided the original stimulus for this work and tried (unfortunately with little success) to educate me in the proper use of the "Queen's English".

Jim Gunn offered much invaluable advice on matters ranging from galaxy formation to RN65E resistors.

Construction of the P60 SIT Spectrograph offered me many hours of amusement, and its completion would have been impossible without the assistance of Jim Gunn (design), Steve Knapp (technical consultant), Doug Rabin (procurement), Larry Blakée (trivia), Barbara Zimmerman (programming), and many others.

Alan Dressler, John Stauffer, Bob Schommer, Rob Kennicutt, Jorge Melnick, Jon Romney, Steve Gull, and of course the good Dr. Young provided much assistance in the way of data, programs, and lively discussions.

A whole crew of night assistants at Palomar, including Buffalo Chip Williams, Ranney Adams, Skip Staples, Steve Barry, Gary Tuton, and Juan Carrasco provided considerable entertainment in addition to expert assistance in operating a variety of telescopes.

My officemate John Hoessel receives a warm acknowledgement for the fine music he provided over the years.

The expert typing skills of Marilyn Rice, Helen Holloway, and Elsa Titchenell are gratefully appreciated.

The Fannie and John Hertz Foundation provided the all important source of financial support during most of my tenure as a graduate student.

Finally a big wad of thanks goes to that gang of idiots known collectively as the graduate students in astronomy who maintained the required level of insanity needed for survival at Cal Tech.

ABSTRACT

The influence of a hot medium on the formation and evolution of galaxies in rich clusters is investigated. Part I begins with an observational study of the two peculiar systems of emission line filaments around the galaxy NGC1275 in the Perseus cluster. It is concluded that one system consists of condensations in an accretion flow from a surrounding medium onto an underlying elliptical galaxy while the second system arises in a superposed but unrelated spiral galaxy. Part II investigates the problem of whether S0 galaxies can be formed by the ram pressure sweeping of spirals due to their motion through a hot intracluster medium. It is found that while the ram pressure may do considerable damage to spirals it is too weak by a large factor to produce the required numbers of S0's. In Part III observations of emission lines from spiral galaxies in the x-ray cluster A1367 reveal that they are deficient in gas content relative to field galaxies and this deficiency is strongest for galaxies closest to the region of x-ray emission. This is taken as evidence that spirals can lose a significant fraction of their gas content by interaction with a hot medium and is therefore a manifestation of the considerable damage predicted in Part II. Finally in Part IV the systematic trends in morphological populations observed in clusters are explained as resulting from a truncation of disks in spirals and S0's during their formation due to

cluster collapse. Remarkably good agreement is obtained between the predictions of this scenario and a number of observed properties of galaxies in clusters.

TABLE OF CONTENTS

INTRODUCTORY NOTE

Each chapter of this thesis is presented in the form of an independent paper. The unifying theme behind this work is the multitude of ways in which the properties of a galaxy can be affected by its presence in a cluster environment. The first three chapters focus on the effect that a hot intracluster medium can have on the gas content of galaxies. In chapter 1 evidence is found which suggests that NGC1275 is accreting material from this medium. In chapter 3 it is shown that the opposite has happened for spiral galaxies in A1367: they have lost material. Chapters 2 and 4 delve into the question of why rich clusters are dominated by elliptical and S0 galaxies, types which are so rare in the field. In chapter 2 the possibility that ram pressure effects could sweep spirals and convert them into S0's is considered and rejected. In chapter 4 a scenario is developed whereby the disks of spiral and S0 galaxies are presumed to be systematically fainter in regions of high density. With a few additional assumptions regarding the division of disk galaxies into spirals and S0's this picture successfully explains a variety of phenomena regarding galaxies in clusters. The cause of this trend in disk brightness remains obscure.

CHAPTER I

IONIZATION AND EXCITATION MECHANISMS IN THE FILAMENTS AROUND NGC1275

THE ASTROPHYSICAL JOURNAL, 230:667–680, 1979 June 15

IONIZATION AND EXCITATION MECHANISMS IN THE FILAMENTS AROUND NGC 1275

S. M. KENT AND W. L. W. SARGENT
Hale Observatories, California Institute of Technology, Carnegie Institution of Washington
Received 1978 October 16; accepted 1978 December 21

ABSTRACT

New observations of the filaments around NGC 1275 are presented. Absolute intensities of the emission lines in the two velocity systems at 5300 and 8200 km s^{-1} are given. The possible sources of ionization and excitation are investigated in detail. The spectra of the high-velocity filaments strongly resemble those of giant H II regions in the outer parts of spiral galaxies. The low-velocity spectra can be equally well explained by collisional ionization in strong shocks or in terms of photoionization by the Seyfert nucleus. Current observations support the hypotheses that (*a*) the high-velocity system is an infalling spiral galaxy bound to the Perseus cluster, and (*b*) the low-velocity filaments are condensations in an accretion flow onto NGC 1275.

Subject headings: galaxies: individual — galaxies: intergalactic medium — galaxies: structure — X-rays: sources

I. INTRODUCTION

The system of filaments around NGC 1275 has presented an intriguing puzzle ever since Minkowski (1957) discovered two discrete emission-line redshift systems at 5300 and 8200 km s^{-1}. The filaments at the lower velocity (LV system) form an irregular cloud distributed roughly symmetrically about the galaxy, while those at the higher velocity (HV system) are confined to a smaller region north and west of the nucleus (Burbidge and Burbidge 1965; Lynds 1970). Our objective in this paper is to determine the source or sources of excitation of the emission lines. To provide new information on the filaments we have made spectroscopic observations using the Hale 5 m telescope and new digital detector systems. From these observations we derive absolute intensities and line widths for the emission lines and information on the kinematics of the HV system.

NGC 1275, which is at the redshift of the LV system, is a powerful radio and X-ray emitter. It has a Seyfert-like nucleus with a strong, nonthermal optical continuum source. On photographs, several filaments around NGC 1275 are seen to contain blue knots which could be associations of young stars. The Perseus cluster (of which NGC 1275 is the brightest member) is also a strong X-ray source and is filled with a hot intracluster medium. All of these varied phenomena are possible sources for ionizing and exciting the filaments. We shall find that the expected characteristic properties (mainly the emission-line spectra) of the filaments are different for each source, and that observationally we can distinguish among the various possibilities.

In spite of numerous investigations, the nature of the filaments is still a matter of considerable concontroversy. Minkowski (1957) originally thought that they result from two spiral galaxies in collision. Burbidge and Burbidge (1965) and Burbidge, Smith, and Burbidge (1978) maintain that all the filaments have been ejected from the nucleus in one or more violent outbursts. After De Young, Roberts, and Saslaw (1973) found 21 cm absorption at 8100 km s^{-1} (i.e., the *high* redshift) against the radio source in NGC 1275, Rubin *et al.* (1977, hereafter RFPO) again suggested that the HV system is a spiral galaxy superposed on an underlying elliptical. Fabian and Nulsen (1977) interpret the LV filaments as being condensations in the intracluster medium infalling toward the core of NGC 1275.

For the rest of this paper we shall assume a distance to NGC 1275 of 106 Mpc ($H' = 50, v = 5300$ km s^{-1}). At this distance 1″ corresponds to 500 pc.

II. OBSERVATIONS

Observations of NGC 1275 were made during 1976 October–December using the Digital SIT spectrograph of Gunn and Oke at the Cassegrain focus of the Hale telescope. Spectra were taken at the slit positions marked in Figure 1; this photograph is a 40 minute exposure in blue light taken by Zwicky at the prime focus of the Hale telescope. Two different gratings gave resolutions of 3.5 and 7.0 Å per channel covering 3700–5300 Å and 3600–6800 Å, respectively. In the spatial direction 40 channels were obtained at a scale of 1″.5 per channel and with a slit width of 1″. Absolute fluxes of the emission lines were calibrated by observation of standard stars tied to the absolute calibration of α Lyr given by Oke and Schild (1970). Details of each observation are given in Table 1.

Observations of the nuclear regions were made using the University College London Image Photon Counting System (Boksenberg 1972; Boksenberg and Burgess 1973) at the 36 inch (91 cm) camera of the Hale telescope coudé spectrograph. One spectrum

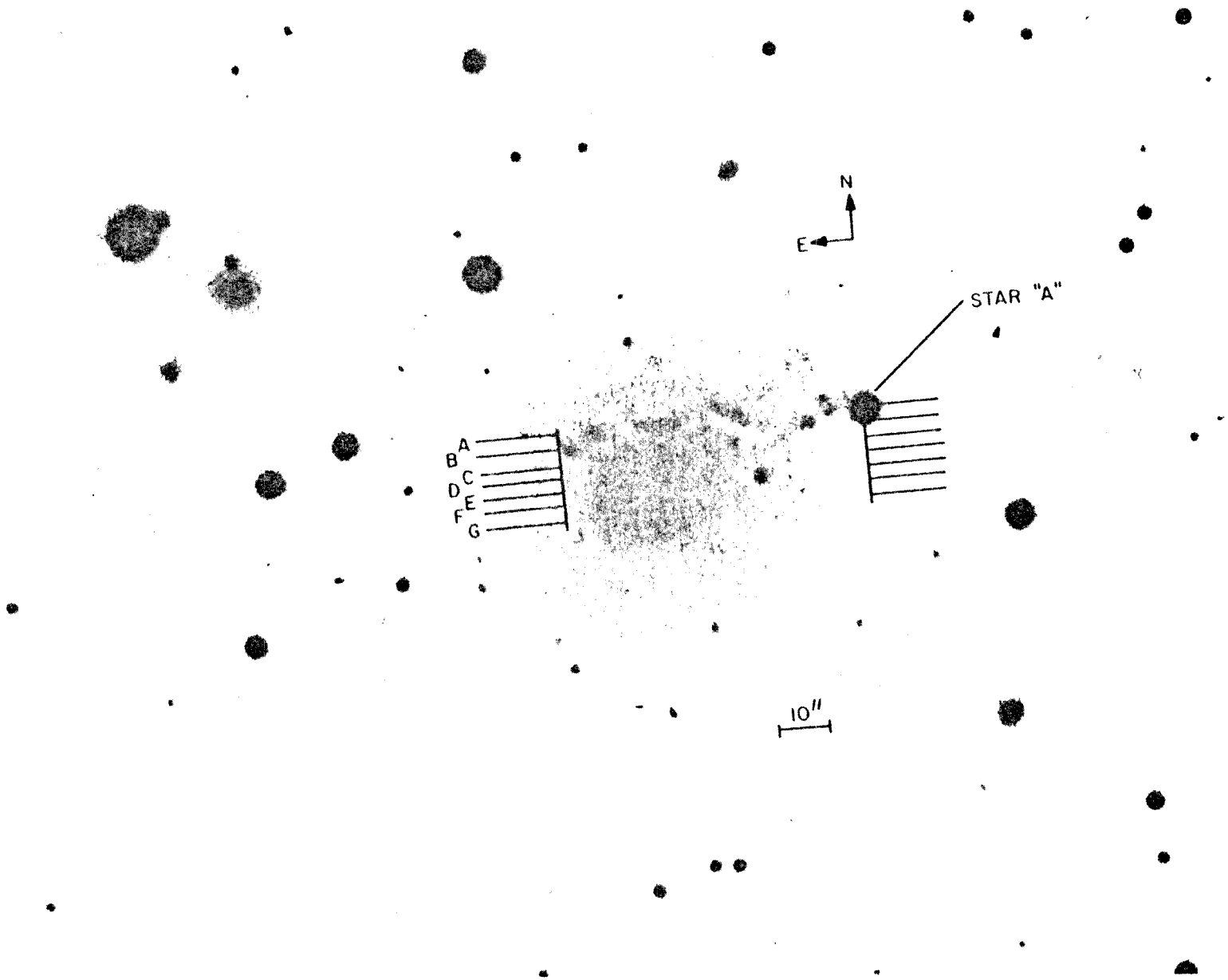

FIG. 1.—NGC 1275: 5 m prime-focus plate taken by Zwicky. Exposed for 40 minutes, unfiltered 103a-O. Outer limits of slit positions A–G used for SIT observations are marked. Slit position F passes through nucleus.

TABLE 1

SPECTROSCOPIC OBSERVATIONS

Slit Position	Instrument	Integ. Time (min)	Resolution (Å)	Wavelength Coverage (Å)
A	SIT	50	7.0	3600-6800
A	SIT	33	3.5	3700-5300
B	SIT	25	3.5	3700-5300
C	SIT	17	3.5	3700-5300
D	SIT	25	3.5	3700-5300
E	SIT	8	3.5	3700-5300
F	SIT	17	7.0	3600-6800
G	SIT	17	7.0	3600-6800
coudé Hα	IPCS	50	0.42	6580-6890
coudé Hβ	IPCS	50	0.44	4840-5170

at Hα and one spectrum centered at Hβ were taken with the slit placed across the nucleus in the direction of the star labeled A in Figure 1. Seven hundred and fifty channels in the wavelength direction at a resolution of ~0.45 Å per channel and 20 channels in the spatial direction at a scale of 2″ per channel were recorded. Integration times were 50 minutes for each spectrum.

Figure 2 is a typical high resolution SIT spectrum of a HV filament taken at slit position A, 45″ northwest of the nucleus; this region includes the prominent "knot" seen near star A in Figure 1. For measuring emission-line intensities, a composite HV spectrum was obtained by averaging all the SIT spectra together. Relative line intensities so determined are listed in Table 2, column (1). Fluctuations of up to 30% in the forbidden line intensities were observed in different regions of the HV system. For example, the [O III] λ5007 intensity varied from 1.76 at slit position C to 3.04 at slit position A.

Figure 3 is an average over 10 channels of a low-resolution SIT spectrum of a region with LV emission lines centered 18″ southwest of the nucleus and covered by slit position G. At the distance of NGC 1275 this separation corresponds to a projected distance of 9 kpc from the nucleus. A mean spectrum of this region was formed by averaging together the spectra from slit positions F and G. The relative emission line intensities are listed in Table 3, column (1).

Portions of the two coudé spectra are shown in Figures 4 and 5. In each case the bottom spectrum is at a position 6″ from the nucleus emphasizing the LV emission lines, while the top spectrum is at a position 20″ from the nucleus centered on the HV system. Approximate intensities of the LV emission lines are listed in Table 3, column (3). No absolute intensity calibration was done, so the two spectra were matched by assuming $H\alpha/H\beta = 2.95$. The Hβ intensity is also somewhat uncertain because of the presence of Balmer absorption lines in the underlying continuum near the nucleus (Minkowski 1968).

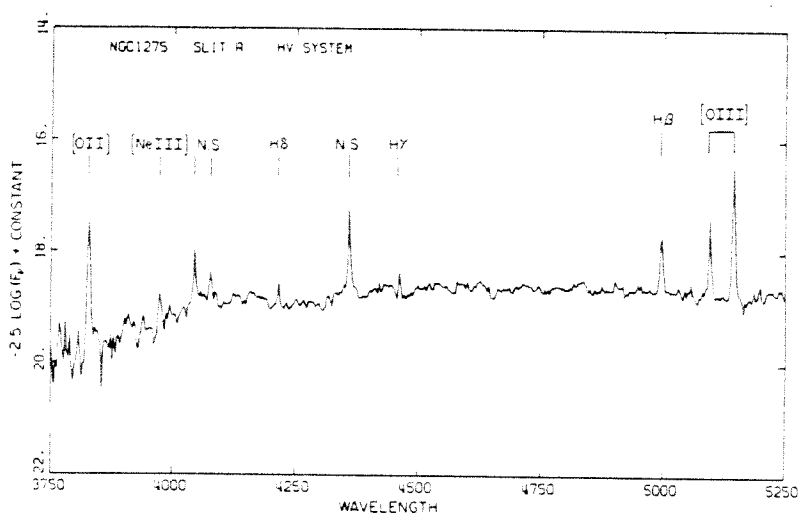

FIG. 2.—High-resolution SIT spectrum of region 45″ NW of nucleus emphasizing emission line system at 8200 km s^{-1}. Average of 12″ length at slit position A.

TABLE 2

RELATIVE LINE INTENSITIES: HIGH-VELOCITY SYSTEM

Line	Mean SIT Spectrum F/F(Hβ) (1)	Mean SIT Spectrum I/I(Hβ)† (2)	HII Region NGC 5455 I/I(Hβ) (3)	Shock Model V_s=141 km s^{-1} I/I(Hβ) (4)	X-Ray Heating T = 7.5 keV I/I(Hβ) (5)
[OII]3727	3.04	3.38	2.14	10.2	3.29
[NeIII]3869	0.36	0.39	...	1.05	0.08
Hγ 4340	0.34	0.36	...	...	0.47
Hβ 4861	1.00	1.00	1.00	1.00	1.00
[OIII]4948	1.24*	1.23	}4.37	0.80	0.18
[OIII]5007	2.64	2.61		2.32	0.55
[NI]5199	...	...	...	0.66	9.21
[OI]6300	<0.5	<0.5	...	0.75	7.77
[NII]6548	...	...	...	0.95	0.66
Hα 6563	3.15	2.82	3.02	2.63	2.95
[NII]6583	<0.22	<0.20	0.43	2.82	1.97
[SII]6717	...	...	...	...	7.09
[SII]6734	...	...	...	...	4.81
I(Hβ)≠	3.4x10^{-6}				

*Contaminated by [O III] 5007 at V = 5300 km s^{-1}.

†Corrected for E(B-V) = 0.10.

≠In ergs cm^{-2} s^{-1} ster^{-1}.

III. ANALYSIS

a) Reddening

The reddening by galactic dust in the direction of the Perseus cluster is $E(B-V) = 0.1$ as derived from Sandage (1973). From Table 2 the measured Hα/Hβ ratio of 3.15 for the HV system is close to the radiative recombination value of 2.95. This indicates little additional reddening intrinsic to the HV filaments. Column (2) of Table 2 lists the HV intensities corrected for $E(B-V) = 0.1$ using Whitford's (1958) reddening law. In contrast, the Hα/Hβ ratio from the SIT spectrum in Table 3 for the LV lines is a much steeper 4.77. If due to reddening, this corresponds to $E(B-V) = 0.43$. Such a steep decrement for the LV lines was also noted by RFPO. Implications for the origin of the reddening are discussed in § V. Corrected intensities for the LV lines using $E(B-V) = 0.43$ are listed in Table 3, column (2).

TABLE 3

RELATIVE LINE INTENSITIES: LOW-VELOCITY SYSTEM

Line	SIT Spectrum 18" Sw of Nuc. F/F(Hβ) (1)	SIT Spectrum 18" Sw of Nuc. I/I(Hβ)† (2)	Coudé Spectrum I/I(Hβ) (3)	Cooling Gas I/I(Hβ) (4)	Vela X SNR I/I(Hβ) (5)	Power Law Ioniz. α=-1 I/I(Hβ) (6)
[OII]3727	3.72	5.85	...	17.35	6.17	4.59
[NeIII]3869	...	...	...	0.59	...	0.06
Hγ 4340	...	...	...	0.47	0.44	0.47
Hβ 4861	1.00	1.00	1.00	1.00	1.00	1.00
[OIII]4958	...	...	2.00	1.93	0.20	0.41
[OIII]5007	0.63	0.60	5.99	5.70	0.60	1.22
[NI]5199	0.52	0.47	...	0.22	0.11	0.86
[OI]6300	1.90	1.26	...	0.26	0.83	2.23
[NII]6548	...	...	...	0.68	0.71	0.83
Hα 6563	4.77	2.95	2.95	2.92	3.16	2.93
[NII]6583	4.09	2.49	2.39	2.05	2.34	2.49
[SII]6717	...	...	3.31	1.47	2.09	3.40
[SII]6734	...	...	3.13	1.04	1.70	2.52
I(Hβ)≠	5.4x10^{-6}					

†Corrected for E(B-V) = 0.43.

≠In ergs cm^{-2} s^{-1} ster^{-1}.

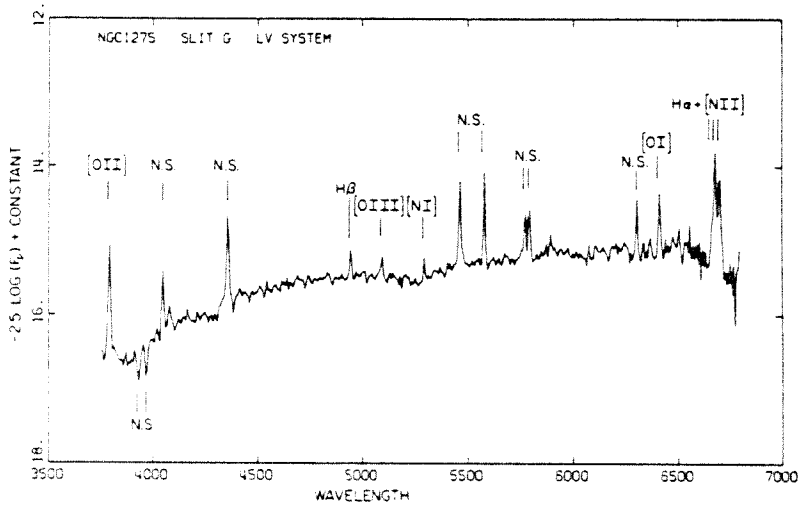

FIG. 3.—Low-resolution SIT spectrum of region 18″ SW of nucleus showing emission line system at 5300 km s^{-1}

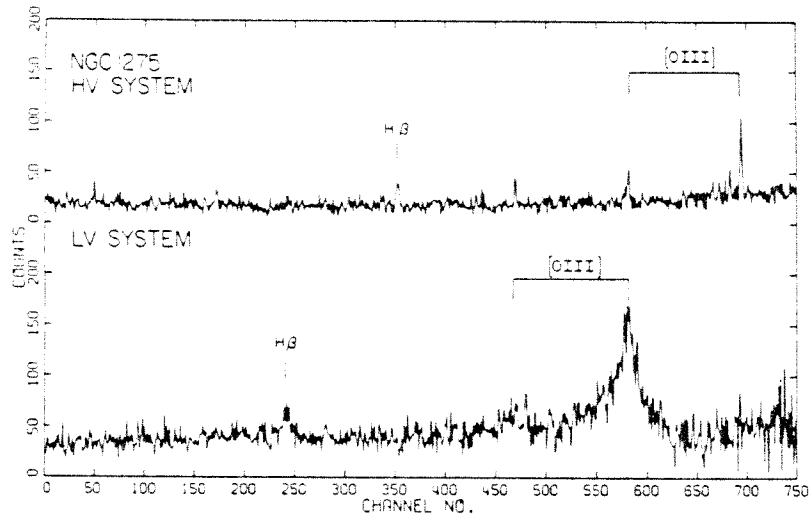

FIG. 4.—Coudé spectrum centered at Hβ showing the two velocity systems. Note coincidence of [O III] λ4957 at 8200 km s^{-1} with [O III] λ5007 at 5300 km s^{-1}.

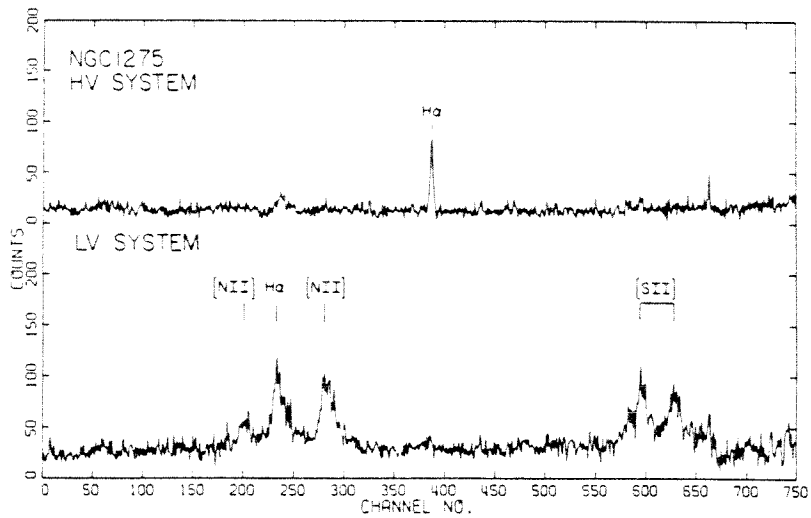

FIG. 5.—Same as Fig. 4 but centered at Hα. In both figures note differences in line widths and relative line strengths between the two velocity systems.

b) Comparison of High-Velocity and Low-Velocity Spectra

Since the work of Burbidge and Burbidge (1965) it has been known that the spectra of the two velocity systems are sharply different. The LV system is generally characterized by a low excitation state. Lines of neutral and singly ionized elements are strong, while usually [O III] λ5007 ≲ Hβ. The high velocity system on the other hand, indicates a more highly excited state. Here, [O III] λ5007 > Hβ, [Ne III] λ3869 is present, and lines of neutral elements are absent. Most striking is the great strength of [N II] λλ6548, 6583 in the LV system compared to the HV system. These lines are not detected in any of our HV spectra, and show up only weakly in other published spectra (e.g., RFPO). In the LV system, however, [N II] is always almost as strong as Hα. It does not seem likely that excitation conditions alone could account for this difference; most likely the N/O abundance ratio is considerably lower in the HV system than in the LV system (Burbidge and Burbidge 1965).

c) High-Velocity System: Velocity Field

Radial velocities for the HV emission lines were measured from the high resolution SIT spectra. Usually 4 to 10 channels in the spatial direction were averaged together to achieve an adequate signal-to-noise ratio. Velocities were determined only from Hβ and the [O II] lines. The typical error is estimated to be 30 km s^{-1} rms based on agreement among the three lines. The velocity field is shown in Figure 6, which also shows the region over which the HV emission lines were detected. Less accurate velocities are marked with a colon (:). RFPO also mapped the high-velocity field, and a comparison with their measurements shows reasonable agreement. The most important feature to note is the velocity gradient from east to west with a peak-to-peak amplitude of 240 km s^{-1} (somewhat smaller than found by RFPO) possibly indicating rotation in the HV system.

d) Densities

Electron densities can be estimated from the [S II] λ6717/λ6731 ratio (Osterbrock 1974). The only measurements we have of this kind are from the coudé spectra of the LV system. From the measured ratio λ6716/λ6731 of 1.06 we find $N_e/T_4^{1/2} = 1200\ \mathrm{cm}^{-3}$, where $T_4 = T/10^4$ K.

Unfortunately, we have no such measurements for the emission line regions of the HV system. However, Romney (1978) has measured the neutral hydrogen density in the 21 cm absorbing cloud at 8100 km s^{-1} discovered by De Young, Roberts, and Saslaw (1973). Using VLBI techniques, he showed the cloud to have a temperature $T < 300\ K$ and a density $N_H \approx 10$–$100\ \mathrm{cm}^{-3}$. The exact value for the density depends upon the unknown spin temperature of the gas and the somewhat uncertain geometry of the cloud; however, $N_H \lesssim 100$ is a fairly firm upper limit.

e) Total Fluxes

The total Hβ flux from the LV system is difficult to estimate due to the large and irregular extent of the filaments. From the Hα photograph of Lynds (1970) which emphasizes the LV system we estimate that the filaments cover ~1000 arcsec^2. Taking as a mean intensity the value listed in Table 3, column (1), the total Hβ flux is 1.3×10^{-13} ergs cm^{-2} s^{-1}, which corresponds to a total luminosity of 2×10^{41} ergs s^{-1} at NGC 1275.

The situation is less uncertain for the HV system. The total Hβ flux detected at the five high-resolution slit positions is 1×10^{-14} ergs cm^{-2} s^{-1}. About one-third of the HV system was covered by these measurements; consequently, the total Hβ flux becomes 3×10^{-14} ergs cm^{-2} s^{-1}, and the luminosity at NGC 1275 is 5×10^{40} ergs s^{-1}.

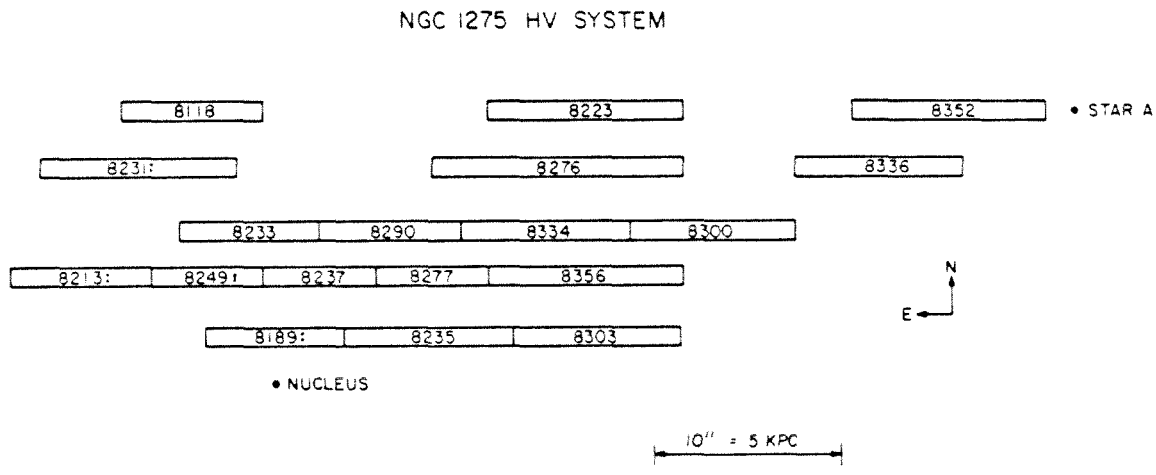

FIG. 6.—Velocity field of HV system as measured from high-resolution SIT spectra (slit positions A–E). Diagram indicates the area covered by each position. Gaps along the top two slit positions are regions where emission lines were weak or absent. No HV emission was detected at slit position F or G.

f) Line Widths

The coudé spectra in Figures 4 and 5 show a striking contrast between the widths of the LV and HV emission lines. The LV lines are quite broad, having a full width at half-maximum (FWHM) of 350 km s^{-1}. This value is similar to the spread in radial velocities among the different LV filaments as measured by Burbidge and Burbidge (1965). In contrast, the HV lines are much narrower, although still resolved. From the iron-arc comparison spectrum, the instrumental resolution is found to be 40 km s^{-1}. After correction for this, the widths of the HV lines are found to range from 57 to 100 km s^{-1}. These widths are much larger than the 6 km s^{-1} found for the 21 cm absorption line in the HV system by De Young, Roberts, and Saslaw (1973).

IV. X-RAY STRUCTURE

Part of our later analysis depends upon results derived from X-ray observations of the Perseus cluster, which we shall review here. The X-ray structure of the Perseus cluster has been discussed, among others, by Kellogg *et al.* (1973), Kellogg and Murray (1974), Kellogg, Baldwin, and Koch (1975), Wolff *et al.* (1976), and Helmken *et al.* (1978). Three separate components have been identified by these authors:

1. An extended component of size ~1 Mpc centered on the chain of galaxies in the middle of the Perseus cluster. The measurements are best fitted by a thermal bremsstrahlung spectrum of temperature 7.5 keV and a luminosity of 1.5×10^{45} ergs s^{-1} in the band 2–10 keV.
2. An extended component of size 120 kpc centered on NGC 1275. If fitted by a bremsstrahlung spectrum, the temperature is also 7.5 keV. The luminosity is 5×10^{44} ergs s^{-1} in the band 2–10 keV.
3. A point source centered on NGC 1275 with a luminosity of 8×10^{43} ergs s^{-1} in the band 2–10 keV and a power-law index of −1. The existence of this last component is not certain.

The origin of the first component is generally agreed to be thermal bremsstrahlung from a hot, intracluster medium (ICM). Bahcall and Sarazin (1977) have calculated a central temperature and density for the ICM of $T = 10^8$ K and $N_e = 5 \times 10^{-3}$ cm^{-3}. The most likely source of the second component is an increase in density of the ICM in the gravitational potential of NGC 1275, thereby producing enhanced X-ray emission (Fabian and Nulsen 1977).

The point source centered on NGC 1275 is inferred from the observations of Helmken *et al.* (1978). If the X-ray flux is a continuation of the nonthermal optical emission from the nucleus measured by Shields and Oke (1975), then the combined optical and X-ray measurements yield a spectrum for the nucleus of

$$L_\nu = 2.8 \times 10^{28}(\nu/\nu_R)^{-1.1} \text{ ergs s}^{-1} \text{ Hz}^{-1}, \quad (1)$$

where ν_R = 1 rydberg. Shields and Oke find a spectral index of −1.5, although their value depends on a somewhat uncertain correction for reddening and underlying stellar continuum. A measurement of the UV flux from NGC 1275, e.g., by the *IUE* satellite, would be helpful.

V. THE HIGH-VELOCITY SYSTEM

a) Ionization and Excitation Sources

In this section we consider three possible excitation sources for the HV system. We are interested mainly in reproducing the general features of the observed emission-line spectrum. Ionization by hot stars has been suggested in the past by several authors. However, the presence of a hot, intracluster medium and multiple X-ray sources in the region around NGC 1275 may have a significant influence on the HV gas. Collisional ionization from supersonic motions in the ICM and X-ray heating are possible excitation sources.

i) *Hot Stars*

Shields and Oke (1975), among others, have noted that the HV emission line spectrum is quite similar to those of giant H II regions in the outer parts of spiral galaxies. An extensive survey of H II regions in external galaxies was made by Searle (1971). In Table 2, column (3), we list his measurements for the region NGC 5455 in M101, which most closely matches the HV spectrum. Agreement with our observations is fairly good, the main characteristics being moderately strong [O III], strong [O II] λ3727, and weak [N II] λλ6548, 6583. As discussed by Shields and Searle (1978), H II regions like NGC 5455 are depleted in heavy elements relative to the Sun and also have abnormally low N/O abundance ratios. Support for the presence of hot stars in the HV system comes from the UV photograph of NGC 1275 taken by Adams (1977), which shows blue knots coincident with known regions of HV emission.

ii) *Collisional Ionization*

The motion of a gas cloud through the ICM at 3000 km s^{-1} is highly supersonic, and such motion should send a strong shock wave into the cloud (a countershock will also be sent out into the ICM). If the shock is strong enough the resulting ionization and heating of the gas could produce the observed emission line spectrum. This situation is illustrated schematically in Figure 7. In a frame at rest with respect to the shock front in the gas cloud, let n_1, v_1 be the density and velocity of the ICM, and n_2, v_2 be the same quantities for the HV gas cloud. The velocity of the shock v_2 passing through the HV cloud can be estimated by assuming conservation of momentum and ignoring thermal pressure and gravitational forces:

$$n_1 v_1^2 = n_2 v_2^2,$$

or

$$v_2 = v_1(n_1/n_2)^{1/2}.$$

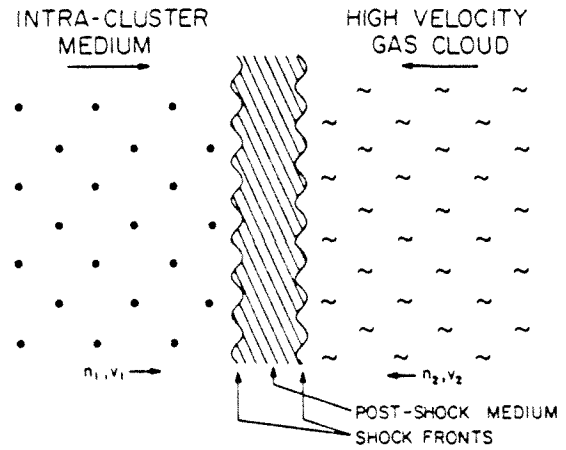

FIG. 7.—Schematic representation of collision between a HV cloud and the ICM.

From § IV we have $n_1 = 5 \times 10^{-3}$ cm^{-3}. Taking $v_1 = 3000$ km s^{-1} and (somewhat arbitrarily) $n_2 = 5$ cm^{-3}, we get $v_2 = 100$ km s^{-1}. Collisional ionization models with shock velocities of this magnitude have been calculated by Cox (1972) and Dopita (1976, 1977) in their analysis of the shock fronts produced by supernova remnants. In Table 2, column (4), we list the emission-line intensities from a model of moderate excitation state computed by Cox. This model, which has a shock velocity of 141 km s^{-1}, closely matches the measurements by Parker (1967) of filaments in the Cygnus Loop.

A general feature of the emission from shocks is the strength of neutral and singly ionized lines even in spectra of otherwise high excitation. Thus, Cox's model, which matches the [O III] intensity in the HV spectrum, predicts much more [O I] and [O II] than is observed. Some of the line strengths (e.g., the [N II] lines) could be brought into better agreement by varying the relative element abundances, but in general the collisional ionization calculation does not give good agreement with the observed spectrum. It is interesting to note, however, that the $H\beta$ intensity predicted by Cox for $v_{shock} = 100$ km s^{-1} and a preshock density of 5 cm^{-3} is 3.8×10^{-6} ergs cm^{-2} s^{-1} sr^{-1} perpendicular to the shock front. This is very close to the observed value of 3.4×10^{-6} ergs cm^{-2} s^{-1} sr^{-1}. If the emission from a shock front is not being seen, then either the mean density in the HV cloud is much larger than 5 cm^{-3} or the interaction between the HV gas and the ICM is so complicated that the simple picture presented here is invalid.

We shall reconsider shock models in analyzing the low-velocity system.

iii) *Thermal X-Rays*

The 120 kpc X-ray component of the ICM centered on NGC 1275 is capable of ionizing gas at the densities inferred for the HV material. To determine if such a flux could produce the HV emission lines, we have computed photoionization spectra for gas clouds excited by a thermal bremsstrahlung spectrum. The X-ray emission was assumed to be from a point source with the luminosity given in § IV for the 120 kpc component and to have a temperature of 7.5 keV. The gas clouds were assumed to be optically thin and to be at a distance of 65 kpc from the X-ray source. Models were computed for a range of densities for the clouds. Details of the calculations are given in the Appendix.

Results for one model with a density $N_H = 100$ cm^{-3} are listed in Table 2, column (5). Comparison with our observations shows severe disagreement; in particular, lines of neutral elements ([O I] and [N I]) are predicted to be much stronger than is observed. The reason is that the mean energy of an ionizing photon is high, and, although the gas is hot, it is still mostly neutral. X-ray excitation is thus unlikely. It should be noted, however, that if the limits of $N_H < 100$ cm^{-3} and $T < 300$ K from Romney (1978) for the 21 cm absorbing cloud are correct, then *such a cloud could not survive unless it were much farther than 65 kpc from the center of NGC 1275, or unless it were heavily shielded against the X-ray radiation.*

b) *Origin of the Material*

Minkowski (1957) originally suggested that NGC 1275 was a collision between two spirals, in keeping with the idea at the time that radio galaxies were formed by galaxy-galaxy collisions. Burbidge and Burbidge (1965) proposed that both the LV and HV systems were formed by one or more explosive outbursts from the nucleus of NGC 1275. This hypothesis is contradicted by the 21 cm absorption measurements which place the HV system in front of the nucleus. As shown by Ekers, van der Hulst, and Miley (1976) and Romney (1978), the absorption at 8100 km s^{-1} occurs against the compact nuclear source rather than the more extended radio components of NGC 1275. In their study of the HV system, RFPO proposed that the HV emission lines arise in a late-type spiral galaxy superposed on but otherwise unrelated to an underlying giant elliptical galaxy. The relative velocity difference of 3000 km s^{-1} is near the limit for a galaxy bound to the Perseus cluster. RFPO gave a number of observations to support their hypothesis, including (1) heavier reddening of LV lines relative to the HV lines; (2) apparent rotation of the HV system; (3) apparent obscuration of the continuum of the underlying galaxy in regions of HV emission; (4) association of emission knots and dust lanes with the HV system; (5) similarity of the HV spectrum to those of giant H II regions; and (6) 21 cm absorption.

The present study provides additional support for the spiral hypothesis. Our observations confirm the apparent rotation of the HV system and the steeper Balmer decrement of the LV lines. This latter effect implies that the LV system is *behind* and thus more reddened by dust *within* the HV system. In addition, we find new evidence that the HV emission arises in H II regions in a late-type spiral:

1. As shown in the previous section, the high-velocity emission-line spectrum is quantitatively

similar to the spectra of giant H II regions such as those found in M101. In his study of spiral galaxies Searle (1971) found that the excitation state of an H II region spectrum increased with increasing distance from the nucleus of a galaxy. Our observations show some evidence for this effect in that the [O III]/Hβ ratio is lower in the middle of the HV system (slit positions C and D of Fig. 1) than at the edges (slit positions A, B, and E), although the effect is not nearly as strong as found by Searle. This may be partly due to our poor spatial resolution combined with the fact that the spiral in NGC 1275 is probably close to edge-on. It is perhaps significant that NGC 5455, which best matched our observations, lies in the middle of the range of excitation found by Searle for M101.

2. The widths of the HV lines are found to be 57–100 km s^{-1} FWHM from the coudé spectra. The lower value (which corresponds to an *e*-folding width of 34 km s^{-1}) is the same value found by Smith and Weedman (1970) and Melnick (1977) for the largest H II regions in M101. The largest widths we find could be due to the presence of multiple H II regions in the field of view of the slit.

3. The total Hβ luminosity measured for the HV system is 5×10^{40} ergs s^{-1}. Comparable measurements for other galaxies are difficult to come by. Cohen (1976) measured the integrated Hα flux from a number of field spiral galaxies. Converting her measurements to absolute luminosities and assuming an Hα/Hβ ratio of 2.95, we find the Hβ luminosity of the HV system to lie well within the range of measurements for the brightest spiral galaxies.

Finally, we note that the VLBI measurements of Romney (1978) show that the 21 cm absorbing cloud has properties that are typical of large clouds in our own Galaxy ($R \approx 4$ pc, $N_H \sim 10$–100, $T < 300$ K).

An argument against the spiral hypothesis is the apparently small probability for seeing two unusual galaxies superposed. As noted by van den Bergh (1977), late-type spirals are rare in the Perseus cluster, especially in the core regions. Also, no detectable nucleus or disk of stars is seen for the spiral on published photographs, although such features may be weak enough to be obscured by dust or lost in the continuum of the underlying galaxy. However, any alternative explanation involving a local origin for both the LV and HV systems must account for the large velocity difference and markedly different spectral characteristics of the two sytsems and the need for the HV system to be in front of the LV system. With present observations, infall of a spiral galaxy still remains the most reasonable explanation.

VI. THE LOW-VELOCITY SYSTEM

a) Ionization and Excitation Sources

As in the case of the HV system, there are several possible sources of excitation for the LV emission lines, including photoionization by the Seyfert nucleus, collisions among turbulent gas clouds, and condensation from the hot ICM. In this section we shall compare model predictions primarily with our SIT observations for which we have the most complete information.

i) *Cooling ICM*

Fabian and Nulsen (1977) suggested that the LV filaments are materials condensing out of the ICM in the vicinity of NGC 1275. We have therefore investigated the possibility that the LV emission lines are produced by the cooling of such gas. Using methods described in the Appendix, we have computed the cumulative emission-line spectrum of a gas cloud as it cools isobarically from 10^8 K to recombination. This spectrum is the same as that which would be emitted from a medium in which matter initially at 10^8 K is continuously freezing out at a constant rate with time. The main uncertainty with this calculation is the optical thickness of the cooling gas to UV ionizing photons. An optically thick cloud would be affected mainly in the hydrogen recombination regions where UV photons are converted to hydrogen recombination lines and the forbidden lines of neutral elements. Somewhat arbitrarily we have assumed case B recombination coefficients for hydrogen but otherwise assumed the gas to be optically thin. The results for this model are listed in Table 3, column (4). Comparison with the observed spectrum shows rather poor agreement; in particular, the lines of neutral elements are predicted to be weaker than is observed, while lines of ionized elements (especially [O II] and [O III]) are predicted to be much stronger than is observed. Since each hydrogen recombination produces 4×10^{-13} ergs in Hβ, a total condensation rate of $1.2 \times 10^4\ M_\odot$ yr^{-1} is required to produce the observed Hβ flux of 2×10^{41} ergs s^{-1}. This rate greatly exceeds the estimate of 100 $M_\odot$ yr^{-1} of Fabian and Nulsen (1977). Condensation will be further discussed below regarding the origin of the LV filaments.

ii) *Collisional Ionization*

The turbulent velocities in the LV filaments ($\Delta v \approx 350$ km s^{-1}) are large enough that cloud-cloud collisions could produce strong shocks ($v_s \approx 100$ km s^{-1}) similar to those discussed for the HV system (§ V). Emission-line spectra produced in such shocks are much more characteristic of the LV system. As an example of such a low-ionization-state shock spectrum we list in Table 3, column (5), emission-line intensities for the Vela X supernova remnant as measured by Osterbrock and Costero (1973). The agreement with the observed spectrum is surprisingly good, especially considering the grossly different nature of the two objects. In particular, the intensity ratios of the three oxygen species are reproduced well, as are the strengths of the nitrogen lines. Element abundances for Vela X were determined by Dopita, Mathewson, and Ford (1977) using the shock wave models of Dopita (1977); their results indicate that the abundances of oxygen and nitrogen are within factors of 2–4 of the solar value, and that the N/O

ratio is, if anything, greater than the solar value. Collisional ionization models could be further checked by observation of [Ne III] λλ3869, 3968, [S II] λλ4068, 4076, and [O III] λ4363, all of which are predicted to be moderately strong (Cox 1972; Dopita 1977), but which are below our detection limit.

iii) *Photoionization by the Seyfert Nucleus*

The nonthermal continuum source in the nucleus of NGC 1275 can easily ionize gas out to large distances from the nucleus (Shields and Oke 1975). Unlike ordinary H II regions, however, nebulae ionized by power-law spectra can exhibit a wide range of ionization states. We have therefore computed photoionization spectra for gas clouds excited by the ionizing source of equation (1). In Table 3, column (6), we list the emission line intensities for a model with an optically thin cloud of density $N_H = 1200\ cm^{-3}$ at a distance 10 kpc from the ionizing source. Again the general features of the observed spectrum are reproduced, although not quite as well as with the collisional ionization model. Better agreement might be achieved by including collisional de-excitation in the models and varying the slope of the power law and the element abundances.

The density for these models was varied to give a best fit to the observed spectrum. Since the models only determine the parameter F/N_H, where F is the radiation flux incident on the clouds, the actual density will depend on the luminosity of the ionizing source and distance of the cloud from the source. Our value for the density is not unreasonable, however, since it is also the density derived from the [S II] lines for the nuclear regions of the LV system. The resulting thermal pressure $nT = 8 \times 10^6$ is of the same order as (although somewhat larger than) the pressure required to be in equilibrium with the surrounding ICM ($nT \approx 10^6$). As shown in § IV, the luminosity of the nucleus is quite uncertain. Reducing it by a factor 8 would bring the density and thermal pressure of the LV filaments much closer to the values needed for equilibrium with the ICM.

From equation (1) the total ionizing flux from the nucleus is $Q(H_0) = 4 \times 10^{54}$ photons s^{-1}. If each ionization and subsequent recombination produces 2×10^{-13} ergs in Hβ (Osterbrock 1974), then the nucleus can ionize enough gas to produce the observed Hβ flux of 2×10^{41} ergs s^{-1}. If the luminosity of the nucleus has in fact been overestimated by a factor of 8, however, this conclusion is no longer secure.

To summarize, the collisional and photoionization calculations are both in reasonably good agreement with the observed LV emission line spectrum. Future observations should be able to distinguish between the two models, e.g., [S II] λ4072 and [Ne III] λ3869 are predicted to be much stronger in the collisional model. Also, the photoionization model would predict a decrease in excitation state of the LV lines with increasing distance from the nucleus, while the collisional ionization model would predict no such dependence.

b) Origin of the Material

The LV filaments have usually been thought of as being ejected from the nucleus of NGC 1275 (Burbidge and Burbidge 1965) in a violent outburst similar to, but on a much larger scale than, the event which occurred in M82. The main evidence for such an outburst is the extensive and irregular nature of the LV filaments as seen, e.g., on the Hα photographs of Lynds (1970) and the large variations in radial velocity among the different filaments. Unlike the case of M82, however, the kinematics show no clear pattern of expansion. In fact, while these observations are suggestive, there is no compelling evidence to support an outburst.

Recently, Fabian and Nulsen (1977) and Mathews and Bregman (1978) have found that slow-moving giant ellipticals in the centers of X-ray clusters can accrete gas from an ICM; the gas density in these deep potential wells is high enough that the cooling times become shorter than a Hubble time. Fabian and Nulsen interpret the LV filaments as being condensations in the gas flow accreting onto NGC 1275. This idea can explain a number of peculiar features of NGC 1275. First, the 120 kpc X-ray component is produced by the enhanced emission from the increased density in the accretion flow. Condensation followed by star formation could explain the presence of blue knots far from the nucleus seen on the UV photograph of Adams (1977) and the unusually blue color of NGC 1275 outside the nucleus (van den Bergh 1977). Star formation at the inner radius of the accretion flow could explain the A-type absorption spectrum seen by Minkowski (1968). Finally, accretion into the core could power the Seyfert nucleus and non-thermal continuum source. From the X-ray luminosity of the 120 kpc component Fabian and Nulsen derive an accretion rate of $\sim 100\ M_\odot\ yr^{-1}$.

The formation of filaments in the accretion flow is discussed by Mathews and Bregman (1978). In summary, the accretion flow is thermally unstable, and any perturbations in the flow (e.g., due to magnetic field variations) will grow and produce cool, collapsed clouds of gas. As shown in the previous section, emission-line radiation produced during the cooling stages is probably too weak to be observed. However, Mathews and Bregman have pointed out that, as the clouds cool, strong shocks will be sent into them by the surrounding ICM. In order to produce the observed Hβ flux material must be passing through shocks at a rate of $\sim 10^4\ M_\odot\ yr^{-1}$. Since the accretion rate is $\sim 100\ M_\odot\ yr^{-1}$, each element of condensing material must be shocked ~ 100 times during the period of infall onto NGC 1275, which would require the accreting ICM to be quite turbulent. As an alternative to shock heating, the condensing clouds, once formed, could be photoionized by the Seyfert nucleus. Either process (or possibly a combination of both) would produce emission line spectra which, as we have seen, are characteristic of the LV spectrum.

As in the case of the outburst hypothesis, there is no direct evidence which supports the presence of

an accretion flow onto NGC 1275. Our considerations of the ionization and excitation of the LV system are consistent with either explanation of the origin of the filaments. The main argument in favor of the accretion flow is that it is a direct consequence of the presence of an ICM in the deep gravitational potential of a galaxy. Such an explanation for the origin of the filaments does not require the arbitrary assumptions about unknown physical processes which must be invoked by the violent outburst hypothesis.

VII. CONCLUSIONS

The results of this paper can be summarized as follows:

1. The most probable source of excitation for the high-velocity emission lines is photoionization by hot stars.

2. Our observations support the idea that the high-velocity system is an infalling spiral galaxy unrelated to (and possibly quite distant from) an underlying elliptical galaxy.

3. The low-velocity emission lines are equally well explained by collisional ionization from shocks formed between colliding clouds and photoionization by the nonthermal continuum source in the Seyfert nucleus. Future observations should distinguish between the two possibilities.

4. The origin of the low-velocity filaments is most easily explained by condensation from an accretion flow of the intracluster medium onto NGC 1275. No explosive ejection from the nucleus is necessary, although there is no direct evidence against such an event.

We have shown that the presence of a hot, intracluster medium can play an important role in interpreting the variety of phenomena that are seen in NGC 1275. It would be of interest to find similar objects in other rich clusters of galaxies. The existence of two velocity systems requires unlikely superposition of two galaxies; however, any attempt at a more plausible explanation is hampered by the strong spectroscopic differences between the two systems, by their large velocity separation, and by the requirement that the high-velocity system be in front of the nucleus of NGC 1275.

We are indebted to Jon Romney for providing the results of his thesis prior to its completion and for many stimulating conversations. We wish to thank Gary Tuton and Juan Carrasco for their assistance at the telescope. W. L. W. S. thanks A. Boksenberg and his Flying Circus for permission to use portions of our coudé observations of NGC 1275. S. M. K. is supported by a fellowship from the Fannie and John Hertz Foundation. This work was partially supported by NSF grant AST 75-00555.

APPENDIX

EQUILIBRIUM AND COOLING IN A HOT GAS

a) Photoionization Models

In this paper we have calculated two models for a photoionized gas, one with a power law ionizing spectrum and one with a thermal bremsstrahlung spectrum. At the temperatures and densities considered here, all ions can be taken to be in the ground state. Equilibrium between adjacent ionization states requires:

$$4\pi n_i \int_{\nu_T^{(i)}}^{\infty} \frac{J_\nu a_\nu^{(i)}}{h\nu}\, d\nu = n_{i+1} n_e \alpha_{i+1}(T_e)\,, \tag{A1}$$

where n_i is the density of ion i, $\nu_T^{(i)}$ is the threshold frequency for ionization, J_ν is the mean intensity of the radiation field, $a_\nu^{(i)}$ is the photoionization cross section, and α_{i+1} is the recombination coefficient for ion $i + 1 \rightarrow i$. For a_ν we use the approximation

$$a_\nu = a_T[\beta(\nu/\nu_T)^{-s} + (1 - \beta)(\nu/\nu_T)^{-(s+1)}]\ \mathrm{cm}^2\,. \tag{A2}$$

Values of a_T, β, ν_T, and s are taken from Osterbrock (1974), Daltabuit and Cox (1972), Chapman and Henry (1971, 1972), Silk and Brown (1971), Ditchburn and Marr (1953), Weisheit (1974), and Weisheit and Collins (1976). For Si I and S I–IV, the more complicated formula of Chapman and Henry (1971) is used. Both valence shell and inner shell ionization are considered. Recombination coefficients of hydrogenic ions are taken from Seaton (1959); those for other ions, from Aldrovandi and Péquignot (1973).

For O and N the resonant charge exchange reactions

$$\mathrm{O} + \mathrm{H}^+ \rightleftarrows \mathrm{O}^+ + \mathrm{H}$$

and

$$\mathrm{N} + \mathrm{H}^+ \rightleftarrows \mathrm{N}^+ + \mathrm{H}$$

are included with the rates given by Osterbrock (1974).

Simultaneously, thermal equilibrium requires equality of the heating and cooling rates:

$$\sum_i 4\pi n_i \int_{\nu_T^{(i)}}^{\infty} \frac{J_\nu a_\nu^{(i)}}{h\nu} h(\nu - \nu_T^{(i)}) d\nu = \sum_i n_e n_i (l_r^{(i)} + l_f^{(i)}) , \tag{A3}$$

where $l_r^{(i)}$ is the energy loss rate from recombination and $l_f^{(i)}$ is the energy loss rate from collisionally excited forbidden lines. The summation is over all ions of all elements. Energy loss from radiative recombination is calculated using the method described by Cox and Tucker (1969). For forbidden line radiation we use the formula:

$$l_f^{(i)} = \sum_{n'} 8.63 \times 10^{-8} \left(\frac{\Omega_{nn'}}{\omega_n}\right) E_{nn'} T^{-1/2} \exp\left(-\frac{E_{nn'}}{kT}\right) \text{ ergs cm}^3 \text{ s}^{-1} , \tag{A4}$$

where $E_{nn'}$ is the energy of the transition $n \rightarrow n'$ in ergs, $\Omega_{nn'}$ is the collision strength, and ω_n is the statistical weight of the lower level. The summation is over all transitions from the ground state. Collision strengths are taken from Osterbrock (1974), Saraph *et al.* (1969), Dopita, Mason, and Robb (1976), Eissner and Seaton (1974), and Seaton (1975).

Our models include the elements H, He, C, N, O, Ne, Mg, Si, and S. Abundances are taken from Allen (1973).

In our calculations a number of simplifactions are made. First the gas clouds are assumed to be optically thin. The gas density is assumed to be low enough that collisional de-excitation is unimportant. The size of the cloud is assumed to be small compared with its distance from the radiation source so J_ν can be taken constant in the cloud. With these assumptions, a given model requires that one specify J_ν/n_e. Equations (A1) and (A2) are solved iteratively to find the electron temperature and ionization distribution. The total density (which depends on the fractional ionization of H and He) is then found and the resulting emission spectrum calculated.

For ionization by a thermal bremsstrahlung spectrum, a few additional effects have been ignored. Ionization of heavy elements by removal of a K-shell electron is usually followed by emission of an Auger electron. Thus, nonadjacent ionization stages are coupled. The Auger electron deposits its energy in heating and/or subsequent ionizations of hydrogen. These processes are ignored because (1) heating is still dominated by H and He and (2) the lowest ionization stages of the heavy elements (which are of greatest interest) are not seriously affected. For optically thick models these effects would need to be included.

b) Radiative Cooling of a Hot Gas

The behavior of a collisionally ionized gas has been considered, e.g., by Cox and Tucker (1969), Cox (1972), and Shapiro and Moore (1976). The gas is initially assumed to be in ionization equilibrium:

$$C_i(T) n_i = \alpha_{i+1}(T) n_{i+1} , \tag{A5}$$

where C_i is the collisional ionization rate for ion $i \rightarrow i + 1$, and α_{i+1} now includes the contribution of dielectronic recombination. Expressions for the collisional ionization rates are taken from Lotz (1967) and Cantó and Daltabuit (1974), extrapolating along isoelectronic sequences where necessary. Dielectronic recombination rates are taken from Aldrovandi and Péquignot (1973).

The rate of change of the ionization distribution is given by:

$$\frac{dn_i}{dt} = C_{i-1} n_{i-1} n_e + \alpha_{i+1} n_{i+1} n_e - (C_i + \alpha_i) n_i n_e . \tag{A6}$$

The rate of energy loss is given by:

$$\frac{dh}{dt} = L(T) n_e , \tag{A7}$$

with $h = \epsilon + (5/2)(1 + f)kT$, and

$$L(T) = l_B + \sum \frac{n_i}{n} (l_f^{(i)} + l_s^{(i)} + l_p^{(i)} + l_r^{(i)} + l_d^{(i)}) ,$$

where h is the enthalpy per ion, ϵ is the mean ionization energy per ion, f is the fractional ionization n_e/n, n is the total density of ions, and the cooling function $L(T)$ contains the following contributions:

1. *Bremsstrahlung.*—The expression of Cox and Tucker (1969) is used:

$$l_B = 2.3 \times 10^{-27} T^{1/2} \text{ ergs cm}^3 \text{ s}^{-1} . \tag{A8}$$

2. *Collisional excitation of heavy elements, including forbidden (l_f), semiforbidden (l_s), and permitted (l_p) line radiation.*—Collision strengths for semiforbidden lines are taken from Osterbrock (1970), Osterbrock and Wallace

(1977), and Jackson (1973). For permitted lines, the collision strength is usually approximated by

$$\frac{\Omega_{nn'}}{\omega_n} = 14.5(E_H/E_{nn'})g_{nn'}f_{nn'}, \tag{A9}$$

where $E_H = 1$ rydberg, $g_{nn'}$ is an effective Gaunt factor, and $f_{nn'}$ is the oscillator strength of the transition. Gaunt factors are taken from van Regemorter (1962), Bely, Tully, and van Regemorter (1963), Bely (1966), Burke and Moore (1968), Sampson (1969), Roberts (1970), and Mewe (1972). These values are evaluated at a temperature $kT = 1.5\,E_{nn'}$. Oscillator strengths are taken from Wiese, Smith, and Glennon (1966), Wiese, Smith, and Miles (1969), Smith and Wiese (1971), and Morton and Smith (1972). Energy levels are taken from Wiese, Smith, and Glennon (1966), Wiese, Smith, and Miles (1969), and Striganov and Sventitskii (1968).

3. *Recombination radiation, both radiative and dielectronic.*—The latter rate is assumed to be

$$l_d^{(i)} = \alpha_{d_i}{}^{(i)}\bar{E}_i, \tag{A10}$$

where α_{d_i} is the dielectronic recombination rate and $\bar{E}_i$ is a mean energy of the lowest excited levels of ion i.

Finally, for isobaric cooling we have

$$\frac{dP}{dt} = \frac{d}{dt}[(1+f)nkT] = 0. \tag{A11}$$

The gas cloud is assumed to be in equilibrium at an initial temperature T_i (for our model $T_i = 10^8$ K) and then allowed to cool. Equations (A6), (A7), and (A11) are numerically integrated to follow the changes in ionization distribution, temperature, and density. For each element the equations (A6) for ionization change for each ion are coupled. The numerical integration at each step is performed by finding the exact solution of the coupled equations assuming constant values for the ionization and recombination coefficients. At each stage of the integration the energy per atom emitted for each emission line of interest is accumulated. The integrations are terminated when hydrogen completes recombination.

Because we do not include iron in our calculations, the cooling rate above 10^6 K is underestimated. Since no emission lines of interest are emitted at these temperatures, the main effect of ignoring iron will be to alter the ionization distribution in this temperature range. However, cooling above 10^6 K is slow enough that departures from a steady-state equilibrium are small, and this effect should not be serious. As a check on our calculations a comparison of our time-dependent cooling function with that of Shapiro and Moore (1976) shows good agreement below 5×10^5 K; these authors include iron, but start at $T_i = 10^6$ K.

REFERENCES

Adams, T. F. 1977, *Pub. A.S.P.*, **89**, 488.
Aldrovandi, S. M. V., and Péquignot, D. 1973, *Astr. Ap.*, **25**, 137.
Allen, C. W. 1973, *Astrophysical Quantities* (London: Althone).
Bahcall, J. N., and Sarazin, C. L. 1977, *Ap. J. (Letters)*, **213**, L99.
Bely, O. 1966, *Ann. d'Ap.*, **29**, 131.
Bely, O., Tully, J., and van Regemorter, H. 1963, *Ann. Phys.*, **8**, 303.
Boksenberg, A. 1972, in *Auxiliary Instrumentation for Large Telescopes*, Proc. of the ESO–CERN Conference, ed. S. Lausten and A. Reitz, p. 295.
Boksenberg, A., and Burgess, D. E. 1973, in *Astronomical Observations with Television Type Sensors*, ed. J. W. Glaspey and G. A. H. Walker (Vancouver: University of British Columbia), p. 21.
Burbidge, E. M., and Burbidge, G. R. 1965, *Ap. J.*, **142**, 1351.
Burbidge, E. M., Smith, H. E., and Burbidge, G. R. 1978, *Ap. J.*, **219**, 400.
Burke, P. G., and Moore, D. J. 1968, *J. Phys. B.*, **1**, 575.
Cantó, J., and Daltabuit, E. 1974, *Rev. Mexicana Astr. Ap.*, **1**, 5.
Chapman, R. D., and Henry, R. J. W. 1971, *Ap. J.*, **168**, 169.
———. 1972, *Ap. J.*, **173**, 243.
Cohen, J. G. 1976, *Ap. J.*, **203**, 587.
Cox, D. P. 1972, *Ap. J.*, **178**, 143.
Cox, D. P., and Tucker, W. H. 1969, *Ap. J.*, **157**, 1157.
Daltabuit, E., and Cox, D. P. 1972, *Ap. J.*, **177**, 855.
De Young, D. S., Roberts, M. S., and Saslaw, W. C. 1973, *Ap. J.*, **185**, 809.
Ditchburn, R. W., and Marr, G. V. 1953, *Proc. Phys. Soc.*, **A66**, 655.
Dopita, M. A. 1976, *Ap. J.*, **209**, 395.
———. 1977, *Ap. J. Suppl.*, **33**, 437.
Dopita, M. A., Mason, D. J., and Robb, W. D. 1976, *Ap. J.*, **207**, 102.
Dopita, M. A., Mathewson, D. S., and Ford, V. L. 1977, *Ap. J.*, **214**, 179.
Eissner, W., and Seaton, M. J. 1974, *J. Phys. B*, **7**, 2533.
Ekers, R. D., van der Hulst, J. M., and Miley, G. K. 1976, *Nature*, **262**, 369.
Fabian, A. C., and Nulsen, P. E. J. 1977, *M.N.R.A.S.*, **180**, 479.
Helmken, H., Delvaille, J. P., Epstein, A., Geller, M. J., Schnopper, H. W., and Jernigan, J. G. 1978, *Ap. J. (Letters)*, **221**, L43.
Jackson, A. R. G. 1973, *M.N.R.A.S.*, **165**, 53.
Kellogg, E., Murray, S., Giacconi, R., Tananbaum, T., and Gurskey, H. 1973, *Ap. J. (Letters)*, **185**, L13.
Kellogg, E., and Murray, S. 1974, *Ap. J. (Letters)*, **193**, L57.
Kellogg, E., Baldwin, J. R., and Koch D. 1975 *Ap. J.*, **199**, 299.
Lotz, W. 1967, *Ap. J. Suppl.*, **14**, 207.
Lynds, R. 1970, *Ap. J. (Letters)*, **159**, L151.
Mathews, W. G., and Bregman, J. N. 1978, *Ap. J.*, **224**, 308.
Melnick, J. 1977, *Ap. J.*, **213**, 15.
Mewe, R. 1972, *Astr. Ap.*, **20**, 215.
Minkowski, R. 1957, in *IAU Symposium No. 4, Radio Astronomy*, ed. H. C. van de Hulst (Cambridge: Cambridge University Press), p. 107.
———. 1968, *A.J.*, **73**, 836.
Morton, D. C., and Smith, W. H. 1973, *Ap. J. Suppl.*, **26**, 333.
Oke, J. B., and Schild, R. E. 1970, *Ap. J.*, **161**, 1015.
Osterbrock, D. E. 1970, in *Nuclei of Galaxies* (Vatican City: Pontifical Academy of Sciences), p. 176.

Osterbrock, D. E. 1974, *Astrophysics of Gaseous Nebulae* (San Francisco: Freeman).
Osterbrock, D. E., and Costero, R. 1973, *Ap. J. (Letters)*, **184**, L71.
Osterbrock, D. E., and Wallace, R. K. 1977, *Ap. Letters*, **19**, 11.
Parker, R. A. R. 1967, *Ap. J.*, **149**, 363.
Roberts, D. E. 1970, *J. Phys. B*, **3**, 676.
Romney, J. D. M. 1978, Ph.D. thesis, California Institute of Technology.
Rubin, V. C., Ford, W. K., Peterson, C. J., and Oort, J. H. 1977, *Ap. J.*, **211**, 693 (RFPO).
Sandage, A. R. 1973, *Ap. J.*, **183**, 711.
Sampson, D. H. 1969, *Ap. J.*, **155**, 575.
Saraph, H. E., Seaton, M. J., and Shemming, J. 1969, *Phil. Trans. R. Soc.*, **A264**, 77.
Searle, L. 1971, *Ap. J.*, **168**, 327.
Seaton, M. J. 1975, *M.N.R.A.S.*, **170**, 475.
Shapiro, P. R., and Moore, R. T. 1976, *Ap. J.*, **207**, 460.
Shields, G. A., and Oke, J. B. 1975, *Pub. A.S.P.*, **87**, 879.
Shields, G. A., and Searle, L. 1978, *Ap. J.*, **222**, 821.
Silk, J., and Brown, R. L. 1971, *Ap. J.*, **163**, 495.
Smith, M., and Weedman, D. 1970, *Ap. J.*, **161**, 33.
Smith, M. W., and Wiese, W. L. 1971, *Ap. J. Suppl.*, **23**, 103.
Striganov, A. R., and Sventitskii, N. S. 1968, *Tables of Spectral Lines* (New York: Plenum Press).
van den Bergh, S. 1977, *Astr. Nach.*, **298**, 285.
van Regemorter, H. 1962, *Ap. J.*, **136**, 906.
Weisheit, J. C. 1974, *Ap. J.*, **190**, 735.
Weisheit, J. C., and Collins, L. A. 1976, *Ap. J.*, **210**, 299.
Whitford, A. E. 1958, *A.J.*, **63**, 201.
Wiese, W. L., Smith, M. W., and Glennon, B. M. 1966, *Atomic Transition Probabilities* (Washington: Government Printing Office), Vol. **1**.
Wiese, W. L., Smith, M. W., and Miles, B. M. 1969, *Atomic Transition Probabilities* (Washington: Government Printing Office), Vol. **2**.
Wolff, R. S., Mitchell, R. J., Charles, P. A., and Culhane, J. L. 1976, *Ap. J.*, **208**, 1.

S. M. KENT and W. L. W. SARGENT: Department of Astronomy 105-24, California Institute of Technology, Pasadena, CA 91125

CHAPTER II

RAM PRESSURE SWEEPING OF SPIRAL GALAXIES BY A HOT INTRACLUSTER MEDIUM

I. INTRODUCTION

The discovery that rich clusters of galaxies are often filled with a hot, diffuse, intra-cluster medium (ICM) has led to the realization that such a medium should have a profound effect on the interstellar gas content of galaxies within these clusters. The thermal pressure of this medium ($nT \sim 10^5$) is alone high enough to drastically alter the properties of a normal interstellar medium (ISM) in a galaxy. Furthermore, the motion of such a galaxy within the cluster can generate a ram pressure which may be capable of sweeping out its ISM. For this reason ram pressure sweeping has received considerable attention in recent years as a possible means of transforming an existing population of spirals into the large numbers of S0's found in clusters (Gunn and Gott 1972, Tarter 1975, Lea and De Young 1976, Melnick and Sargent 1977, Bahcall 1977b,Butcher and Oemler 1978, Tytler and Vidal 1978, Gisler 1979, Himmes and Biermann 1979).

One objective of this paper is to examine the nature of the sweeping process in somewhat greater detail than has been done in previous treatments and to formulate a more quantitative estimate of the efficiency with which sweeping can occur. In particular, some emphasis is placed on the fact that a substantial fraction of material may exist in dense clouds which are more difficult to sweep than uniformly distributed matter. These results are presented in §§III and IV. Some

observational predictions regarding the sweeping of individual galaxies are given in §V.

The second objective is to construct a simple model for sweeping in a cluster and determine if the ram pressure experienced by galaxies is capable of sweeping a sufficient number of spirals to reproduce the observed numbers of S0's. In §VI it will be shown that, contrary to previous opinion, the ram pressure is probably too low by more than an order of magnitude to sweep the required number of spirals. A summary of conclusions is given in §VII.

II. PRELIMINARIES

For the purposes of this paper thermal conduction and viscosity in the ICM will be ignored. The importance of these processes depends very much on the presence or absence of magnetic fields. In the absence of magnetic fields the rate coefficients are (Spitzer 1962):

$$\kappa = \frac{1.85\times10^{-5}\ T^{5/2}}{\ln\ \Lambda}\ \text{erg cm}^{-1}\ \text{K}^{-1}\ \text{s}^{-1}\ \text{(conductivity)}$$

$$\mu = \frac{2.2\times10^{-15}T^{5/2}}{\ln\ \Lambda}\ \text{g cm}^{-1}\ \text{s}^{-1}\ \text{(viscosity)}$$

where $\ln\Lambda \simeq 30\text{-}40$ and $T \sim 10^8$ K for the ICM. In the limit of low density κ (and also presumably μ) are reduced by saturation effects (Cowie and McKee 1977). Cowie and Songaila (1977) have stressed the importance of thermal conductivity

as being an efficient means of evaporating material from a galaxy. However, the importance of viscosity has not been recognized: for the flow of an ICM around a galaxy the Reynolds number $R = \rho v L/\mu$ is less than 1 ($L \sim 10$ kpc, $v \sim 10^3$ km s^{-1}, $\rho \sim 2 \times 10^{-27}$ g cm^{-3}). In the presence of even a weak magnetic field transport processes across the field are reduced drastically. For a field strength of 10^{-8} gauss, as might typically exist in an ICM, this reduction factor is 10^{-12}. In this case the actual transport rates will be determined by anomalous processes such as turbulence, Bohm diffusion (Hochstim 1969), and magnetic field line reconnection. Unless these modes are extremely efficient, conductivity and viscosity are not likely to be important.

Also ignored here is mass loss from stars. The problem being considered is the removal of a preexisting medium from a galaxy. Until this is accomplished, mass loss from stars will be of only secondary importance.

For convenience many of the commonly used symbols in this paper are defined in Table 1.

III. LOCAL EFFECTS OF SWEEPING

The basic condition for removing the ISM from a disk is that the ram pressure exceed the gravitational restoring force:

$$P_{ram} > 2\pi G \Sigma_* \Sigma_g \qquad (1)$$

where Σ_* and Σ_g are the surface mass densities of stars and gas respectively. Equation (1) approximates the stars and

gas as uniform thin slabs, neither of which is accurate. This section explores some of the consequences of using a more realistic treatment of the stellar and gas distributions. It will be shown that equation (1) still gives the correct criterion for sweeping under most conditions, although other effects can occur at much lower pressures. In what follows it will be assumed that the scale height of the stellar and gas distributions is much smaller than the dimensions of a galaxy, so a one-dimensional approximation is valid.

a) Uniform Medium

The first case to be considered is one in which the stellar and gas distributions are uniform but extended perpendicular to the galactic plane. It will be assumed that the gravitational field is determined by the stars only which form a self-consistent isothermal potential with velocity dispersion σ_*. The gas, which may have a different dispersion, is in hydrostatic equilibrium in this potential.

The solutions for this problem are derived in Appendix A. The distributions are found to be

$$\rho_* = \rho_*(0)\ \mathrm{sech}^2\ (\tfrac{z}{h}) \tag{2}$$

$$\rho_g = \rho_g(0)\ [\mathrm{sech}\ (\tfrac{z}{h})]^{2\beta} \tag{3}$$

where $\beta = \sigma_*^2\ (kT_g/\mu)^{-1}$ and $h = [\sigma_*^2/2\pi G\rho_*(0)]^{1/2}$. In the presence of magnetic fields equation (3) must be modified. If the magnetic pressure is everywhere proportional to the

gas pressure, i.e. $B^2/8\pi = \varepsilon P_g$, then β is replaced by $\beta/(1+\varepsilon)$.

Normally the ISM is distributed symmetrically about the galactic midplane at z = 0. If an external pressure P_{ext} is applied to one side of the disk, the ISM will redistribute itself until the pressure at the interface matches P_{ext} (Fig. 1a). A critical point is reached when the interface reaches z = 0 and the ISM occupies only one half of the disk (Fig. 1b). Designating this pressure as $P_{1/2}$ it can be determined as a function of Σ_*, Σ_g, and β. From Appendix A,

$$P_{1/2} = 2\pi G\, \Sigma_* \Sigma_g \left\{ \frac{\Gamma\,(\beta+\frac{1}{2})}{\pi^{\frac{1}{2}}\Gamma(\beta+1)} \right\} . \qquad (4)$$

When $\beta = 0$ the stars are confined to a thin disk and the quantity in brackets is 1. For large β this quantity is $\simeq 1/(\pi\beta)^{\frac{1}{2}}$. In other words, if the gas temperature is much smaller than the stellar velocity dispersion, the pressure needed to displace the gas to one side of the disk is much smaller than the value given by equation (1), which treats the stars and gas as thin slabs.

The significance of $P_{1/2}$ is as follows. If P_{ext} lies in the range $P_{1/2} < P_{ext} < 2\pi G\Sigma_*\Sigma_g$ the ISM could achieve an equilibrium state as in Figure 1c. However, this state is Rayleigh-Taylor unstable, since a cold, dense material is supported by a hot, rarefied medium in a gravitational field. Any perturbations will quickly grow and cause the ISM to break up. Under these conditions the exact behavior of the

ISM requires a closer look at its detailed properties. The essential point to be made is that a uniform medium can be disrupted at a pressure much lower than that which is required to sweep it.

b) Realistic ISM

The conditions for sweeping become somewhat more complicated when the realistic properties of an interstellar medium are considered. This section explores some of the consequences of the two-phase model of the ISM. The steps involved in the sweeping of an ISM typical of the solar neighborhood are discussed in some detail.

i) ISM Description

The two-phase model (Field et al. 1969, Field 1970) predicts the existence of two discrete components to the ISM: cold clouds at $T \sim 100$ K, $n \sim 10$ cm^{-3}, and a warm, intercloud medium at $T \sim 10^4$ K, $n \sim 0.1$ cm^{-3}. The state of ISM is determined by the requirement that heating and cooling be in equilibrium. For a given pressure (within a wide range) two thermally stable phases are possible, which are identified as the two components of the ISM. Above a pressure P_{max} the intercloud medium becomes unstable and all material is forced into clouds.

More modern viewpoints (McKee and Ostriker 1977, McCray and Snow 1979) picture the ISM as being in a more violent state with supernovae dominating the energetics and dynamics. However, even in these models most of the matter is in clouds

and the intercloud medium, so the following discussion should still be appropriate.

The size distribution of clouds is arbitrary in these models and observationally the situation is uncertain. In fact, 21 cm surveys often have trouble even finding clouds (Heiles 1967, Verschuur 1974b), although other surveys and other lines of evidence, e. g. interstellar absorption line studies, do point to the existence of discrete clouds. The minimum cloud sizes that can be identified are typically 4 $M_\odot$ (Verschuur 1974a), although lower mass structures may exist which are too small to be recognized. The maximum cloud sizes are less well known, and Kwan (1979) has suggested that they may depend strongly on the local mean ISM density. In the inner regions of our galaxy giant molecular clouds of up to 10^6 $M_\odot$ may contain a significant fraction of the ISM (Solomon and Sanders 1979). Typical parameters for the clouds are $M \sim 5 \times 10^5$ $M_\odot$, $n(H_2) \sim 300$ cm^{-3}, $T \sim 10$ K, $R \sim 20$ pc. For the solar neighborhood a cloud mass function $n(m) \sim m^{-2}$ (McKee and Ostriker 1977) with mass limits of 4 - 4000 $M_\odot$ reproduces the mean mass density and the cloud density found by Verschuur (1974a).

ii) The ISM in the solar Neighborhood

Discussions on the nature of the ISM in the solar neighborhood abound in the literature. A recent treatment which closely follows the approach used here is given by Fuchs

and Thielheim (1979). Parameters for the stellar distribution, intercloud medium, and cloud distribution as determined by these authors are given in Table 2, using the notation of this paper. The cloud distribution requires a few words. If clouds were in equilibrium, they would settle to the galactic midplane and form a thin layer. In fact it is observed that they are stirred up (presumably by supernovae) to a velocity dispersion of $\sim$7 km s^{-1}. If clouds are assumed to have a mean density of 16 cm^{-3}, their filling factor in the galactic plane is $\sim$4%.

iii) Ram Pressure Effects

Now consider what happens when an external ram pressure is applied to one side of the galactic plane. Initially, the intercloud medium is displaced as described in section A. However, once the pressure at the galactic midplane reaches P_{max}, the intercloud medium becomes unstable and begins forming new clouds. If P_{ext} rises above P_{max}, no equilibrium state can be achieved, and the intercloud medium will be converted completely into clouds or swept away. For the ISM in the solar neighborhood this pressure ($nT[1+\varepsilon] = 4100$) is a factor 8 less than the value given by equation (1) which is required for sweeping.

Even with the intercloud medium gone, the external ICM is still not free to flow through the galaxy since clouds still present a considerable cross section. For example, using the cloud mass function above, a line of sight in the solar neighborhood through the galactic plane should inter-

sect, on average, about two clouds. A more accurate description might be that the ICM leaks its way between the clouds.

Determing the fate of the clouds is more difficult. Although they are too dense to be swept directly, one might imagine that bits of material could be shredded and removed in a piecemeal fashion. The minimum time scale for this process can be estimated by the requirement that this material be accelerated to the escape velocity. It is easily shown that $t_{min} \simeq \Sigma_g v_e / P_{ext}$. In the solar neighborhood $v_e \simeq 350$ km s^{-1}. Taking $P_{ext} = 6 \times 10^{-13}$ dyne cm^{-2} (for which the intercloud medium is destroyed) yields $t_{min} \simeq 3 \times 10^9$ years. The actual time scale will be much longer, since (a) the ICM is not free flowing and therefore not capable of accelerating as much material, and (b) bits of material will not necessarily shed at the maximum rate with which the ICM is capable of removing them. Most likely this nibbling away is only of marginal importance.

Once the ram pressure approaches $2\pi G \Sigma_* \Sigma_g$, it is capable of sweeping the bulk of the ISM away. This value is $\sim 4.6 \times 10^{-12}$ dyne cm^{-2} for the solar neighborhood. Only the largest clouds with a mean projected density larger than $P_{ext}/2\pi G \Sigma_*$ will survive.

The sizes of clouds at this point are rather uncertain because the ambient pressure is 8 times higher than for an undisturbed ISM. The time scale for cloud formation and destruction is short enough (10^7 - 10^8 years) that the mass spectrum will be altered considerably to some new (unknown) function. Because clouds are generally asymmetric in shape, it is unlikely that they will compress uniformly and become impervious to the

ICM; in fact, any compression is most likely to be one-dimensional, in which case the projected surface density of these clouds or fragments formed from them remains unchanged.

It was assumed that the largest clouds in the solar neighborhood have a mass of $\sim 4000\ M_\odot$. If these clouds were initially spherical with a mean density of 100 cm^{-3}, they would have had a surface density of $\sim 42\ M_\odot\ pc^{-2}$. This value is large enough that such clouds, or fragments formed from them will survive the initial sweep-out.

The behavior of these dense clouds, which resist sweeping, is of some interest. They will rise in the gravitational field of the disk until the ram pressure is balanced by the gravitational restoring force. This problem is elucidated further in Appendix B, where the equilibrium shape and position are derived for a cloud in a free-flowing ICM. The clouds assume a highly flattened shape (see Fig. 2), which lends support to the idea that compression of such clouds will be essentially one-dimensional.

The giant molecular clouds have such high column densities ($\Sigma_c \sim 400 M_\odot\ pc^{-2}$) that enormous ram pressures (much larger than will be encountered in a cluster environment) are needed to sweep them. These clouds are also gravitationally bound and therefore quite difficult to break up or fragment. The only way to sweep them would be if they were to disrupt by internal causes. Whether this can happen is uncertain; Kwan (1979) estimates the lifetime of molecular clouds to be $> 2 \times 10^8$ years.

In view of our uncertainty regarding the behavior of the ISM in the presence of an ICM it is unclear how much material (if any) can ultimately survive once the bulk of the ISM has been removed. Hereafter the most favorable case of no material remaining will be assumed.

c) Accelerations Parallel to the Disk

Up to now only motion perpendicular to the disk has been considered. Accelerations parallel to the disk are somewhat different, since the ISM is supported by rotation rather than pressure. Sweeping parallel to the disk is itself of no importance because of the huge column densities of material in this direction.

If the ram pressure is strong enough to sweep all but the densest clouds from a galaxy, an interesting phenomenon can still occur regarding the remaining clouds. For simplicity consider a galaxy in which the ICM is flowing perpendicular to the disk. Because a cloud is in rotation about the center of a galaxy, the net velocity of the ICM as seen by the cloud is $\vec{v}_f - \vec{v}_\theta$, where $\vec{v}_\theta$ is the rotation velocity. The total ram pressure felt by the cloud is $\rho_f(v_f^2 + v_\theta^2)$, which acts in a direction $(\vec{v}_f - \vec{v}_\theta)/|v|$. In addition to a ram pressure in the z direction, the cloud feels a drag opposing its rotational motion of magnitude $\rho_f v_\theta (v_f^2+v_\theta^2)^{1/2}$, which causes it to spiral in towards the galactic center. The time scale for a cloud to lose an amount of energy equal

to its original kinetic energy is $\sim\bar{\Sigma}_c/2\rho_f(v_f^2+v_\theta^2)^{1/2}$. It can be shown that this analysis is still qualitatively correct for an arbitrary flow direction. As typical values take $\rho_f = 1.7 \times 10^{-27}$ g cm^{-3}, $v_f = 1000$ km s^{-1}, $\bar{\Sigma}_c = 40$ M$_\odot$ pc^{-2}; the time scale for drag to operate is 8×10^8 years. In a rich cluster like Coma the ICM is dense enough that even the giant molecular clouds are capable of being dragged into the centers of galaxies on a time scale comparable to a Hubble time. Note that this mechanism requires the ICM to be essentially free flowing; otherwise a galaxy could "spin up" the local ICM and significantly reduce the drag effect.

IV. SWEEPING FROM A GLOBAL VIEWPOINT

The next step is to examine the efficiency of ram pressure sweeping for a galaxy as a whole. Two questions to be investigated are: (1) what is the nature of the ICM flow around a galaxy, and (2) for a given ram pressure, what fraction of the ISM will be swept? In particular, what ram pressure is needed to completely sweep a galaxy?

a) Flow of ICM around a Galaxy

For the purposes of determining the main features of the ICM flow, a reasonable approximation is to treat a galaxy as a solid disk of some radius r. This radius would represent the outermost point at which the ISM resists sweeping. For simplicity consider the ICM to be flowing along the z axis. This situation is illustrated in Figure 3, where various

details are labeled. On the front surface is a stagnation point with pressure P_s. Away from this point the pressure decreases towards the edge of the disk. At the edge, a detached boundary layer forms and behind the galaxy is a turbulent zone with mean pressure P_z. If the flow is supersonic, a bow shock will form in front.

The stagnation pressure can be calculated from Bernouilli's law plus (for supersonic flow) the shock jump conditions (Landau and Lifschitz 1959):

$$\frac{P_s}{P_f} = \left(1+ \frac{\gamma-1}{2} M^2\right)^{\frac{\gamma}{\gamma-1}} \qquad M < 1$$

$$\frac{P_s}{P_f} = M^2 \left(\frac{\gamma+1}{2} \right)^{\frac{\gamma+1}{\gamma-1}} \left(\gamma - \frac{\gamma-1}{2M^2} \right)^{\frac{1}{\gamma-1}} \qquad M > 1$$

where $M = \mu v_f/\gamma k T_f$ and $\gamma = 5/3$. Writing $P_s = P_f + P_{ram}$, the net ram pressure has the limiting forms

$$P_{ram} \simeq 0.5\ \rho_f\ v_f^2 \qquad M << 1$$

$$P_{ram} \simeq 0.88\ \rho_f v_f^2 \ . \qquad M >> 1$$

It is seen that the ram pressure depends very little on the ICM temperature. For low velocities a measurable contribution to P_{ram} is also made by the potential well of a galaxy.

Away from the stagnation point the pressure is not so easily estimated. Considering the bluff nature of a disk, it is probably not a bad estimate to take this pressure constant

across the entire face. In the turbulent zone P_z is also difficult to estimate. A common approximation is to take it equal to the free flow value P_f, although in practice it is often found to be less. If the z axis is inclined by an angle θ with respect to the ICM flow, the ram pressure will be reduced by an amount $\sim\cos^2\theta$.

As a check on these ideas a numerical calculation was done of the axisymmetric steady state flow around a circular disk using a hydrodynamic code written by S. Gull (1975) and described briefly in Gisler (1976). The case considered was a flow along the z axis for a galaxy and ICM with the following parameters: $r = 5$ kpc, $T_f = 2 \times 10^7$ K, $v_f = 1400$ km s^{-1}, $n_f = 10^{-3}$ cm^{-3}, $M = 2$. Plotted in Figures 4-6 are the resulting pressure contours, velocity field, and x-ray emission from the ICM. A consequence of the ICM compression is that x-ray emission is enhanced, a point which will be returned to in §V. Along the front disk face the pressure falls from a maximum value at the stagnation point to ~75% of this value at the edge. Behind the disk the pressure fluctuates but is about 1/2 the free-flow pressure. It is thus seen that the qualitative picture of flow around a galaxy with a net ram pressure of $\sim\rho_f v_f^2$ across the disk is reproduced.

b) Distribution of Stars and Gas in a Galaxy

Freeman (1970) has shown that the distribution of light in a spiral galaxy can be well represented by an exponential disk plus a spheroidal component. It is the disk which binds

the ISM to a galaxy and controls its dynamics. The spheroidal component seldom dominates the mass distribution and will be ignored here. A massive halo will likewise have little effect on binding the ISM in a disk. Freeman furthermore finds that the central surface brightness of disks is constant at $\mu_B(0) \sim 21.65$ mag arcsec^{-2}, which implies that disks form a one-parameter family of objects with only a variable scale length. Aaronson et al. (1979) also present dynamical evidence that the central mass density of spirals is constant. Assuming $M/L \simeq 10$, the corresponding value of $\Sigma_*(0)$ is 1.5×10^3 $M_\odot$ pc^{-2}, and the surface density has the form $\Sigma_* = \Sigma_*(0) \exp(-r/r_s)$.

The gas distribution in spiral galaxies is not so simple. 21-cm maps of spirals show that the extent of H I relative to the optical disk is correlated with morphological type with later types having more extended disks (Bottinelli 1971). In some galaxies, e.g., M31 (Roberts 1975) there is a deficiency of H I in the center, while in others, e.g. M33 (Huchtmeier 1978) little or no such deficiency is seen. In addition, the distribution is not smooth but concentrated in spiral arms, as for M101 (Allen et al. 1973). Molecular H_2 may also form a substantial fraction of the ISM in regions where arms are prominent, as in our own galaxy (Solomon and Sanders 1979). Bottinelli (1971) suggests that the mean H I surface density is constant among galaxies and only the relative size of the H I disk varies. To approximate these results it will be assumed that the H I distribution is again an exponential disk of constant central surface density but with a second

scale length r_H. Within a radius which contains half the H I mass Bottinelli finds a mean surface density of 1.3×10^{-3} g cm^{-2}. For an exponential disk the corresponding central surface density becomes $\Sigma_g(0) = 3.8 \times 10^{-3}$ g cm^{-2}. For an average galaxy $M(HI)/M_T \sim 5\%$ (Roberts 1975), which for the distributions here requires $r_H/r_s = 2$.

c) Efficiency of Sweeping

The portion of a galaxy which can be swept for a given ram pressure is now readily calculated. Sweeping will be complete beyond a radius at which $P_{ram} > 2\pi G \Sigma_* \Sigma_g$. This function is plotted in Figure 7 for the typical stellar and gas distributions adopted here. It is evident that the ram pressure required to sweep beyond a given radius is a strong function of that radius. The inner regions of a galaxy are considerably more difficult to sweep than the outer regions. If gas distributions actually decline in the centers of galaxies, the ram pressure required to sweep these central regions is probably less than indicated here. However, it is clear that ram pressures on the order of $1\text{-}5 \times 10^{-10}$ dyne cm^{-2} are required for sweeping to be complete.

V. SOME OBSERVATIONAL PREDICTIONS OF SWEEPING THEORY

A comparison of predictions with observations is somewhat difficult to make since to date no case of a galaxy being swept has been unequivocally established, although a number of candidates have been proposed. This section examines some consequences of sweeping with regard to the properties of individual galaxies; a discussion on the formation of S0's is deferred to §VI.

a) Hydrogen Content

Galaxies which have been partially swept should exhibit a deficiency in H I content relative to undisturbed galaxies. In particular the extensive H I envelope of late type galaxies should be easily removed. Evidence for an H I deficiency in cluster spirals has been presented by Davies and Lewis (1973) and Krumm and Salpeter (1979) for galaxies in the Virgo cluster and by Sullivan and Johnson (1978) for galaxies in A1367 and the Coma cluster.

b) Optical Appearance

Wilkerson et al. (1977) and Strom and Strom (1978) have pointed out the existence of galaxies in clusters which have spiral patterns apparently formed by the stellar distribution alone without the usual population I tracers such as H II regions or young stars. They suggest that these "smooth-armed" spirals have been recently swept and that the remnant spiral pattern will eventually fade away leaving behind a smooth

disk characteristic of an S0 galaxy.

Even if the ram pressure is not high enough to sweep a galaxy clean a second effect may still alter its optical appearance. If the pressure is high enough to destroy the intercloud medium, the galaxy will be permeated by the hot ICM. In this case star formation normally instigated by shock compression of clouds crossing spiral arms should be suppressed since the ICM is essentially incompressible. This is also an argument against our own galaxy being pervaded with a hot (10^6 K) medium left behind from supernova remnants (Shu 1978). A galaxy which might be in such a state is NGC4921 in the Coma cluster.

Finally it has been noted that the drag on large clouds which resist sweeping is capable of pulling them into the center of a galaxy. Such galaxies may have active nucleii but otherwise barren disks. Several galaxies are found in the Coma cluster (e. g. Zw 160-73, 160-76, 160-106, and IC4040) which have just such characteristics. They are low surface brightness, anemic objects but with very blue, strong emission line nuclei indicating the presence of active star formation in the central regions of these galaxies.

c) Shock Spectra

A feature of the ram pressure effect is that a large pressure differential can exist across the disk of a galaxy. Under various conditions this pressure differential might drive shock waves into the ISM. If these shocks are strong

enough ($v_s \sim 100$ km s^{-1}) they could be detected spectroscopically from the characteristic shock emission line spectrum. A possible candidate for such activity is NGC4438 in the Virgo cluster which John Stauffer (private communication) has shown exhibits a very characteristic shock type spectrum. This galaxy is also quite distorted,although the presence of a nearby companion complicates any interpretation.

d) X-Ray Emission

It was pointed out in §IV that a consequence of the compression of the ICM as it flows around a galaxy is that the x-ray emission will be enhanced. This enhancement is not large, but the Einstein Observatory is capable of detecting such galaxies and has, in fact, found several in the Virgo cluster (Forman et al. 1979). The luminosity enhancement can be found from the hydrodynamic model in §IV. For the 0.5-3.0 kv band of the Einstein detectors the flux was calculated to be 2.2×10^{40} erg s^{-1}. The actual x-ray luminosities of the Virgo spirals as measured by Forman et al. (1979) range from 0.25 to 1.7×10^{40} erg s^{-1}, so compression of the ICM is quite capable of producing the required emission provided a galaxy presents a cross-section to the ICM comparable to its optical size.

VI. THE FATE OF SPIRALS IN A CLUSTER ENVIRONMENT

The problem to be investigated in this section is whether or not the ram pressure encountered by spiral galaxies in a cluster is high enough to sweep them and thus presumably form the S0's found in clusters. The approach taken here is to construct a simple model for sweeping which involves making a dynamical model for clusters filled with an ICM and then assuming that all spirals which encounter a ram pressure greater than a certain critical value are swept to form S0's. A recent paper by Himmes and Biermann (1979, hereafter HB) presents a similar although more detailed computation. The primary observations on the population distribution of galaxies in clusters which will be considered here are taken from Oemler (1974), Melnick and Sargent (1977), and Dressler (1980).

a) Preliminary Discussion

The morphological population fractions E/S0/Sp are observed to range from 11/45/75 for field galaxies (Tammann et al. 1979) to 33/45/22 for the richest clusters like Coma (Oemler 1974). One important point which is often ignored can be made immediately from these data: the sweeping of spirals to make S0's is alone not enough to reproduce the morphological populations in clusters. The reason is simply that ellipticals are three times as numerous in rich clusters as the field whereas the sweeping of spirals should have no

effect on this fraction.

At least three possibilities may be offered to explain this effect. The first is that for some reason ellipticals are formed preferentially in the dense central regions of clusters (Gott and Thuan 1976). However if one were to assume this then for consistency one must also admit to the possibility that S0's will also form preferentially,in which case the justification for sweeping theory is weakened. The second possibility is that mergers between galaxies in dense regions can form new elliptical systems from old disks (Toomre 1977), although the viability of this mechanism is disputed by some (Ostriker 1977). The final possibility is that some disk galaxies are destroyed at some stage during the evolution of a cluster, raising the relative number of ellipticals. This is not so unlikely in view of current beliefs that disks have relatively long formation times (Gott and Thuan 1976). As a variant on this idea HB picture some spirals as being swept at a time when most of their mass is still in a gaseous state. These galaxies become gravitationally unbound and are dispersed. For lack of a better alternative it will be assumed that this last possibility is correct.

The model presented here does not follow the time evolution of galaxies but only considers the effects of sweeping on a population with properties characteristic of present day galaxies. It is unable to reproduce the

destruction of galaxies at early times but should correctly determine which galaxies remain unswept, since as time progresses the gas content of galaxies declines through normal star formation activity and hence the efficiency of sweeping increases. Thus this model should correctly reproduce the spiral/elliptical ratios in clusters (provided the elliptical population is not being enhanced); the S0 population depends on the number of galaxies that are destroyed.

One final point which must be addressed is at what ram pressure will sweeping make a spiral look like an S0. Determining a reliable value from the model galaxy calculations in §IV is difficult because of the uncertainties in these models. Instead the problem will be inverted to ask what critical value of ram pressure (P_{crit}) is required to produce the observed populations in clusters and then check to see if this value is reasonable.

b) Model Description

The cluster distribution and dynamics are assumed to be represented by one of a family of models computed by King (1966). The application of this type of model to a cluster of galaxies is clearly debatable, although Rood et al. (1972) have shown that at least for the Coma cluster such a model does reproduce the observed profiles in luminosity and velocity dispersion. Nominal parameter values are taken to be r_c = 200 kpc, r_t = 10 Mpc, and σ_v = 1000 km s^{-1}. The first two values are appropriate for the Coma cluster although r_t has

been taken to be a more modest value. The corresponding central mass density is $\rho_v = 2.8 \times 10^{-25}$ g cm^{-3}. Bahcall (1975) has shown that rich clusters often have similar core radii and luminosity profiles.

The most detailed x-ray studies of the ICM in clusters have been done by Gorenstein et al. (1978, 1979) for the Perseus and Coma clusters. It is found for both clusters that the x-ray emission is more extended than the galaxy distribution. If the ICM is in hydrostatic equilibrium with the cluster potential then this implies that the parameter $\beta = \sigma^2(kT_f/\mu)^{-1}$ is ~ 0.5 or $T_f = 10^8$ K. The central density is taken to have a typical value $n_f = 5 \times 10^{-3}$ cm^{-3} (Bahcall and Sarazin 1977).

The time scale for sweeping a galaxy is short compared with the orbital time scale through a cluster so the efficiency of sweeping is determined only by the maximum ram pressure experienced along an orbit.

At a given radius r from the cluster center galaxies have a velocity distribution given by

$$f(v,J)\,dv\,dJ \propto \frac{8\pi v J}{r^2(v^2 - J^2/r^2)^{1/2}}\{\exp[-(\tfrac{1}{2}v^2+\phi(r))/\sigma_v^2] - 1\}\,dv\,dJ$$

where v is the velocity, J is the angular momentum, and $\phi(r)$ is the "depressed" potential defined such that $\phi=0$ at $r=r_t$. For a given value of v and J, the maximum ram pressure along such an orbit can be calculated. 20 steps each in v and J

were used to determine a new distribution of galaxies as a function of ram pressure. This procedure was repeated at a total of 41 radii from the cluster center. Finally these distributions were projected onto the plane of the sky.

The initial population is taken to be a typical field distribution E/S0/Sp of 11/14/75 which yields an initial ratio Sp/E of 6.8 .

c) Results

As mentioned above this model should only provide a good representation of the spiral/elliptical ratio and only this quantity is considered.

i) Sp/E Distribution

This function is presented in two ways. In Figure 8 the cumulative [Sp/E] ratio relative to the initial ratio for field galaxies within a given radius is plotted. The same results are shown in Figure 9 where the differential [Sp/E] ratio is plotted as a function of projected density; this is the format in which Dressler (1980) plots his data. The origin for this plot has been arbitrarily offset so that log ρ_{proj} = 2.0 at the cluster center. In each figure five curves are drawn corresponding to different values for the critical pressure at which sweeping is assumed to occur.

ii) [Sp/E] Versus X-Ray Luminosity

The global [Sp/E] ratio as a function of x-ray luminosity is plotted in Figure 10. Here it is assumed that $L_x \propto \rho_f^2$, ρ_f/ρ_v = constant, and that the [Sp/E] ratio scales with

mass density ρ_v as described in the next section.

iii) Scaling Relations

The curves in Figures 8 and 9 can be scaled to other cluster parameters by noting that $P_{ram} \propto \rho_f \sigma_v^2$ and $\sigma_v^2 \propto \rho_v r_c^2$. For example, if $\rho_v \rightarrow \alpha\rho_v$, $\rho_f \rightarrow \alpha\rho_f$, then $P_{ram} \rightarrow \alpha^2 P_{ram}$. Note also that in Figure 9 the origin of log ρ_{proj} needs to be shifted according to the relation $\rho_{proj} \propto \rho_v r_c$.

The effect of changes in r_t/r_c and β cannot be determined by scaling but must be calculated individually. As an example, in Figure 11 the differential [Sp/E] ratio is again plotted showing the effects on curve 3 from Figure 8 of changing a) r_t/r_c from 50 to 158; b) β from 0.5 to 1.0 . As can be seen, increasing the concentration of a cluster steepens the gradient of [Sp/E] with radius while increasing β raises the overall [Sp/E] ratio without changing the gradient appreciably.

d) Comparison With Observations

i) Determination of P_{crit} from [Sp/E]

In Table 3 eight clusters are listed for which information exists on the morphological content, velocity dispersion, and x-ray emission. The quantities listed are: 1) Abell number; 2) [Sp/E] ratio relative to the field; 3) radius at which this ratio is measured assuming r_c = 250 kpc for all clusters; 4) velocity dispersion; 5) central ICM density ρ_f; 6) x-ray luminosity; 7) derived value of P_{crit}. The quantity ρ_f is taken from self-consistent isothermal sphere models for x-ray emission for those clusters where the x-ray core radius has

been measured, or scaled from the Coma cluster value assuming $\rho_f^2 \propto L_x$. Although one should more correctly use a hydrostatic model in computing these densities in practice similar results are obtained.

The value of P_{crit} is derived by taking the observed [Sp/E] ratio, finding the requisite value of P_{ram} from Figure 8, and scaling according to the observed values of σ^2 and ρ_f. There is a rather large scatter in these values of P_{crit}, part of which is undoubtedly due to uncertainties in many of the parameters used. For use later a nominal value for P_{crit} of 4×10^{-12} dyne cm^{-2} will be taken.

ii) Population Gradients

Dressler (1980) has measured the differential population gradients in 55 clusters and finds an excellent correlation between population and projected density of galaxies which is obeyed by all clusters. This relation represents a combination of gradients within a cluster and population differences between clusters. In Figure 12 his observed relation for [Sp/E] is plotted along with two curves from Figure 11 corresponding to $r_t/r_c = 50$ and 158. An arbitrary offset in log ρ_{proj} has been applied to the computed curves. It is seen that the general trend is reproduced although detailed agreement is perhaps not so good. Also the high concentration model provides a somewhat better fit. In Figure 13 curves from a series of models in which ρ_v has been varied are plotted; P_{ram} and ρ_{proj} have been scaled accordingly. In order for these curves to form a single continuous relation it is

necessary to assume that the ICM density ρ_f be constant for all clusters. When this is done it is seen that the observed curve in Figure 12 would again be reasonably well reproduced. To summarize, the observed population gradients, both within and between clusters,are reproduced by the sweeping model provided ρ_f is constant among all clusters.

iii) Correlation with X-Ray Luminosity

Data from Table 3 for [Sp/E] and the x-ray luminosity are plotted with the predicted relation in Figure 10. An arbitrary shift in the computed L_x has been made to match the Coma cluster point. Agreement is quite reasonable. The relation suggested by Bahcall (1977b) of $L_x \propto \rho^{2.8}$ would be less acceptable.

e) Discussion - Difficulties with Sweeping

In spite of the apparent success of the sweeping model a closer look reveals several severe problems.

The major difficulty is that the derived value for P_{crit} of 4×10^{-12} dyne cm^{-2} is extremely low. It was shown from the model galaxy calculations in §IV that a value of $1\text{-}5 \times 10^{-10}$ dyne cm^{-2} is needed to sweep the interior regions of a spiral, i. e. a factor 25-100 times higher. A ram pressure of 4×10^{-12}, while capable of disrupting the outer H I envelope of a galaxy, should have no effect on the gas-rich spiral arm regions. If galaxies actually are swept at this low value of P_{crit}, then the simple picture by which a galaxy is swept must be completely erroneous.

A second problem is that if the population gradients for clusters form a continuous relation as suggested by Dressler's data, then it is necessary to assume that the ICM density is the same for all clusters. If instead the more reasonable assumption is made that ρ_f/ρ_v is constant, then the population changes between clusters will be a more rapid function of ρ_{proj} than is observed. As shown in Table 3, ρ_f is clearly not constant among clusters but can vary by an order of magnitude. The seriousness of this contradiction is lessened if the overlap between clusters does not have to be as strong as suggested.

Two additional problems present difficulties not only for sweeping theory but for any mechanism which converts spirals into S0's. The first is the well-known fact that S0's both in and out of clusters have bulge to disk ratios that are much larger than for spiral galaxies (Sandage and Visvanathan 1978, Dressler 1980). Swept spirals should have small bulges and low surface brightness disks, which are not the characteristics of cluster S0's. Models for "puffing up" disks by tidal interactions (Marchant and Shapiro 1977) or violent relaxation following rapid mass loss (Biermann and Shapiro 1979) are most likely of dubious importance.

A final problem has been pointed out by Dressler (1980) who notes that many irregular cluster contain large populations of S0's. If, as Dressler suggests, these clusters are still collapsing, then ram pressure effects will not yet have developed and sweeping could not possibly have produced these S0's.

f) Comparison with Other Calculations

In view of the discrepancy regarding the efficiency of sweeping between this paper and other authors, it is of some importance to compare these results. Two quantitative calculations comparable to those here have been published by HB and Bahcall (1977b).

HB have made a far more detailed model for sweeping than here, following the time evolution of galaxies and the growth of the ICM in a cluster. A model was run here with parameters corresponding to those used by HB. It was found that their results for the spiral and elliptical distributions could be reproduced quite well if their value for P_{crit} is taken to be $\sim 1.2 \times 10^{-10}$ dyne cm^{-2}. In spite of this high value of P_{crit} these authors claim to be able to reproduce the population gradients in the clusters studied by Melnick and Sargent (1977). The discrepancy between their conclusions and those here is due to a number of differences regarding initial assumptions. In particular, 1) they assume an initial field population of E/S0/Sp of 17/25/58 which requires less sweeping to reproduce the cluster population than the initial distribution used here; 2) they use a more extended ICM distribution and lower concentration parameter for cluster model than here, both factors being more favorable toward sweeping; 3) for cases where they make specific comparisons between their models and actual clusters, the velocity dispersions (although not stated by the authors) are in general a factor of 2 higher than are actually measured; 4) they take a higher central ICM density than here.

All these factors work in the same direction to increase the apparent efficiency of sweeping.

Bahcall (1977b) constructed a simple model for sweeping in order to compute the global spiral fraction in clusters. She assumed that all swept spirals become S0's and hence ignored the problem alluded to earlier regarding the rising fraction of ellipticals in clusters. She finds a value for P_{crit} which is 40% of the value given by Gunn and Gott (1972) or 10^{-11} dyne cm^{-2}. If the results in Figure 8 are interpreted as representing the ratio [Sp/Sp+S0+E] then a new value of P_{crit} can be determined for all the clusters in Table 3. Doing so yields $P_{crit} \sim 1.4 \times 10^{-11}$ dyne cm^{-2} which agrees with that of Bahcall. Again, however, this value is more than an order of magnitude less than that derived in §IV.

g) Alternatives to Sweeping

If sweeping is not responsible for the formation of S0's, then one might ask 1) what is responsible; 2) why do morphological populations correlate so well with the predictions of sweeping; and 3) what influence will the ICM have on galaxies in a cluster.

Sweeping is only one of many hypotheses which have been advanced to account for the enhanced formation of S0's and ellipticals in clusters. Some argue for the conversion of spirals by other environmental causes (Spitzer and Baade 1951, Cowie and Songaila 1977) while others focus on factors which can influence galaxies at the time of their formation (Gott

and Thuan 1976, Larson and Tinsley 1978, Larson, Tinsley, and Caldwell 1979, Kent 1979).

A common factor in these ideas is that the main influence in a cluster which affects the morphology of galaxies is density and hence any other property of a cluster which depends on density will also correlate with morphology. Furthermore, some of these hypotheses suggest that formation of large numbers of S0's will result in leaving behind considerable debris which will contribute to any ICM. Thus any correlation between morphology and x-ray luminosity or other properties of a cluster, while real, may be of little causal significance but merely a reflection of a common correlation with density.

While ram pressures encountered in clusters may not be powerful enough to transform spirals to S0's they should nevertheless be quite effective at removing the less tightly bound gas from a system and injecting it into the surrounding ICM. Iron-line x-ray observations of clusters (Mitchell et al. 1976, Serlemitsos et al. 1977) suggest that a large fraction, if not all, of the ICM has been processed through galaxies. Finally the high thermal pressure of the ICM alone should be effective at altering the visible appearance of a galaxy and may be responsible for the "anemic" state of many cluster spirals.

VII. CONCLUSIONS

This paper has explored in some detail the numerous ramifications of ram pressure sweeping on the fate of gas in spiral

galaxies. The essential points which have been made can be summarized as follows:

1. The ISM in a galaxy is capable of being disrupted by an external medium at a pressure which is much lower than that needed for sweeping.

2. The response of a galaxy to an applied external pressure can take one of three forms. At low pressures the ISM is merely displaced in the disk. As the pressure rises the intercloud medium is destroyed but clouds are still dense enough to resist sweeping. When the pressure exceeds a critical value all but the densest clouds are swept away.

3. Very dense clouds, particularly giant molecular clouds, will never be swept unless they are first broken up. Nevertheless they will still feel a drag which can pull them into the center of a galaxy on a Hubble time scale.

4. The ram pressure required to sweep a given region of a galaxy is a strong function of radius. The inner regions require pressures in excess of 10^{-10} dyne cm^{-2} while the outer regions can be swept at pressures more than an order of magnitude lower.

5. Several predictions have been made regarding the optical appearance, H I properties, and x-ray emission from individual galaxies.

6) Models for the sweeping of spirals in clusters to form S0's can qualitatively reproduce many of the observed properties of galaxies in clusters but they require that sweeping occur at ram pressures a factor of 25-100 less than those

estimated from the model galaxy calculations. Other lines of evidence also cast doubt on the feasibility of forming S0's from spirals by sweeping.

It is a pleasure to thank Alan Dressler, Jim Gunn, Wal Sargent, and John Stauffer for many stimulating conversations. I am indebted to Steve Gull for providing a copy of his hydrodynamics code.

APPENDIX A.

DISTRIBUTION OF STARS AND GAS OF UNIFORM BUT UNEQUAL TEMPERATURE IN ONE DIMENSION

a) Stellar Distribution

The distribution of stars with velocity dispersion σ_* in a potential ϕ is determined by solving the equation of hydrostatic equilibrium:

$$\frac{d\rho_*}{dz} = -\frac{\rho_*}{\sigma_*^2}\frac{d\phi}{dz} \quad . \tag{A1}$$

If the potential is generated by the stars themselves ϕ is determined by solving the Poisson equation:

$$\frac{d^2\phi}{dz^2} = 4\pi G\rho_* \quad . \tag{A2}$$

Letting $g = d\phi/dz$, (A1) and (A2) are easily integrated to yield:

$$g = g_o \tanh\left(\frac{z}{h}\right) \tag{A3}$$

$$\rho_* = \rho_*(0)\,\mathrm{sech}^2\left(\frac{z}{h}\right) \tag{A4}$$

$$\left.\begin{aligned} \text{where} \quad g_o &= [8\pi G\rho_*(0)]^{1/2} \\ \text{and} \quad h &= \left(\frac{\sigma_*^2}{2\pi G\rho_*(0)}\right)^{1/2} \quad . \end{aligned}\right\} \tag{A5}$$

For disk galaxies one normally specifies the surface density of stars $\Sigma_* = 2\rho_*(0)h$, in which case $g_o = 2\pi G\Sigma_*$. Note

that of the variables $\rho_*(0)$, σ_*, g_o, h, and Σ_* only 2 are independent.

b) Gas Distribution

This is again determined by the equation of hydrostatic equilibrium:

$$\frac{dP_g}{dz} = -g\rho_g \quad . \tag{A6}$$

For an isothermal medium $P_g = \rho_g kT/\mu = \rho_g \sigma_g^2$. So

$$\frac{d\rho_g}{dz} = -\frac{\rho_g}{\sigma_g^2} g \quad .$$

Substituting (A3) for g and using the relations (A5) yields:

$$\rho_g = \rho_g(0) [\mathrm{sech}(\frac{z}{h})]^{2\beta} \tag{A7}$$

where $\beta = \sigma_*^2/\sigma_g^2$. When $\beta = 1$ the stars and gas have the same distribution.

c) External Pressure Applied

When a pressure $P_{1/2}$ is applied to one side of the galaxy, the ISM is displaced to one side of the galactic midplane subject to the constraint that the surface density of gas remain constant. The value of $P_{1/2}$ is determined as follows. The surface density is given by

$$\Sigma_g = \int_0^\infty \rho_g dz = \rho_g(0) \int_0^\infty [\mathrm{sech}(\frac{z}{h})]^{2\beta} dz$$

Letting $x = z/h$ and using the facts that $\rho_g(0) = (P_{1/2})/\sigma_g^2$ and $h = 2\sigma_*^2/g_o$ gives

$$\Sigma_g = \frac{P_{1/2}}{g_o} \times 2\beta \int_0^\infty (\text{sech } x)^{2\beta} dx$$

This integral is evaluated by using the substitution $u = \text{sech}^2 x$:

$$\int_0^\infty (\text{sech } x)^{2\beta} dx = \frac{1}{2}\int_0^1 u^{\beta-1}(1-u)^{-1/2} du$$

$$= \frac{\Gamma(\beta)\Gamma(\frac{1}{2})}{2\Gamma(\beta+\frac{1}{2})}$$

(Abramowitz and Stegun 1964). And therefore

$$P_{1/2} = 2\pi G \Sigma_* \Sigma_g \frac{\Gamma(\beta+\frac{1}{2})}{\pi^{1/2}\Gamma(\beta+1)} . \qquad \text{(A8)}$$

APPENDIX B.

CLOUD SUPPORTED BY A WIND IN A GRAVITATIONAL FIELD

A cloud which is dense enough to resist sweeping will rise above the galactic plane until gravitational forces balance the ram pressure. The treatment given here for the flow past a cloud closely follows that by Batchelor (1970) for the similar problem of bubbles rising through a dense fluid.

The cloud will form itself into a flattened shape perpendicular to the ICM flow (Figure 2). In the case of highly subsonic flow an approximate solution is possible.

A stagnation point with pressure P_s is formed on the front face of the cloud. By Bernouilli's law the pressure at any other point on the face is given by

$$P = P_s - \frac{1}{2}\rho_f v^2 - \rho_f g z \qquad \text{(B1)}$$

where g is the gravitational acceleration. This must be balanced by the hydrostatic pressure within the cloud:

$$P = P_s e^{-z/h} \sim P_s(1-\frac{z}{h}) \qquad \text{(B2)}$$

where $h = kT_c/\mu g$ is the isothermal scale height. The key step is to treat the front face of the cloud as if it were part of a sphere of radius R. In this case it can be shown that the velocity v is given by

$$v = \frac{3}{2} v_f \sin\theta \quad . \qquad \text{(B3)}$$

Noting that $kT_c/\mu g = P_s/\rho_c g$ and $z = R(1-\cos\theta)$, (B1), (B2), and (B3) can be combined to yield

$$\frac{1}{2}\rho_f v_f^2 \left(\frac{3}{2}\sin\theta\right)^2 = (\rho_c-\rho_f)gR(1-\cos\theta) \quad .$$

Expanding for small values of θ and ignoring ρ_f compared with ρ_c finally gives

$$R = \frac{\left(\frac{3}{2}v_f\right)^2\rho_f}{g\rho_c} \quad . \tag{B4}$$

The maximum angle θ_o is determined by the requirement that the velocity at the edge of the cloud be $\sim$ the free-flow velocity (actually it will be somewhat greater) which occurs at $\sin\theta = 2/3$ or $\theta \sim 42^o$. The mass contained in a cloud is

$$M_c = \frac{\pi R^3}{3}\rho_c[2-(\cos\theta_o)(\sin^2\theta_o+2)] = .19\rho_c R^3 \quad , \tag{B5}$$

and the mean surface density is

$$\bar{\Sigma}_c = \frac{M_c}{\pi R^2 \sin^2\theta_o} = .14\rho_c R \quad . \tag{B6}$$

Depending on whether mass or surface density is specified a cloud will rise until it feels a gravitational force

$$g = 1.3\rho_f v_f^2 M_c^{-1/3}\rho_c^{-2/3} = \frac{.32\rho_f v_f^2}{\bar{\Sigma}_c} \quad . \tag{B7}$$

For the cloud described in §III<u>b</u> typical numbers are $\rho_f v_f^2 = 2.3 \times 10^{-12}$ dyne cm^{-2}, $\bar{\Sigma}_c = 40\ M_\odot$ pc^{-2}. Then such a cloud rises until it feels an acceleration $g = 3.4 \times 10^{-10}$ cm s^{-2} which occurs at 20 pc above the galactic plane.

In the case of supersonic flow the details will change, but (B7) should still be qualitatively correct.

The stability of this configuration is questionable. The cloud is subject to the usual Rayleigh-Taylor and Kelvin-Helmholtz instabilities (Blake 1972) as well as the neglected thermal conduction. It is possible that the cloud will be broken up into fragments which individually are capable of being swept.

TABLE 1

COMMONLY USED SYMBOLS

ρ_*, Σ_*, σ_*	Volume density, surface density, velocity dispersion of stars
ρ_g, Σ_g, T_g	Volume density, surface density, temperature for interstellar gas in general
ρ_c, Σ_c, T_c	Same for interstellar clouds
ρ_f, T_f, P_f, v_f	Density, temperature, pressure, and velocity of undisturbed ICM
ϕ	Gravitational potential
g	Gravitational acceleration
β	$= \sigma_*^2 (kT_g/\mu)^{-1}$
P_{ext}	External pressure applied to ISM
$P_{1/2}$	Value of P_{ext} needed to displace ISM to one side of galactic midplane.
P_s	Stagnation pressure
P_{crit}	Critical ram pressure needed to completely sweep ISM from a galaxy
r_s	Scale length for stellar exponential disk
r_H	Same for gaseous disk
r_c, r_t	Core and tidal radii for a cluster
ρ_v	Virial mass density in a cluster
σ_v	Cluster velocity dispersion
ρ_{proj}	Projected density of galaxies

TABLE 2

INTERSTELLAR MEDIUM AND STELLAR PARAMETERS

FOR SOLAR NEIGHBORHOOD

	Stars
$\rho_*(0)$	$= 0.10\ M_\odot\ pc^{-3}$
σ_*	$= 8.3\ km\ s^{-1}$
h	$= 175\ pc$
Σ_*	$= 35\ M_\odot\ pc^{-2}$
g_0	$= 3 \times 10^{-9}\ cm\ s^{-2}$
	Intercloud Medium
$\rho_g(0)$	$= 0.16\ cm^{-3}$
σ_g	$= 9\ km\ s^{-1}$
T_g	$= 10^4\ K$
B	$= 2.9 \times 10^{-6}$ gauss
ε	$= 1.56$
Σ_g	$= 2.9\ M_\odot\ pc^{-2}$
β	$= 0.33$
	Clouds
$\overline{\rho_g(0)}$	$= 0.57\ cm^{-3}$
σ_{turb}	$= 7.1\ km\ s^{-1}$
Σ_g	$= 4\ M_\odot\ pc^{-2}$

TABLE 3

X-RAY CLUSTERS FOR DETERMINATION OF P_{crit}

Abell # (1)	[Sp/E] (2)	r/r_c (3)	σ_v (km s^{-1}) (4)	ρ_f (10^{-3} cm^{-3}) (5)	L_x(2-10 kv) (10^{44} erg s^{-1}) (6)	P_{crit}(10^{-12} dyne cm^{-2}) (7)
262	0.40[a]	4	439[c]	0.6[e]	0.4[i]	2.7
426	0.02[a]	13	1396[c]	4.3[f]	12.4[i]	1.8
576	0.30[a]	18	1080[a]	2.0[e]	4.9[j]	16.
1060	0.81[a]	5	771[c]	0.4[e]	0.2[k]	20.
1367	0.37[b]	13	847[c]	1.0[g]	0.5[i]	9.1
1656	0.07[b]	15	900[c]	2.5[f]	7.6[i]	1.6
2199	0.10[b]	14	843[c]	1.2[e]	1.8[i]	1.0
Virgo	0.42[a]	16	700[d]	0.6[h]	0.3[i]	4.1

Notes to Table 3:
a) Melnick and Sargent (1977)
b) Oemler (1974)
c) Faber and Dressler (1976)
d) Sandage and Tammann (1976)
e) Scaled from Coma and L_x
f) Bahcall and Sarazin (1977)
g) Scaled from L_x and r_x (Jones et al. 1979)
h) Forman et al.^{x}(1979)^x
i) Mushotzky et al. (1978)
j) Bahcall (1977a)
k) Forman et al. (1978)

REFERENCES

Aaronson, M., Huchra, J., and Mould, J. 1979, Ap. J., 229, 1.

Abramowitz, M., and Stegun, I. 1964, Handbook of Mathematical Functions (Washington: Government Printing Office), p. 258.

Allen, R.J., Gross, W.M., and van Voerden, H. 1973, Astr. Ap., 29, 447.

Bahcall, J.N., and Sarazin, C.L. 1977, Ap. J. (Letters), 213, L99.

Bahcall, N. A. 1975, Ap. J., 198, 249.

_____ 1977a, Ap. J. (Letters), 217, L77.

_____ 1977b, Ap. J. (Letters), 218, L93.

Batchelor, G.K. 1970, An Introduction to Fluid Dynamics (Cambridge: Cambridge University Press).

Biermann, P., and Shapiro, S.L. 1979, Ap. J. (Letters), 230, L33.

Blake, G.M. 1972, M.N.R.A.S., 156, 67.

Bottinelli, L. 1971, Astr. Ap., 10, 437.

Butcher, H., and Oemler, A. 1978, Ap. J., 226, 559.

Cowie, L.L., and McKee, C.F. 1977, Ap. J., 211, 135.

Cowie, L.L., and Songaila, A. 1977, Nature, 266, 501.

Davies, R.D., and Lewis, B.M. 1973, M.N.R.A.S., 165, 231.

Dressler, A. 1980, Ap. J., in press.

Faber, S.M., and Dressler, A. 1976, Ap. J. (Letters), 210, L65.

Field, G.B., Goldsmith, D.W., and Habing, H.J. 1969, Ap. J., 158, 173.

Field, G.B. 1970, in I.A.U. Symposium No. 39, Interstellar Gas Dynamics, ed. H. J. Habing (Dordrecht: D. Reidel), p. 51.

Forman, W., Jones, C., Cominsky, L., Julien, P., Murray, S., Peters, G., Tannabaum, H., and Giacconi, R. 1978, Ap. J. (Suppl.), 38, 357.

Forman, W., Schwarz, J., Jones, C., Liller, W., and Fabian, A.C. 1979, Ap. J. (Letters), submitted.

Freeman, K.C. 1970, Ap. J., 160, 811.

Fuchs, B., and Thielheim, K.O. 1979, Ap. J., 227, 801.

Gisler, G.R. 1976, Astr. Ap., 51, 137.

Gisler, G.R. 1979, Ap. J., 228, 385.

Gorenstein, P., Fabricant, D., Topka, K., Harnden, F.R., and Tucker, W.H. 1978, Ap. J., 224, 718.

Gorenstein, P., Fabricant, D., Topka, K., and Harnden, F.R. 1979, Ap. J., 230, 26.

Gott, J.R., and Thuan, T.X. 1976, Ap. J., 204, 649.

Gull, S. 1975, Ph. D. Thesis, University of Cambridge.

Gunn, J.E., and Gott, J.R. 1972, Ap. J., 176, 1.

Heiles, C. 1967, Ap. J. (Suppl.), 15, 97.

Himmes, A., and Biermann, P. (HB) 1979, preprint.

Hochstim, A.R. 1969, Kinetic Processes in Gases and Plasmas (New York: Academic Press), p. 199.

Huchtmeier, W.K. 1978, in I.A.U. Symposium No. 77, Structure and Properties of Nearby Galaxies, ed. E.M. Berkhuijsen, and R. Wielebinski (Dordrecht: D. Reidel), p. 197.

Jones, C., Mandel, E., Schwarz, J., Forman, W., Murray, S.S., and Harnden, F. 1979, Ap. J. (Letters), submitted.

Kent, S.M., preprint.

King, I.R. 1966, A. J., 71, 64.

Krumm, N., and Salpeter, E.E. 1979, Ap. J., 227, 776.

Kwan, J. 1979, Ap. J., 229, 567.

Landau, L.D., and Lifschitz, E.M. 1959, Fluid Mechanics (Oxford: Pergamon Press), p. 458.

Larson, R.B., and Tinsley, B.M. 1978, M.N.R.A.S., 186, 503.

Larson, R.B., Tinsley, B.M., and Caldwell, C.N. 1979, preprint.

Lea, S.M., and De Young, D.S. 1976, Ap. J., 210, 647.

Marchant, A.B., and Shapiro, S.L. 1977, Ap. J., 215, 1.

McCray, R., and Snow, T.P. 1979, Ann. Rev. Astr. Ap., 17, 213.

McKee, C.F., and Ostriker, J.P. 1977, Ap. J., 218, 148.

Melnick, J., and Sargent, W.L.W. 1977, Ap. J., 215, 401.

Mitchell, R.J., Culhane, J.L., Davison, P.N., and Ives, J.C. 1976, M.N.R.A.S., 175, 29P.

Mushotzky, R.F., Serlemitsos, P.J., Smith, B.W., Boldt, E.A., and Holt, S.S. 1978, Ap. J., 225, 21.

Oemler, A. 1974, Ap. J., 194, 1.

Ostriker, J.P. 1977, in Evolution of Galaxies and Stellar Populations, ed. B.M. Tinsley and R.B. Larson (New Haven: Yale University Observatory), p. 369.

Roberts, M.S. 1975, in Galaxies and the Universe, ed. A. Sandage, M. Sandage, and J. Kristian (Chicago: University of Chicago Press), p. 309.

Rood, H.J., Page, T.L., Kintner, E.C., and King, I.R. 1972, Ap. J., 175, 627.

Sandage, A., and Tammann, G.A. 1976, Ap. J. (Letters), 207, L1.

Sandage, A., and Visvanathan, N. 1978, Ap. J., 225, 742.

Serlemitsos, P.J., Smith, B.W., Boldt, E.A., Holt, S.S., and Swank, J.H. 1977, Ap. J. (Letters), 211, L63.

Shu, F.H. 1978, in I.A.U. Symposium No. 77, Structure and Properties of Nearby Galaxies, ed. E.M. Berkhuijsen and R. Wielebinski (Dordrecht: D. Reidel), p. 139.

Solomon, P.M., and Sanders, D.B. 1979, in Giant Molecular Clouds in the Galaxy, ed. P. Solomon and M. Edmunds (Oxford: Pergamon Press).

Spitzer, L. 1962, Physics of Fully Ionized Gases (New York: Wiley), p. 143.

Spitzer, L., and Baade, W. 1951, Ap. J., 113, 413.

Strom, S.E., and Strom, K.M. 1978, in I.A.U. Symposium No. 77, Structure and Evolution of Nearby Galaxies, ed. E.M. Berkhuijsen and R. Wielebinski (Dordrecht: D. Reidel), p. 69.

Sullivan, W.T., and Johnson, P.E. 1978, Ap. J., 228, 751.

Tammann, G.A., Yahil, A., and Sandage, A. 1979, Ap. J., in press.

Tarter, J. 1975, Ph. D. Thesis, University of California Berkeley.

Toomre, A. 1977, in Evolution of Galaxies and Stellar Populations, ed. B.M. Tinsley, and R.B. Larson (New Haven: Yale University Observatory), p. 401.

Tytler, D., and Vidal, N. 1978, M.N.R.A.S., 182, 33P.

Verschuur, G.L. 1974a, Ap. J. (Suppl.), 27, 65.

_____ 1974b, Ap. J. (Suppl.), 27, 283.

Wilkerson, M.S., Strom, S.E., and Strom, K.M. 1977, Bull. A.A.S., 9, 649.

FIGURE 1

Schematic representation of three possible configurations of ISM in response to an external pressure.

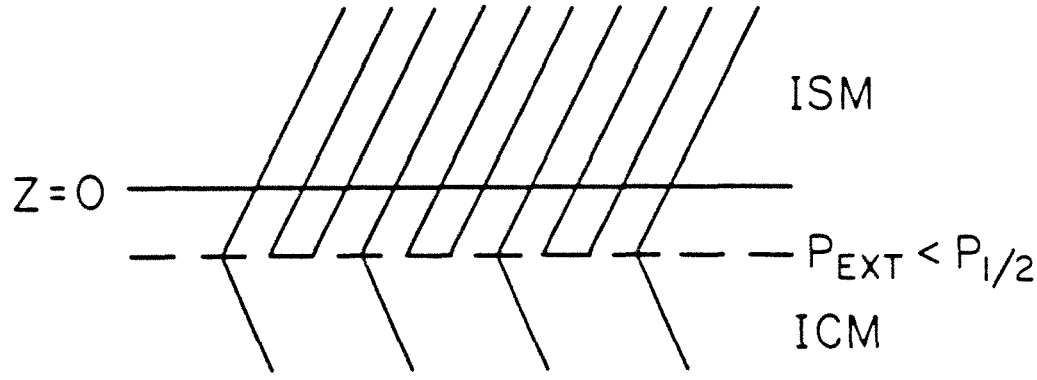

(a)

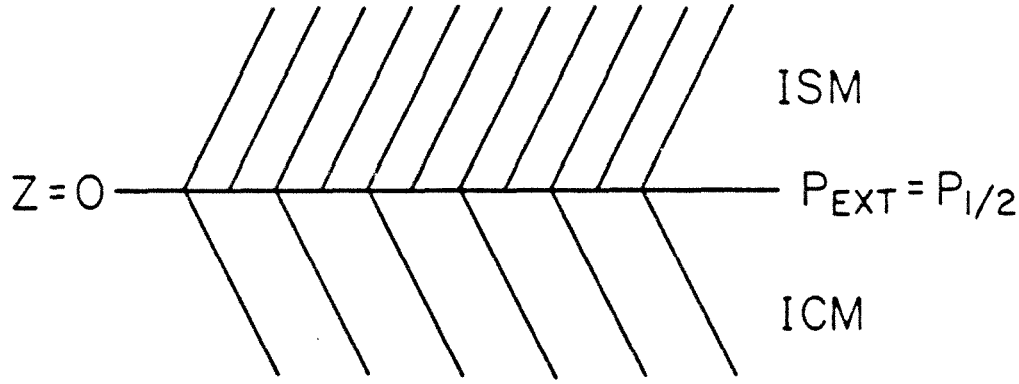

(b)

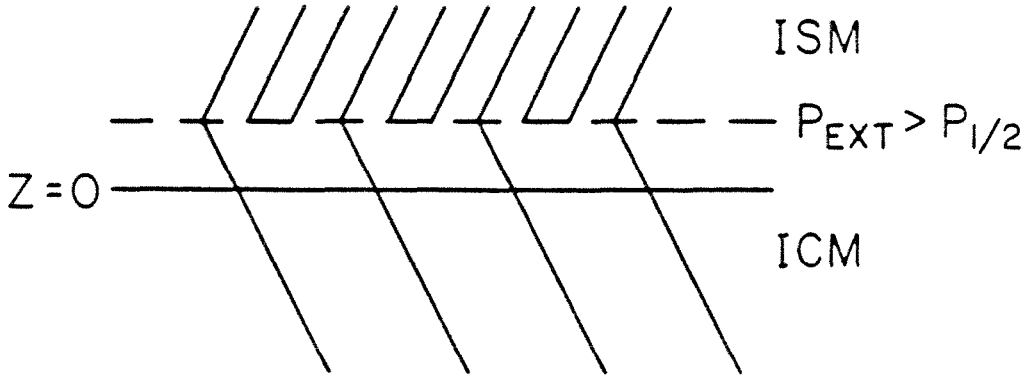

(c)

FIGURE 2

Equilibrium state of a cloud being supported by a wind in a gravitational field. Cloud assumes a flattened shape perpendicular to the wind.

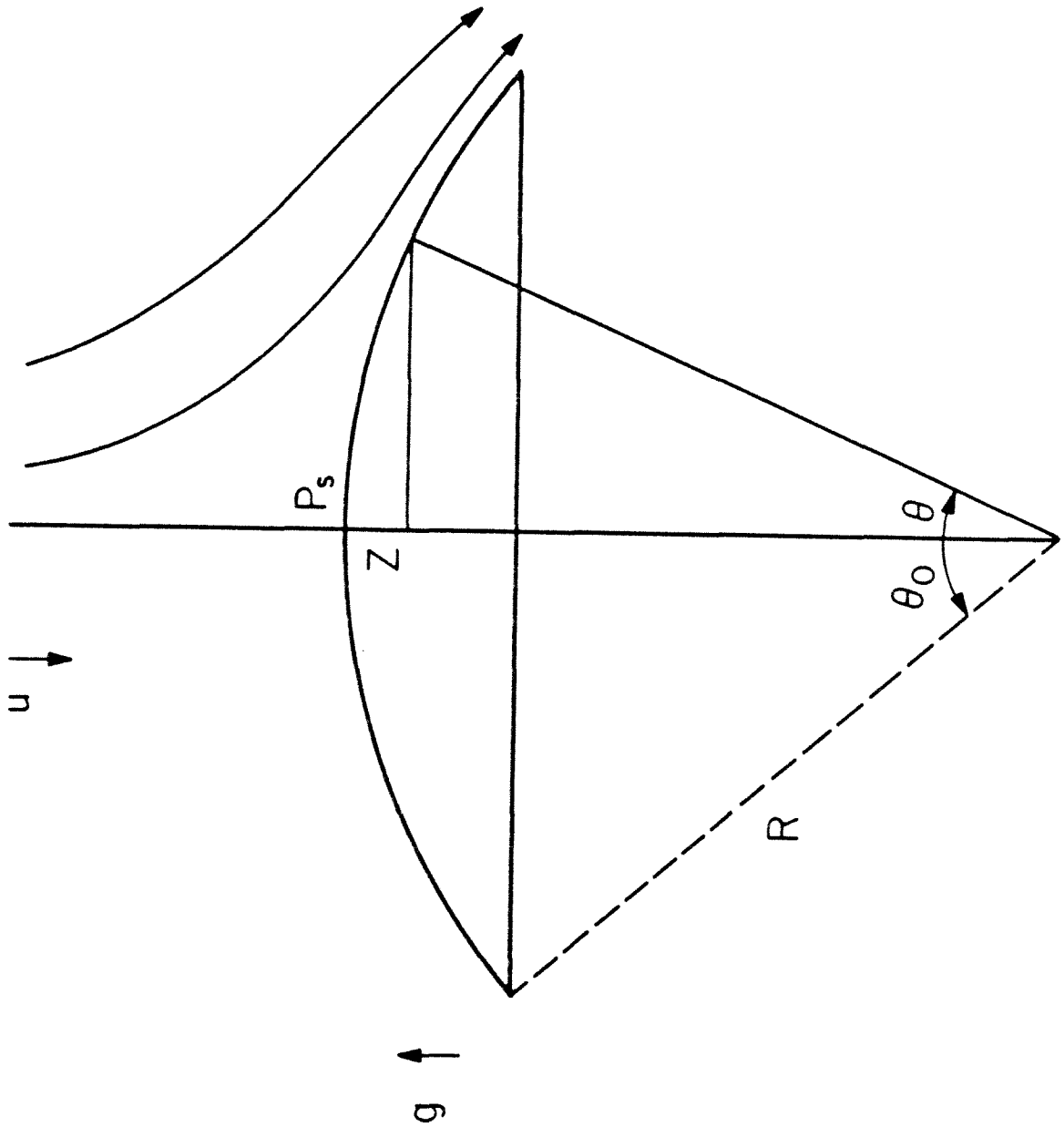
P_s
Z
θ
θ_o
R
u
g

FIGURE 3

Schematic representation of on-axis ICM flow around a galaxy. Galaxy is viewed edge-on.

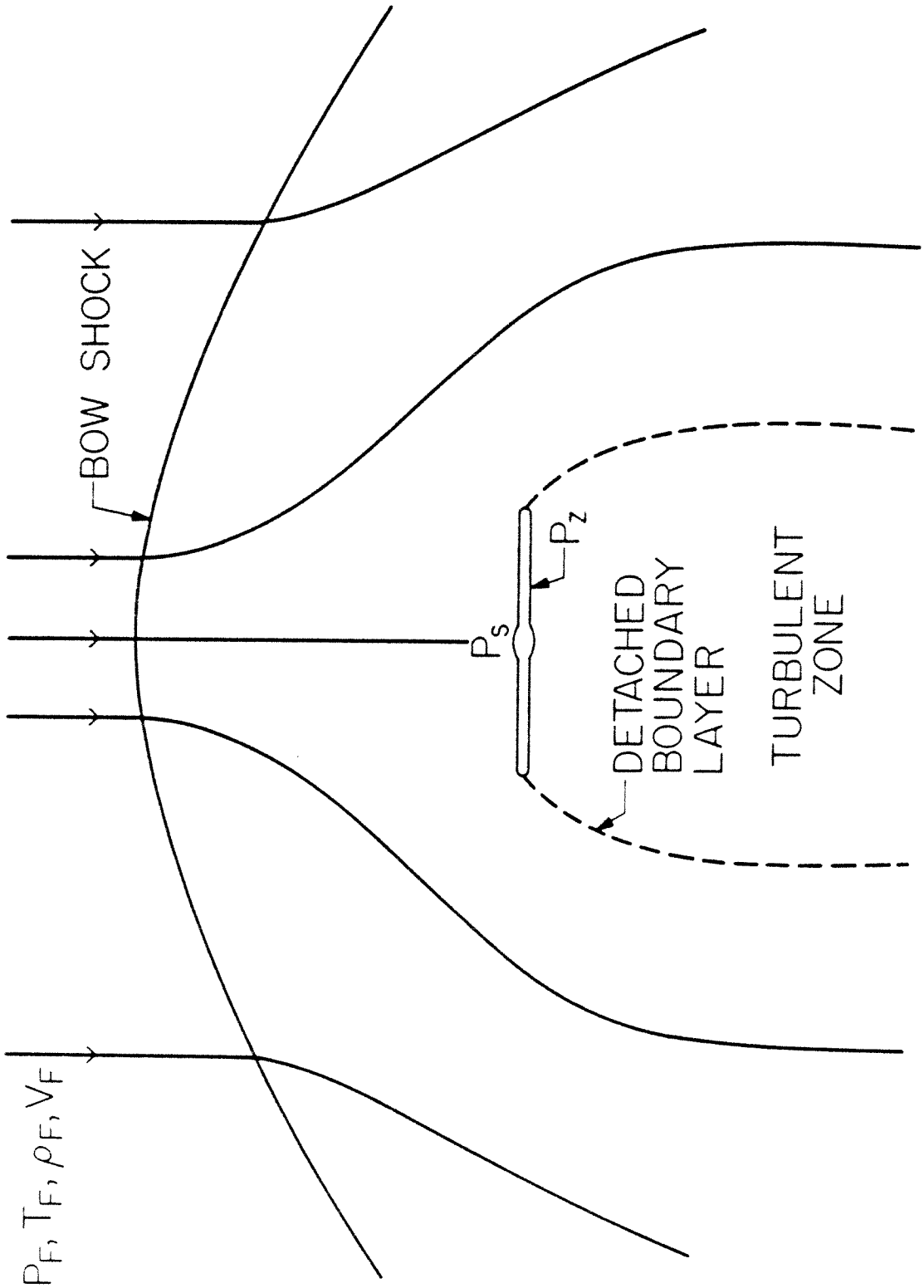
P_F, T_F, ρ_F, V_F
BOW SHOCK
P_s
P_z
DETACHED BOUNDARY LAYER
TURBULENT ZONE

FIGURE 4

Pressure contours for flow depicted in Figure 3 with parameters as described in text. Adjacent contours differ by a factor 1.5 . Flow enters grid at top of figure. Galaxy is located at z = 20 and extends 5 units in r direction. Irregularities in contours are due to plotting routine.

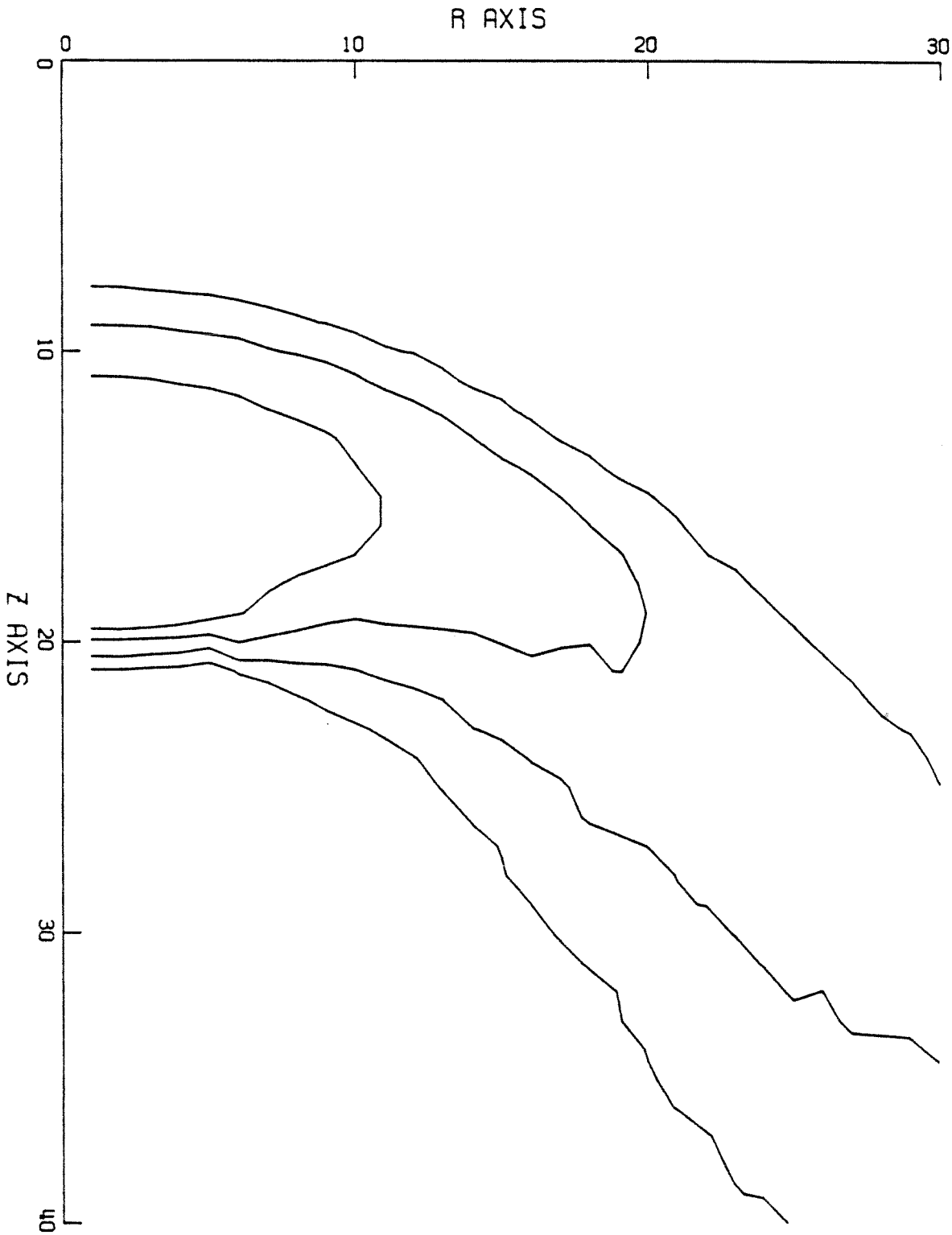
R AXIS
0
10
20
30
Z AXIS
0
10
20
30
40

FIGURE 5

Velocity field for flow in Figure 3. Note bow shock in front of and stagnation zones in vicinity of galaxy.

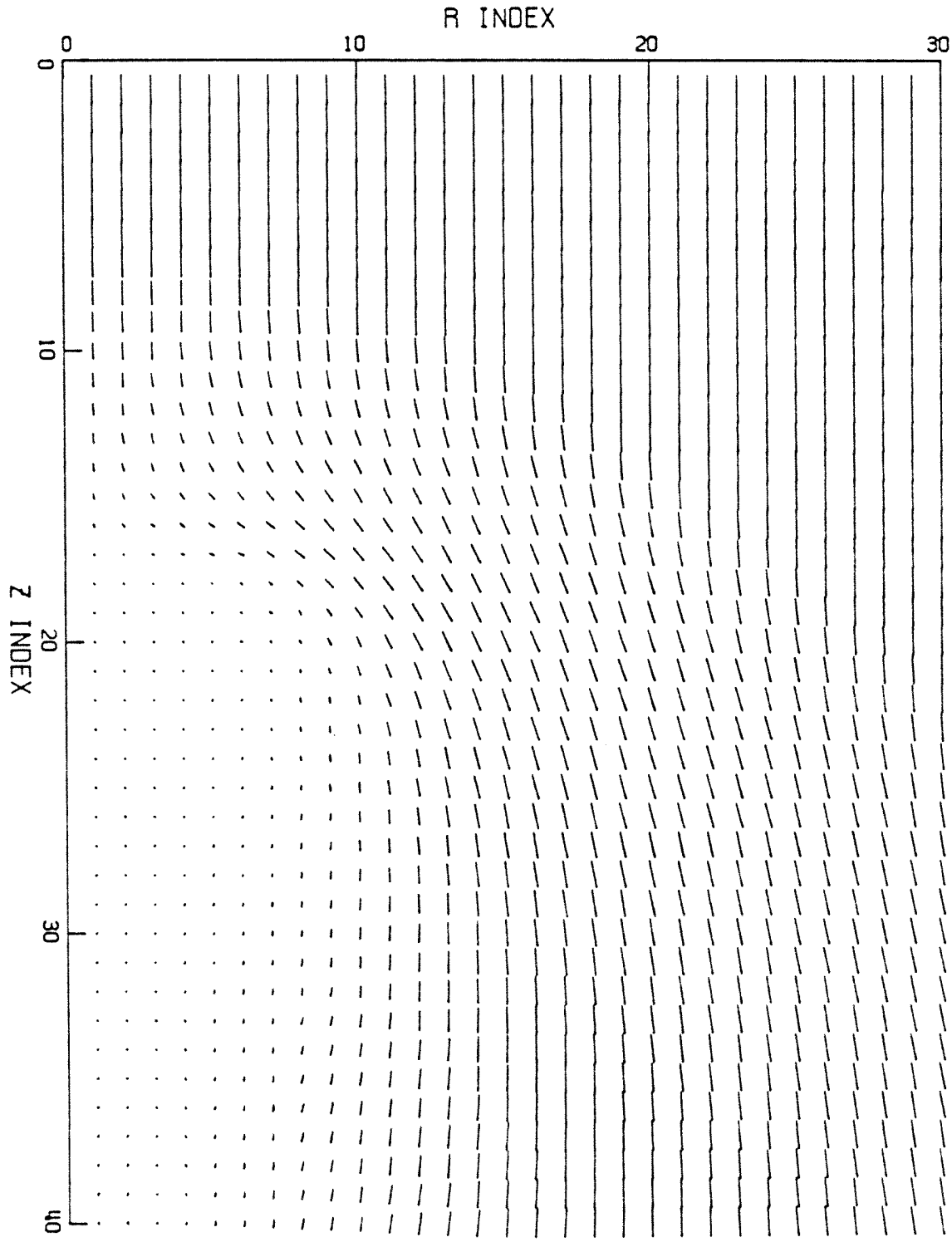
R INDEX
0
10
20
30
Z INDEX
0
10
20
30
40

FIGURE 6

X-ray flux enhancement from flow in Figure 3. Contours represent total emission within an annulus at a given radius. Adjacent contours differ by a factor 2. Note that x-ray flux is strongest along the front face of the galaxy.

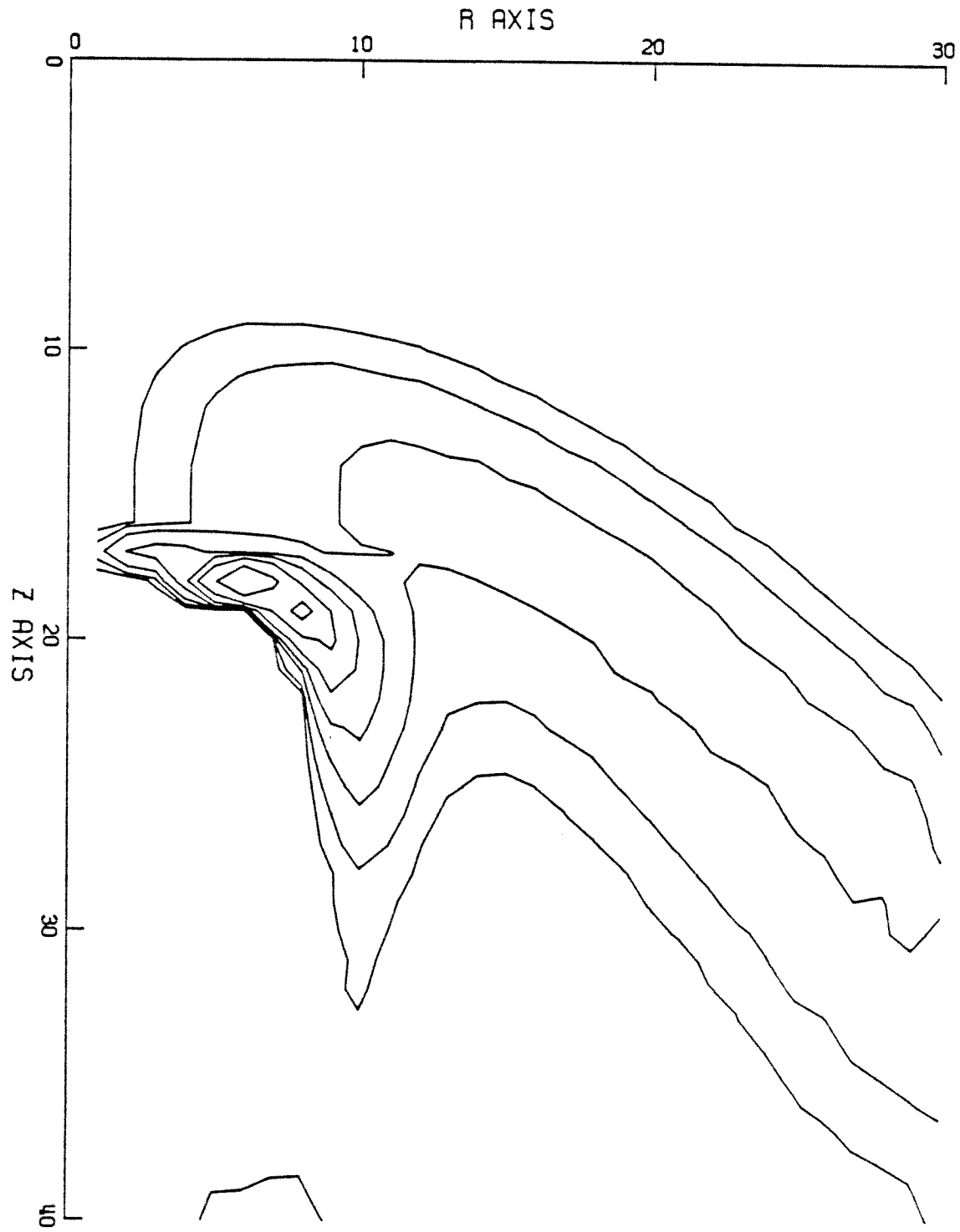
R AXIS
0
10
20
30
Z AXIS
0
10
20
30
40

FIGURE 7

Ram pressure needed to sweep a galaxy beyond a given radius with mass and gas distributions as given in text.

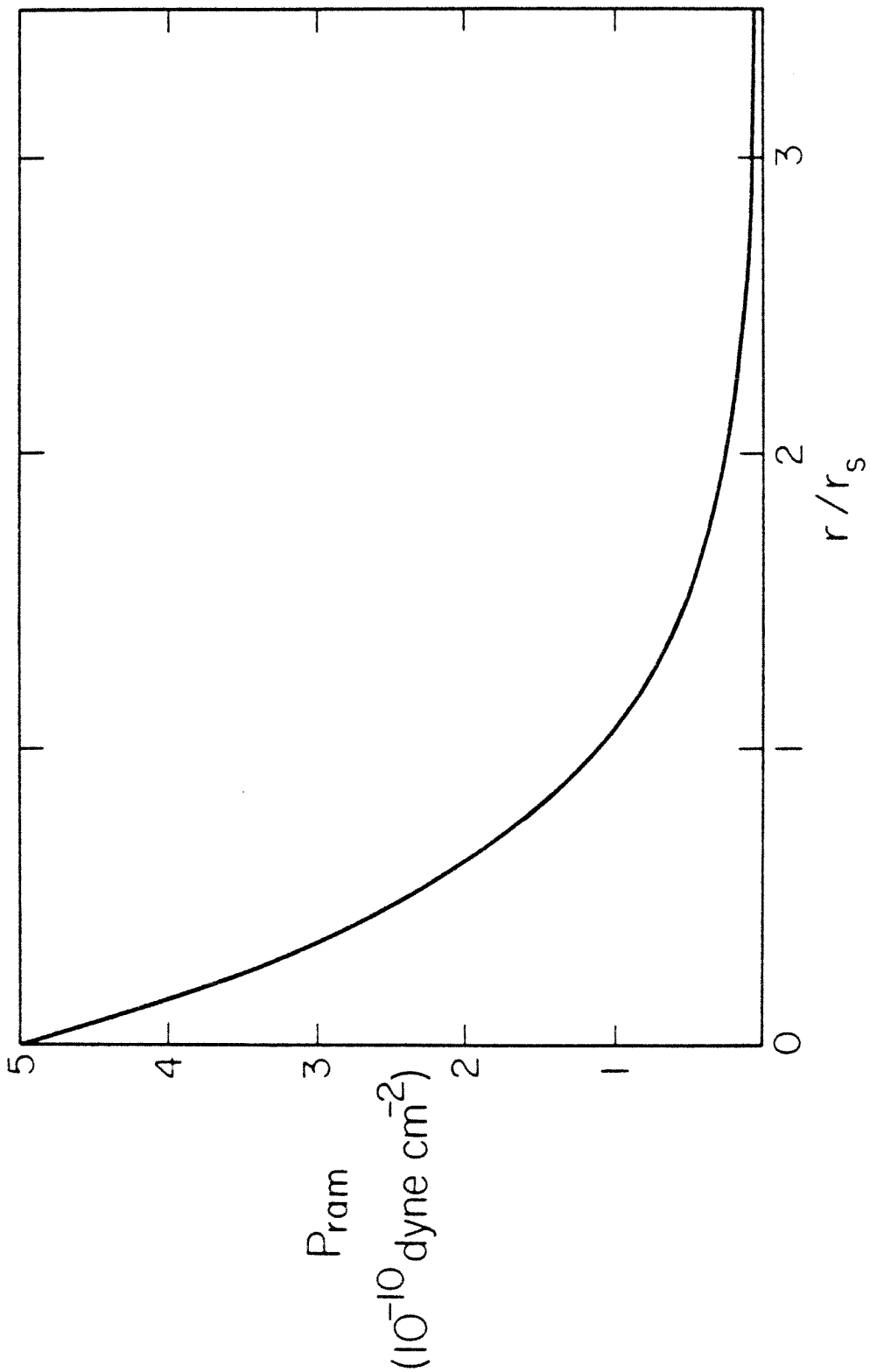
5
4
3
2
1
0
1
2
3
P_{ram}
$(10^{-10}$ dyne $cm^{-2})$
r/r_s

FIGURE 8

Cumulative [Sp/E] ratio within a radius r from cluster center. Values in parentheses correspond to different values of P_{crit} in dyne cm^{-2}.

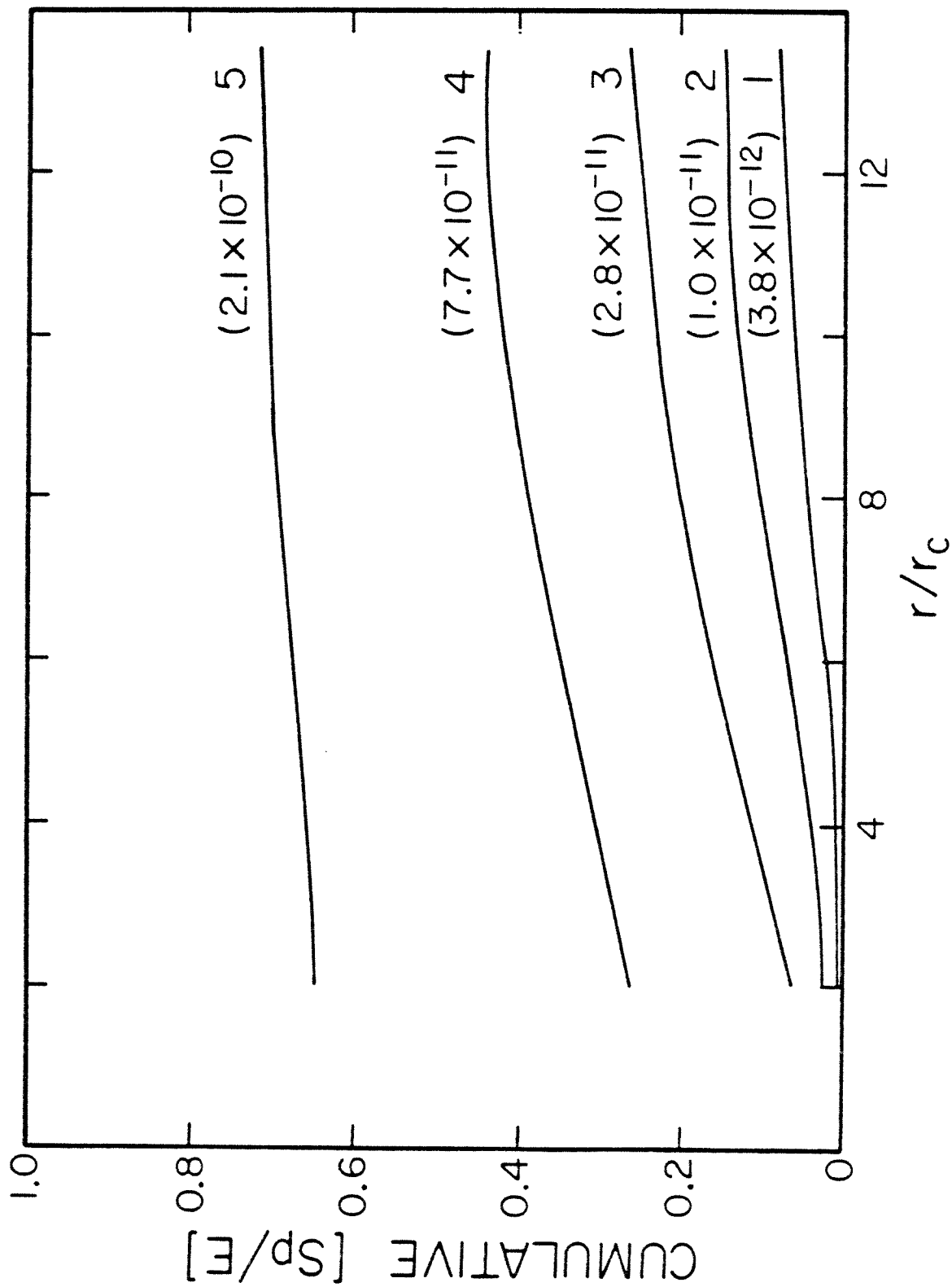
CUMULATIVE [Sp/E]
1.0
0.8
0.6
0.4
0.2
0
4
8
12
r/rc
(2.1×10⁻¹⁰) 5
(7.7×10⁻¹¹) 4
(2.8×10⁻¹¹) 3
(1.0×10⁻¹¹) 2
(3.8×10⁻¹²) 1

FIGURE 9

Differential [Sp/E] ratio as a function of projected density of galaxies. Corresponding radius is indicated in parentheses. Curves are numbered the same as in Figure 8.

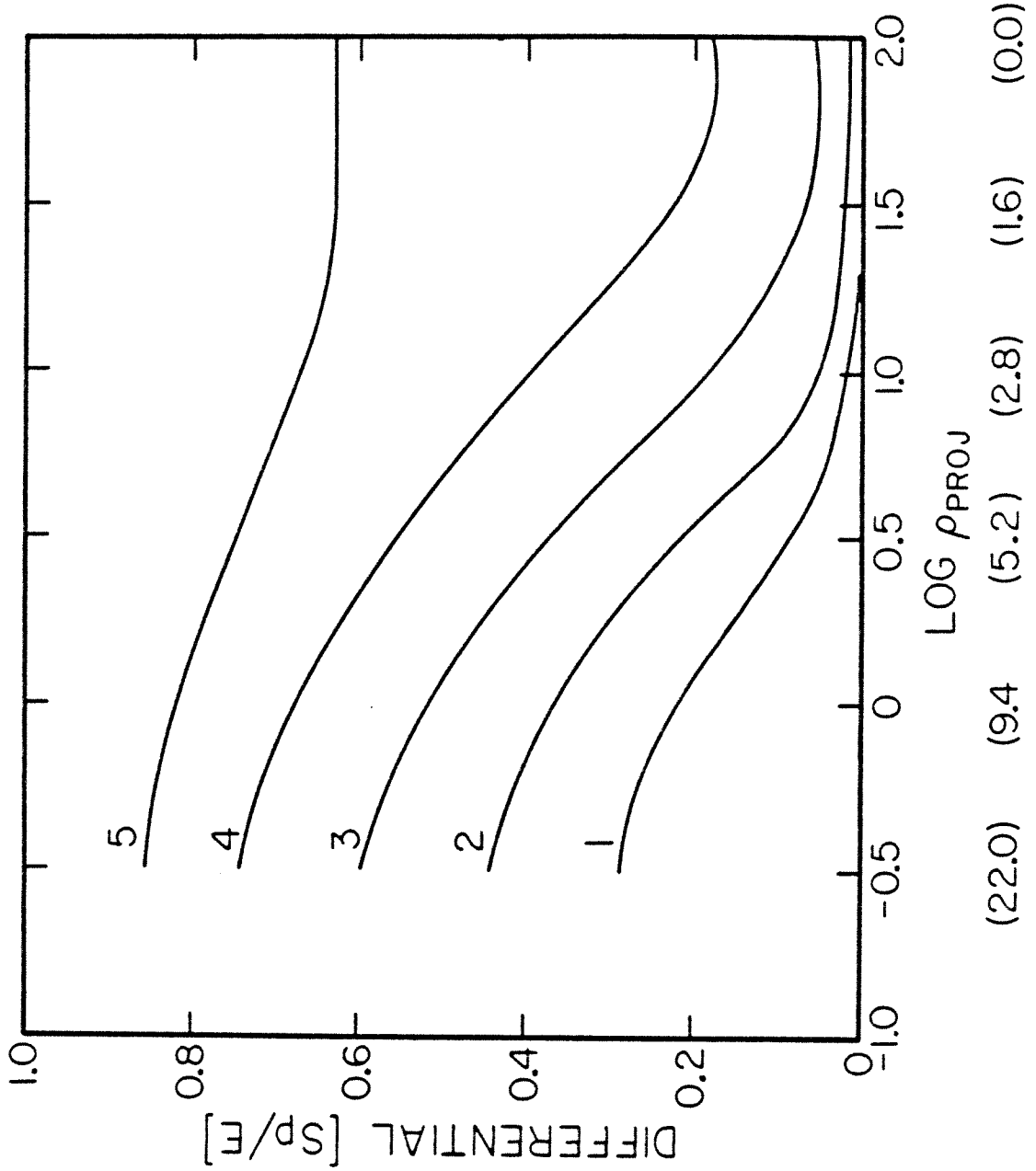
DIFFERENTIAL [Sp/E]
1.0
0.8
0.6
0.4
0.2
0
-1.0
-0.5
0
0.5
1.0
1.5
2.0
LOG ρPROJ
(22.0) (9.4 (5.2) (2.8) (1.6) (0.0)
(r/rc)
5
4
3
2
1

FIGURE 10

Global [Sp/E] ratio as a function of x-ray luminosity. Solid curve: predicted relation (within $14r_c$); crosses: data from Table 3.

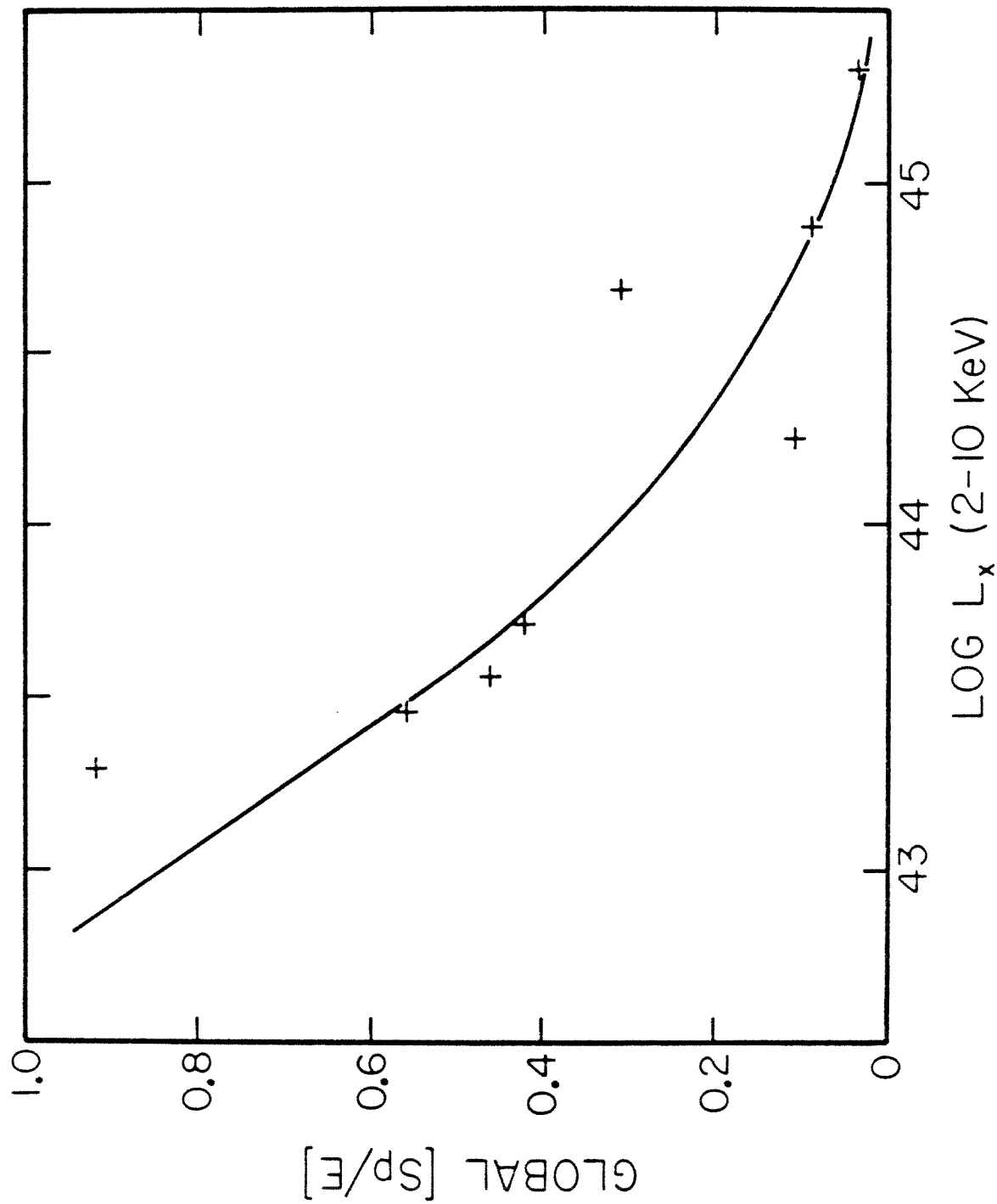
GLOBAL [Sp/E]
1.0
0.8
0.6
0.4
0.2
0
43
44
45
LOG L_x (2-10 KeV)

FIGURE 11

Same as Figure 9, curve 3, showing effects of changing r_t/r_c from 50 to 158 and β from 0.5 to 1.0 .

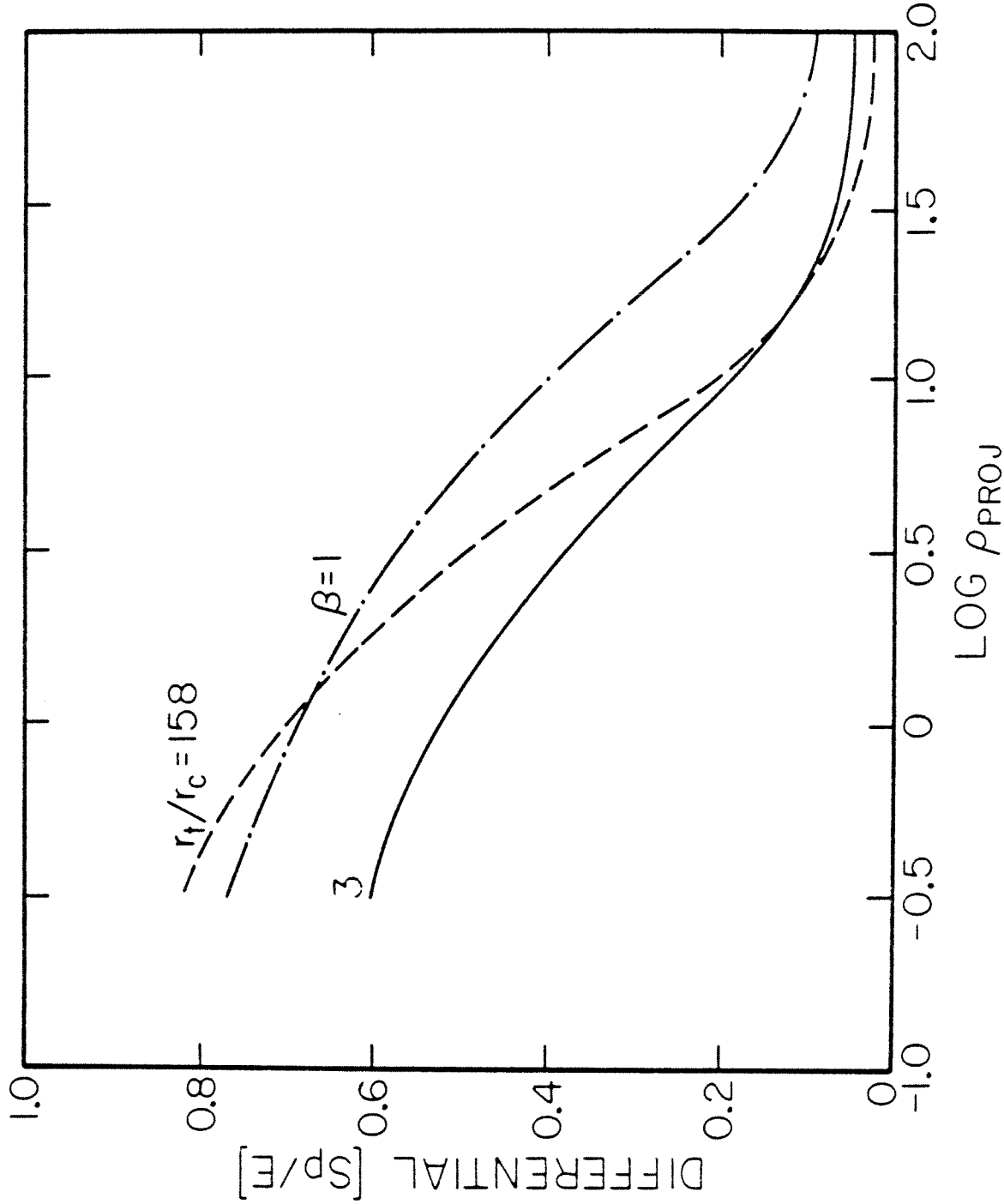
DIFFERENTIAL [Sp/E]
LOG ρPROJ
1.0
0.8
0.6
0.4
0.2
0
-1.0
-0.5
0
0.5
1.0
1.5
2.0
rt/rc=158
β=1
3

FIGURE 12

Two curves from Figure 10 plotted with observed relation for [Sp/E] from Dressler (1980).

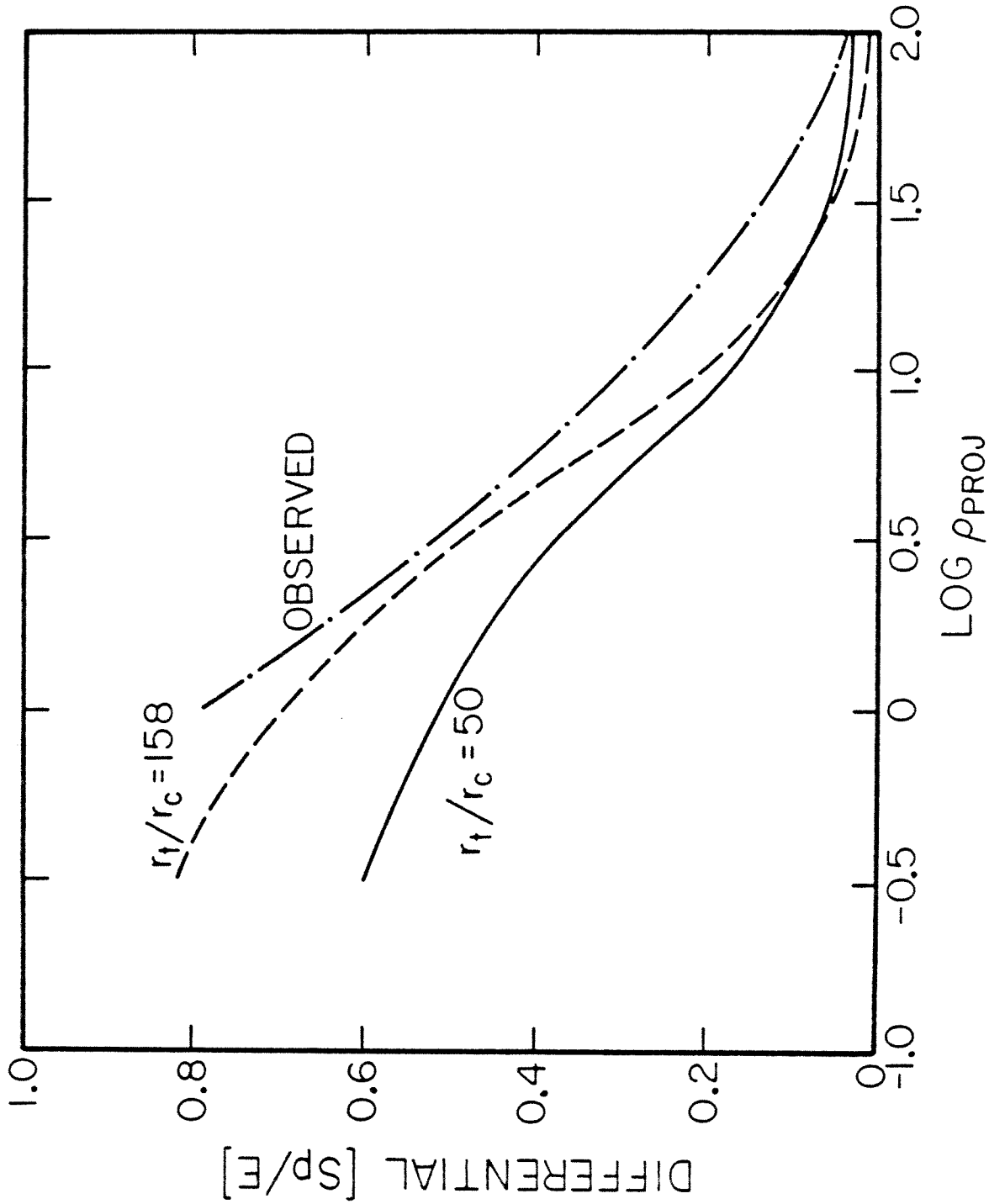
DIFFERENTIAL [Sp/E]
LOG ρPROJ
OBSERVED
r_t/r_c=158
r_t/r_c=50
1.0
0.8
0.6
0.4
0.2
0
-1.0
-0.5
0
0.5
1.0
1.5
2.0

FIGURE 13

Same as Figure 9 but with curves scaled to corresponding values of ρ_{proj} assuming mass density ρ_v is varied but ICM density ρ_f remains fixed. Compare combined profile with observed relation in Figure 12.

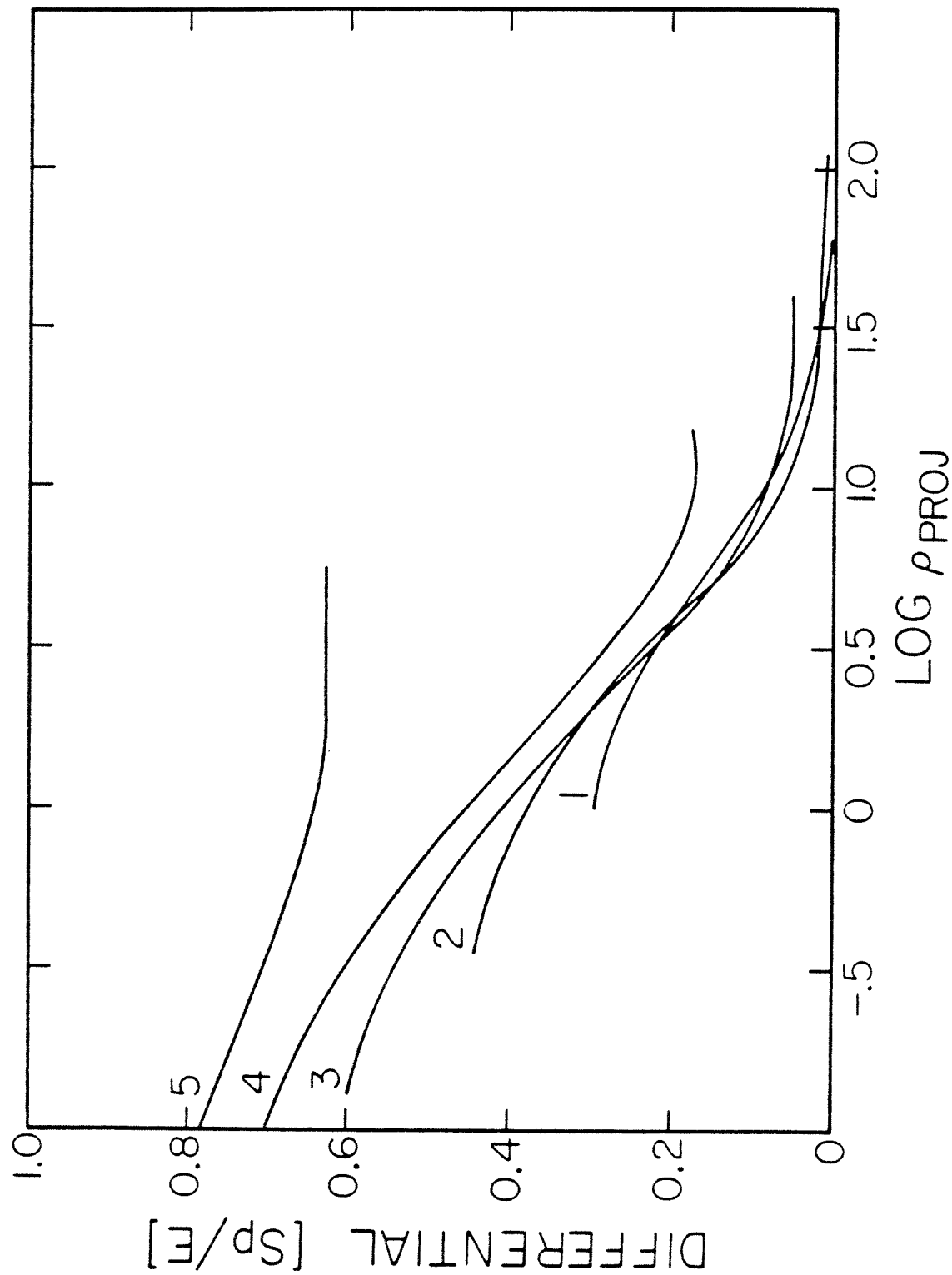
DIFFERENTIAL [Sp/E]
1.0
0.8
0.6
0.4
0.2
0
-.5
0
0.5
1.0
1.5
2.0
LOG ρ PROJ
1
2
3
4
5

CHAPTER III

EVIDENCE FOR A DEFICIENCY OF Hα EMISSION FROM SPIRAL GALAXIES IN ABELL 1367

I. INTRODUCTION

The discovery of the existence of a hot, intra-cluster medium (ICM) in clusters of galaxies has led to much speculation regarding the influence the ICM could have on the galaxies within these clusters. The temperatures and densities for the ICM as inferred from X-ray observations ($T \sim 10^8$ K, $n \sim 10^{-3}$) are large enough that the ICM should have a profound effect on the interstellar medium in a galaxy, possibly removing it entirely. If such an effect could be verified it would have important relevance for studies of the evolution of galaxies in clusters.

This paper investigates the deficiency in gas content of spiral galaxies in the cluster A1367 relative to a sample of field spirals by studying their Hα emission line properties. A study of Hα emission was chosen because of the relative ease with which a large number of galaxies could be observed at Hα with a telescope of modest aperture. Originally it was also hoped that direct evidence for the ram-pressure stripping of galaxies could be found in the form of spectra characteristic of shocks which one might expect to see as a result of stripping, although eventually no such spectra were found. The cluster A1367 was selected for study because it is nearby, relatively rich in spirals, and a known X-ray source, indicating the presence of an ICM.

Several approaches have been used in the past for

studying the gas content of galaxies in clusters. Perhaps the most direct method involves measuring the H I content. Such measurements have been made by Davies and Lewis (1973), Huchtmeier et al. (1976), and Krumm and Salpeter (1979) for galaxies in the Virgo cluster, and by Sullivan and Johnson (1978) for galaxies in A1367 and the Coma cluster. These surveys all point to a deficiency in H I content for spirals in these clusters relative to the field. It should be noted that H I measurements may not reflect the total gas content of a galaxy as much material could be in the form of H_2. The high pressure of a hot ICM may, in fact, favor the formation of H_2 clouds in cluster spirals without actually removing material from them.

Van den Bergh (1976) has used the gas content of a spiral as one parameter in his two-dimensional classification scheme for disk galaxies. The division of galaxies into normal/anemic/S0 depends on a subjective estimate of the vigor with which star formation is occurring in a galaxy, but nevertheless may be useful for detecting trends in gas content among galaxies. Van den Bergh, e.g., notes that the spirals in the Virgo and Coma clusters are much more likely to be anemic than those in the field. He interprets this effect as evidence for gas removal by environmental factors in these clusters.

A third measure of the gas content of a galaxy, and

the approach taken in this paper, is the strengths of emission lines. Such observations only measure the ionized gas component and are therefore more difficult to interpret than H I observations They are, however, fairly easy to make. For example, Gisler (1978) has collected statistics from the literature on the occurrence of emission lines in a large number of galaxies and shows that emission lines are absent much more often for galaxies in the richest clusters than those in open clusters or in the field. Because of the heterogeneity of his sample, his results can be considered only qualitative in nature. Previous work on emission lines in field galaxies only has also been done by Burbidge and Burbidge (1962, 1965) and Cohen (1976).

While all these surveys point to a gas deficiency for galaxies in clusters, a quantitative measure of the deficiency has been difficult to establish, in part due to the intrinsic dispersion in gas content among galaxies. Also, although it has been argued that the deficiency is due to environmental effects (i.e., interaction with an ICM), such a connection has never been unequivocally established. Alternate causes, such as intrinsic deficiency at the time of galaxy formation, cannot be ruled out.

A1367 is an example of what Butcher and Oemler (1978) call low concentration clusters. These clusters are purported to have not yet undergone collapse and have a mass

distribution which still reflects their (irregular) initial conditions. However, A1367 is more centrally condensed than other irregular clusters (Oemler 1974), and the high velocity dispersion (Dickens and Moss 1976; Tifft 1978) plus the presence of a hot ICM suggest that at least the core region has undergone collapse. This cluster should therefore be an ideal place to search for spiral galaxies which are losing or have recently lost their internal gas content to the ICM.

The observations presented here are slit spectra at Hα which have been obtained for a sample of spiral galaxies in A1367 and a comparison sample of field galaxies. The observations of the field sample are given in § II where correlations between Hα and other properties of a galaxy are investigated. These observations are compared with a similar survey by Cohen (1976). In § III the observations of galaxies in A1367 are presented and compared with the field galaxy sample. The evidence for a deficiency in Hα emission is discussed, and it is argued there is a deficiency for galaxies near the region of X-ray emission. In § IV the results are discussed in terms of their implication for the evolution of galaxies.

II. THE FIELD SPIRALS

a) Selection of Galaxies

The sample of field galaxies which were observed was obtained from the Second Reference Catalog of Bright Galaxies (hereafter RC2, de Vaucouleurs et al. [1976]). The only general requirement was that the galaxies be brighter than $M_B = 12.5$. Because it was desired to compare the present measurements with those of Cohen (1976), many objects are in common with her list. Also some attention was paid to selecting objects that have 21 cm measurements, and for this purpose the compilation of Roberts (1975) was used. Objects in the Virgo cluster were generally avoided. Finally, an attempt was made to obtain a reasonable spread in morphological type. In all 57 galaxies were observed and are listed in Table 1.

The distribution of types observed here as compared with the field in general will be of some importance for later purposes. Only the ratio of early (T = 1-3) to late (T = 4-10) types will be considered. This ratio has been determined for the field in two ways. First, de Vaucouleurs (1959) has found the distribution of all morphological types for a complete sample of 200 field galaxies. Considering types Sa-Sm only it is found that the ratio of early/late types is 38/62. A second determination was made using the analysis by Tammann et al. (1979) of the Revised Shapley-Ames (RSA) Catalog. These authors derive actual luminosity functions for galaxies according to type. By integrating

these functions the ratio of types Sa-Sb to Sbc or later was found to be 39/61. A lower limit on the luminosity function corresponding to $M_B = -20$ was imposed because the distribution depends somewhat on magnitude and surveys of clusters generally cover only the bright end of the luminosity function. For the galaxies listed in Table 1 with $T \geq 1$, the corresponding ratio is found to be 39/61 using de Vaucouleurs types, or 45/55 using RSA types (kindly supplied by A. Sandage). Thus from the point of view of early versus late, the present sample of galaxies should provide a good representation of the field, possibly being biased slightly towards early types.

b) Observations

Long-slit spectra were obtained for this sample of galaxies during 1978 November - 1979 August with the Palomar 1.5 m telescope and the Digital SIT Spectrograph (Kent 1979a). A slit size of 3"x3' was generally used, and the slit was always oriented in an E-W direction centered on the nucleus of a galaxy. The wavelength region covered was 5850-7400 Å at a resolution of 3.2 Å per pixel. The scale along the slit was 2".2 per pixel. Exposure times were typically 20 minutes. Usually only one spectrum was obtained for each object, although a few were repeated on different nights as a check on the consistency of these observations.

Standard observation and reduction procedures were used

to calibrate the spectra and convert them to relative fluxes. The spectra were compressed to one dimension for the purpose of measuring the Hα equivalent width. Any other emission lines present were also measured. In a few cases the galaxy extended beyond the 3' length of the slit, thus causing the strips along the edge of the spectrum which are used for sky subtraction to be contaminated by the galaxy. Because of the low surface brightness levels at these distances from the nucleus, this contamination is probably not serious and no attempt at correction was made.

The emission line measurements are given in Table 1 along with the following information: 1) NGC or IC number; 2) morphological type "T" from RC2; 3) Hα equivalent width in Å; 4) [N II] λ6548+6583 strength relative to Hα when measured; 5) [S II] λ6717+6731 strength relative to Hα when measured; 6) neutral hydrogen M_H/L in solar units from Roberts (1975) except where indicated; 7) B magnitude; 8) B-V color; 9) isophotal surface brightness μ_{25}; 10) galactocentric radial velocity. Entries in columns (7)-(10) are from the RC2. In cases where Hα was not detected, the upper limit is typically less than 1 Å. No correction has been made for any underlying absorption; from the spectra with no detectable Hα emission it is estimated that any absorption is $\lesssim$ 2 Å. The [N II] and [S II] lines will not be used further but are included here to illustrate the

range in values that these lines may take.

Because of the two-dimensional nature of the data it is possible to examine the spatial distribution of Hα across a galaxy. This has been done for all the galaxies and is illustrated in Figure 1. For each object the top profile gives the continuum distribution along the slit in a wavelength region near Hα, and the bottom profile shows the net Hα distribution. In a few cases an asymmetric profile in the continuum was caused by a slight irregular trailing of the galaxy along the slit.

A few galaxies are of sufficient interest to merit further comment.

NGC 1569: This unusual galaxy appears to be undergoing extremely active star formation across the entire disk (de Vaucouleurs et al. 1974). Near the nucleus a high excitation H II region was found with lines of He I λλ5876,6678, 7065 and [Ar III] λ7136 present.

NGC 2782: [O I] λ6300 present.

NGC 3227: This galaxy is classified as a Seyfert by Weedman (1977).

NGC 3310: He I λ5876 and [O I] λ6300 present. These last three galaxies are the only ones in which [O I] was detected.

NGC 5005: The emission lines in the nucleus of this galaxy are extremely broad and the Hα + [N II] and [S II] line pairs are blended. If the line intensities were much stronger this galaxy might be classified as a Seyfert.

c) Analysis

Because slit measurements sample only a small portion of a galaxy it is of importance to compare them with a corresponding set of aperture measurements which record the total Hα emission from a galaxy. For this reason the present set of measurements will be analyzed in conjunction with the observations of Cohen (1976) who measured Hα + [N II] equivalent widths for a similar sample of galaxies but using apertures which included a large fraction of the total light of a galaxy.

i) Comparison of Slit and Aperture Measurements

There are 16 galaxies in common between the slit measurements here and the aperture measurements of Cohen. The corresponding values for the equivalent width of Hα + [N II] are plotted in Figure 2 along with a 45° line. Although there is considerable scatter in the points it is clear that the two types of measurement are well correlated. A least squares fit to the points gives $\log W_\lambda$ (slit) = 1.17 $\log W_\lambda$ (aperture) - 0.139 with a scatter in $\log W_\lambda$(slit) of $\sigma = 0.25$. This scatter is almost certainly due to the sampling problem of the slit measurements and will dominate over any statistical noise in the data.

ii) Correlation Between Hα and Other Quantities

This section examines the correlations between the Hα

equivalent width and other properties of a galaxy. Because of the large scatter in many of these relations use will be made of the Kendal rank correlation test for independence (Hollander and Wolfe 1973) which is useful for testing for positive or negative correlations between two random variables X and Y. This test defines the statistic K as

$$K = \sum_{i<j} \xi[(X_i, Y_i); (X_j\ Y_j)]$$

where the $(X_j\ Y_j)$ are the paired observations and

$$\begin{aligned} \xi[(a,b);(c,d)] &= 1 \text{ if } (a-b)(c-d) > 0 \\ &= 0 \text{ if } (a-b)(c-d) = 0 \\ &= -1 \text{ if } (a-b)(c-d) < 0 \quad . \end{aligned}$$

For a large number of points n, if X and Y are independent K is distributed normally with mean 0 and $\sigma^2 = n(n-1)(2n+5)/18$. The rank correlation coefficient $\tau = 2K/n(n-1)$ gives an estimate of the degree of correlation. The quantities $K^* = K/\sigma$ and τ are listed in Table 2 for the following tests:

1. Hα vs. B-V. The measurements are plotted in Figure 3.

2. Hα vs. morphological type T (Fig. 4).

3. Hα vs. surface brightness (Fig. 5).

4. Hα vs. neutral hydrogen M_H/L (Fig. 6).

Only galaxies with positive H I detections are plotted.

5. Hα vs. absolute magnitude (Fig. 7). The absolute

magnitude was determined by using the Hubble distance to a galaxy (H_o = 50). For those galaxies with v < 500 km s^{-1} it was assumed that this distance is ill-determined and such galaxies are not plotted.

Galaxies of type T = 0 have been excluded from the statistical tests, and the slit and aperture data have been considered separately. In plotting the data in Figure 3-7 no corrections have been made to the aperture data for the inclusion of [N II].

An examination of these figures and Table 2 show that the strongest correlation exists between Hα and B-V as has already been noted by Cohen (1976). There is also a moderate correlation between Hα and morphological type. Any other possible correlations are much weaker. An inspection of Figure 5 suggests that galaxies of high surface brightness have strong Hα emission while galaxies with very weak or no Hα emission tend to be of low surface brightness. A similar pattern is also suggested by Figure 6 for Hα vs. M_H/L. Finally, there is no evidence for a correlation between Hα and absolute magnitude.

iii) Distribution of Hα Equivalent Widths

The distribution of galaxies with respect to Hα equivalent width is plotted in Figure 8 for the slit and aperture data individually. Again galaxies of type T = 0 have been excluded. In both plots the main feature that is apparent

is a broadly peaked distribution centered at ~ 20 Å. The aperture data suggest a higher mean value of equivalent width and a narrower distribution than the slit data. These differences are readily understood when it is realized that the aperture data include [N II] with the Hα (often a significant contribution) and that the slit measurements have a large scatter about the intrinsic Hα equivalent width to begin with.

A somewhat more disturbing discrepancy

is the relatively large number of galaxies with no Hα detection in the slit data. This difference does not appear to be due to the slit measurements missing large regions of Hα emission since in the common group of galaxies the only no-detection in the slit data was also not detected in the aperture data. There is also no significant difference in the distribution of morphological types that were surveyed. Part of the discrepancy can be explained by the fact that about half of the no-detections in Hα have measurable [N II] which would have counted as weak detections in the aperture data. Also, the no-detections tend to have lower surface brightness on average whereas the sample for the aperture data is biased towards galaxies of high surface brightness. The remainder of the discrepancy is probably due to chance.

The occurrence of galaxies with little or no Hα

emission will be of some importance in § III, and some further comment on their nature is of interest. A galaxy with no detectable Hα is not necessarily devoid of such emission but rather has an equivalent width less then 1 Å (the average detection limit of the survey). By way of example, a long exposure was obtained of NGC 7217, for which an upper limit is given in Table 1. Hα was, in fact, detected throughout the galaxy with an overall equivalent width of 0.87 Å. A feeling for the morphological appearance of these low Hα-emission objects can be gotten from the Hubble Atlas (Sandage 1961) where several of them are illustrated. Of the nine spirals in the Atlas which were found here to have $W_\lambda(H\alpha) < 4$ Å, six, including NGC 2775, 2841, 3521, 5055, 7217, and 7331, are members of a class of which NGC 2841 is the prototype. Galaxies in this class are characterized as having a bright nucleus and an amorphous lens surrounded by thin, multiple arms that are segmented rather than being continuous. In some cases the disk is of quite low surface brightness. Of the remaining three galaxies, two (NGC 2681 and 5566) are early-type galaxies with amorphous arms that are delineated primarily by weak dust lanes. The final galaxy (NGC 3627) is the only object with weak Hα emission that appears to be an otherwise healthy spiral. Thus morphologically the galaxies with low Hα emission form a rather homogeneous set.

d) Discussion

The first conclusion that can be drawn is that while slit observations cover only a small fraction of a galaxy, they nevertheless provide a reasonable measure of the global Hα emission from a galaxy. This somewhat surprising result implies that the Hα emission in a galaxy is distributed roughly the same as the continuum light.

The distribution of Hα emission within a galaxy can be estimated from Figure 1 where the profiles of Hα and continuum light along the slit are plotted. Quite frequently two separate components to the Hα emission can be identified. The first will be referred to as the bulge component since it is centered on the central bulge of a galaxy. This emission is generally quite strong and is usually extended. It probably originates in large H II region complexes surrounding the nucleus, regions which have been termed "hot spots" by Morgan (1958). Examples of galaxies in the present survey with optically identified hot spots (Sérsic and Pastoriza 1967) are NGC 2903, 3310, 3351, 3359, and 5248. The presence of several other galaxies in Figure 1 with similar emission suggests that hot spots are a rather common phenomenon in spiral galaxies.

The second component of emission will be referred to as the disk component since it usually extends across the visible disk of a galaxy. This emission is usually fainter

than the bulge component although it can include bright outlying H II regions. An example is found in NGC 3294. Almost invariably if there is a bulge component present there will also be a disk component. This suggests that the bulge emission is actually a phenomenon of the inner regions of a disk. It also helps explain why slit and aperture measurements agree well; while slit measurements are most sensitive to the bulge component and aperture measurements reflect mainly the disk emission, both components are correlated to some degree.

A third component is emission that is confined to the nucleus of a galaxy. Emission of this sort was studied by Burbidge and Burbidge (1965) and is characterized by having [N II]/Hα > 1. In several galaxies in this survey only emission of this sort was detected. It is usually weak (W_λ(Hα + [N II]) < 10 Å) and the lines are often broadened noticeably.

The strong correlation between Hα and the B-V color in Figure 3 has already been discussed by Cohen (1976) and simply reflects a correlation between the total Hα emission from ionized regions and the number of hot stars which can produce ionizing radiation. The other positive correlation between Hα and morphological type (Fig. 4) is not as strong but does reflect the fact that morphological type is a measure of gas content and star formation activity in a

galaxy. It should be noted that galaxies of types T = 1 to 3 have similar Hα properties and are significantly different from galaxies of types T ≥ 4. In particular, galaxies with $W_\lambda(H\alpha) < 2$ Å are confined almost exclusively to T = 1 to 3.

The poor correlation between Hα and M_H/L (Fig. 6) is somewhat surprising. There is, however, the suggestion of a threshold effect at $M_H/L \approx 0.08$ in that below this value no Hα is seen, while above it Hα is almost always present with a strength independent of the hydrogen value. The one errant point in the upper left of this figure is the Seyfert NGC 3227. Further evidence for the existence of a threshold effect is provided by the neutral hydrogen surveys of Lewis and Davies (1973) and Balik et al. (1976). In a plot of M_H/L vs. B-V, both surveys show that galaxies with $M_H/L <$ 0.05 to 0.08 are invariably red (B-V > 0.80) while galaxies with larger M_H/L show a sudden increase in the range of B-V. More observations are needed to verify this possibly interesting effect.

The distributions of Hα equivalent width in Figure 8 do not necessarily represent the true distribution for field galaxies since they are biased by any selection effects that were used when galaxies for each sample were originally chosen. The galaxies in the aperture sample were selected with rather restrictive requirements on magnitude and diameter, and consequently this sample will not

be considered further. However, for the slit data the only selection effect that should be of importance is the distribution of morphological types, and it has been shown in § IIa that the distribution here does match that for field galaxies in general. Thus the Hα distribution in Figure 8a should be a representative sample of all field galaxies.

III. THE A1367 SAMPLE

a) Observations

A list of galaxies in A1367 was compiled from the Catalog of Galaxies and Clusters of Galaxies (hereafter CGCG, Zwicky and Herzog [1963]). These galaxies were classified as spirals, S0's, or ellipticals from a 1.2 m Schmidt IIIaJ plate kindly loaned by W. Sargent. A sample of brighter spirals and S0's were selected from this list for observation at Hα. Some preference was given to galaxies which 1) had previous H I measurements (Sullivan and Johnson 1978; Schommer, private communication); 2) were known to have Hα emission from previous spectroscopy (Gudehus 1976; Dickens and Moss 1976, Tifft 1978); 3) exhibited Hα emission as determined from pairs of Hα/continuum plates taken with the Schmidt telescope. These last plates were taken as part of a survey searching for objects in X-ray clusters with unusual Hα emission. Because of the difficulty in identifying early-type spirals on small scale plates, galaxies of this sort are probably missed here. Therefore,

unlike the field sample in § II, the cluster sample does not provide a good representation of all spirals in A1367 but is biased towards late-type galaxies most likely to have Hα emission.

Observations were made during 1978-1979 using the same equipment and procedures for the field galaxies in § II. The results are listed in Table 3 along with the following information: 1) Zwicky number from CGCG; 2) other designation; 3) equivalent width of Hα in Å; 4) morphological type. In this column the first item is the coarse classification from the Schmidt plate, and items in parentheses are the RDDO types as determined by J. Stauffer (private communication) from a KPNO 4-m plate; 5) galactocentric radial velocity from Tifft (1978) except where indicated; 6) magnitude from CGCG. The accuracy of the equivalent widths is only fair (~ 25%). Upper limits are generally less than 3 Å.

b) Analysis

i) Spatial Distribution

A plot on the sky of all the galaxies in A1367 is shown in Figure 10. Above 21°30' only galaxies for which spectra were obtained are plotted. In Figure 11 the spiral galaxies alone are plotted with symbols indicating the strength of Hα that was detected. Also plotted are the

cluster center as determined from galaxy counts and the centroid of X-ray emission as given by Jones et al. (1979).

The galaxy distribution near the center of A1367 is rather irregular, but can be roughly divided into two groups, one concentrated to the northwest of the center and the other extending off to the southeast. The X-ray emission is located around this second group of galaxies, extending ~ 26' from the cluster center southeast to the radio galaxy 3C 264 = NGC 3862. From Figure 11 it is seen that the spiral galaxies associated with each of these two regions have quite different properties. The spirals to the northwest of the cluster center almost always have strong Hα emission, while those to the southeast are mainly devoid of Hα. Of 11 spirals south of 20°10' and east of 11^h40^m, 8 are no-detections. Thus there is an apparent correlation between the region of X-ray emission and Hα deficiency.

ii) Distribution of Hα Equivalent Widths and Comparison with Field Galaxies

The distribution of equivalent widths for the galaxies in Table 3 is plotted in Figure 9. Galaxies with no Hα are plotted at the values of their upper limits.

A detailed comparison between the Hα distribution for A1367 and the field is difficult because of the small samples involved and the relatively high upper limits on Hα for the A1367 measurements. Among the cluster galaxies with

detected Hα there is again a broadly peaked distribution centered around 10-20 Å as in Figure 8a for the field galaxies. The cluster distribution, though, does not appear to be as sharply peaked. More significant, a much larger fraction of cluster galaxies have either weak detections or upper limits to Hα. The median equivalent width for the field sample is ~ 12 Å against 4.6 Å for the cluster sample, nearly a factor 3 difference. When just galaxies near the region of X-ray emission are considered the difference is even more striking. Here, 73% of the galaxies have equivalent widths less than 4.6 Å; the relevant fraction for field galaxies is 33%. Thus there is a deficiency in Hα for galaxies in A1367 compared with the field and the deficiency is strongest for galaxies near the region of X-ray emission.

iii) Correlation Between Hα Emission and Morphology

In the RDDO system the anemic spirals are supposed to be galaxies which, on the basis of optical appearance, are deficient in gas content. It is of interest to see how well this classification correlates with the Hα emission properties of a galaxy. In Table 3 there are 17 galaxies with RDDO types. Of the 7 galaxies classified as normal spirals or irregulars, all have Hα emission detected. Of the 10 anemic spirals only 3 have detectable emission. This good

correlation is actually not terribly surprising since the classification of a galaxy as an anemic relies on the presence or absence of H II regions which are the primary source of Hα.

Two galaxies in A1367 (NGC 3860 and IC 2951) have been identified by Strom and Strom (1978) as being "smooth-armed" spirals, a rather ill-defined class of galaxies. These two galaxies are classified as anemics here. Strom and Strom suggest that NGC 3860 is a spiral in the process of being stripped; they point to blobs of nearby material which may be shreds torn out of the galaxy. Spectroscopically it has healthy Hα emission and an otherwise normal spectrum. IC 2951 has no Hα detected. Thus the spectroscopic evidence for these galaxies being stripped or having been stripped is rather inconclusive.

iv) Correlation Between Hα, H I, and Luminosity

In § II it was found that for field galaxies with $M_H/L < 0.05 - 0.08$ Hα was usually not detected, while above this value it was almost always detected. This relationship can be checked for galaxies in clusters using the data of Sullivan and Johnson (1978). Data on the presence of emission lines in all these galaxies is available either from the present survey for A1367 or from a compilation of redshifts in the Coma cluster by Gregory (1975). Among the galaxies with emission lines 9 out of 12 have H I detections

or upper limits of $M_H/L > 0.08$, while among those with no lines 8 out of 10 have $M_H/L < 0.08$. Thus the trend in § II regarding Hα versus H I for field galaxies is found to hold for cluster galaxies as well.

It was also shown in § II that for field galaxies there is no correlation between Hα and absolute magnitude. This relation can be checked here for the cluster spirals. Taking the data in Table 2 and dividing it into two groups of weak ($W_\lambda(H\alpha) < 4.6$ Å) and strong ($W_\lambda(H\alpha) > 4.6$ Å) sources, it is found that there is again no significant dependence of Hα emission on magnitude.

v) Correlation Between Hα and Velocity Dispersion

The galaxies within 1.2° of the cluster center were again divided into two groups of weak and strong sources. The velocity mean and dispersion were found to be $\bar{v} = 6350$, $\sigma = 747$ km s^{-1} for the weak sources, and $\bar{v} = 6470$, $\sigma = 833$ km s^{-1} for the strong sources. The difference in velocity dispersion between the two groups is probably not significant in view of the small number of galaxies involved.

c) Discussion

From a comparison of the Hα distributions it has been suggested that the A1367 galaxies are deficient in emission relative to the field by perhaps a factor of 3.

However, the possibility must be considered that deficiency is not intrinsic but is due to biases present in the data for the cluster galaxies.

Because the cluster galaxies are biased towards the bright end of the luminosity function the effect of a difference in luminosity between cluster and field galaxies must be considered. This effect is probably unimportant because the absolute magnitude range for the cluster galaxies of -20 to -22 is well covered by the field galaxies, and in any case no correlation between Hα and luminosity was ever found for any sample.

A second possible bias which may arise is that because the galaxies in A1367 are much more distant than the field galaxies, slit observations will cover a much larger fraction of the area of a galaxy and will, in fact, be more like aperture measurements. The magnitude of this effect can be estimated from Figure 2, where the systematic differences between slit and aperture measurements are illustrated. At high levels of Hα emission the aperture values are generally smaller than the slit values, while the opposite is true at low levels. Since deviations at weak levels of Hα are of greatest interest here, it is seen that the cluster galaxies in this domain should, if anything, have slightly higher equivalent widths than the field galaxies. The magnitude of this effect, however, is probably small

(< 10%).

The final and most important bias is that the sample of spirals in A1367 is not representative of the entire spiral population in the cluster. As has been noted previously, early-type spirals are most likely missed.

When these biases are considered, any deficiency between the cluster and field galaxies is likely to be enhanced. It is therefore concluded that the deficiency seen here is intrinsic and, if anything, the magnitude is underestimated.

IV. THE CAUSE OF A GAS DEFICIENCY

The existence of a deficiency in gas content among spiral galaxies in clusters has usually been interpreted in

the past as evidence for gas loss by an interaction between the spirals and an ICM. An alternative explanation that must be considered, however, is that the deficiency was intrinsic to the galaxies of the time of their formation.

A problem related to this gas deficiency in cluster galaxies is the corresponding difference in distribution of morphological types. Some authors (e.g., Sullivan and Johnson [1978]) have attempted to determine the existence of a gas deficiency in cluster galaxies by comparing them to field galaxies of the same type. One problem with this approach is that accurate typing of galaxies in distant clusters is quite difficult. A more fundamental problem, however, is the fact that in the standard classification schemes morphological type is itself partly a measure of gas content. Establishing the existence of a gas deficiency may simply reflect the preferential formation of early-type galaxies in clusters, and conversely, a true loss of gas due to environment may be misidentified as such a trend towards early-type galaxies.

Of course there are other properties of a galaxy correlated with morphological type, such as the bulge-to-disk (B/D) ratio (although this parameter is not a primary consideration when determining the type of a galaxy. In fact, in a study of galaxies in rich clusters, Dressler (1980) found that the B/D ratio for spirals (and S0's) is

systematically higher in regions of high galaxy density. This trend depends only on the local projected density of galaxies and not the other properties of a cluster (such as the presence of an ICM). The cause of this trend is presumably related to the conditions during the formation of the cluster galaxies, and it could also be responsible for any apparent gas deficiency and trend towards early-type galaxies in clusters.

To establish an environmental cause for gas deficiency it is necessary to show that such a deficiency is associated with the ICM specifically and not simply the high density of galaxies in the centers of clusters. In A1367 this is possible because the X-ray emission (and ICM) is offset from the cluster center. The galaxy distribution is more symmetrical with respect to the center and the highest densities are actually on the opposite side of the center from the X-ray emission. As has been stated previously, the spiral galaxies with low Hα emission are not distributed the same as the general galaxy distribution in the cluster but are concentrated towards the region of X-ray emission. Thus it appears that the ICM is responsible for the Hα deficiency.

If the absence of Hα emission is a true indicator of low gas content (as has been argued), the question is then how does the ICM remove gas from a galaxy. Two processes that are frequently mentioned are thermal evaporation and

ram-pressure stripping. A third possibility is that the high pressure of the ICM enhances the rate of star formation, causing a galaxy to rapidly exhaust its gas supply.

Thermal evaporation is effective at removing gas because of the very high temperature of the ICM (Cowie and Songaila 1977). Because of the low x-ray flux from A1367 the temperature of the ICM is not well determined, but Mushotzky et al. (1978) give limits of $1.3 < T_x < 2.8$ kV from OSO-8 data, with the lower value being more likely. The corresponding emission integral is $\langle n_e^2 \rangle V = 1\text{-}7 \times 10^{67}$ cm^{-3} where V is the volume of the emission region. If, as is usually assumed, the gas is distributed like an isothermal sphere, the emission integral is $2.47\ a^2 n_c^3$ where a is the core radius and n_c is the central density. The core radius was measured by Jones et al. (1979) to be $\gtrsim$ 15' or 520 kpc. This yields a central density of $n_c \simeq 1\text{-}3 \times 10^{-3}$ cm^{-3}.

At these temperatures and densities Cowie and Songaila give an evaporation rate for a typical galaxy of a few $M_\odot$ yr^{-1}. Taking a typical H I mass for a spiral galaxy of 5×10^9 $M_\odot$ (Roberts 1975) yields an evaporation time scale of $\sim 1\text{-}2 \times 10^9$ years. Thus any spiral immersed in the ICM should lose its gas on a time scale short compared with a Hubble time. A major problem with evaporation is that the presence of even very small magnetic fields can inhibit conduction perpendicular to field line, and any turbulence

may have the same effect even along field lines. Cowie and McKee (1977) argue that if evaporation is important the magnetic field in a cloud will be well connected to the surrounding medium which is self-consistent with the requirement for thermal conduction to be occurring. However, if a galaxy has substantial motion with respect to the ICM it is difficult to see how a magnetic field could avoid becoming tangled.

The dynamical ram pressure experienced by a galaxy moving through the ICM is proportional to $\rho_{ICM}\ v^2$ and depends very little of the temperature of the ICM. The magnitude of the ram pressure needed to remove material from a galaxy is estimated by Gunn and Gott (1972) to be of order $2\pi G\sigma_*\sigma_g$ where σ_* and σ_g are the surface mass densities of stars and gas respectively. Using the typical parameters for a galaxy given by these authors and a 3-dimensional velocity dispersion of 1200 km s^{-1}, stripping will occur if the ICM density exceeds 10^{-3}, which is just the central density derived above.

A more detailed model for stripping has been developed by Kent (1979b) and can be used here to provide a better estimate of the efficiency of stripping. If the weak Hα galaxies are assumed to have $M_H/L < 0.08$ (section §IIIb) compared with a more normal value of 0.20 for field galaxies (Roberts 1975), then the total gas content must be depleted by a factor $\sim$ 3 or more. For the typical galaxy model given by Kent, this requires stripping to be complete beyond about

r_H (where r_H is the exponential scale length of the gas distribution). The corresponding minimum ram pressure to accomplish this is $\sim 2.5 \times 10^{-11}$ dyne cm^{-2}. From the dynamical cluster model developed in that paper and using the ICM parameters derived here it is found that $\sim$ 40% of all spirals should be stripped by the required amount, which is,in fact, about the excess number of weak Hα objects found here. While this analysis relies on the somewhat tenuous relation between Hα and H I content, it is clear that stripping is quite capable of causing significant deficiencies in the gas content of cluster spirals.

A final question relating to the evolution of galaxies is whether the excessive numbers of S0's in clusters are produced by the stripping of spirals. The spectroscopic evidence presented here,while consistent with this interpretation, is by no means conclusive. Indeed, evidence is accumulating that S0's are not evolved from spirals (Dressler 1980), the primary observation being that S0's do not have the small bulges characteristic of spirals. Nevertheless some contribution to the S0 population by stripped spirals cannot be ruled out. Perhaps more important for the evolution of a cluster is the contribution of gas lost from spirals to the growth of the ICM, which evidence now suggests may be composed in large part of material processed through galaxies (Mushotzky et al. 1978).

V. CONCLUSIONS

The main conclusion of this paper is that the spiral galaxies in A1367 exhibit a deficiency in Hα emission relative to field spirals, and that this deficiency, being strongest for galaxies in the vicinity of the x-ray emission, is caused by the presence of an ICM in the cluster. Because of the selection effects involved in the sample of galaxies that were observed, a more quantitative statement is difficult to make.

These observations provide support for the idea that the environment of a galaxy can affect its characteristics. In particular, the presence of a hot intracluster medium can seriously deplete the interstellar medium from a spiral galaxy. Just how such galaxies evolve, and in particular whether they remain as anemic spirals or eventually become S0's requires considerably more study for a definitive answer.

I wish to thank John Stauffer for providing RDDO classifications for the A1367 galaxies and Allan Sandage for supplying data on the morphological types of field galaxies. I also thank Bob Kennicutt, W.L.W. Sargent, and Bob Schommer for several interesting discussions. Finally, it gives me great pleasure to thank Stirling L. Huntley for continued support during this work.

TABLE 1

FIELD SPIRALS

NGC/ IC	Type	W_λ(Hα)	[NII]/ Hα	[SII]/ Hα	M(HI)/ L	M_B	B-V	μ_{25}	V_r
(1)	(2)	(3)	(4)	(5)	(6)	(7)	(8)	(9)	(10)
N2655	0	1.2	5.8	...	0.091[b]	10.95	0.75	14.2	1623
N2681	0	<	4.0[c]	...	...	11.10	0.72	13.7	760
N3166	0	<	2.8[c]	...	...	11.50	0.80	14.2	1203
N4753	0	<	...	...	...	10.85	0.85	13.7	1137
N5363	0	<	...	...	...	11.2	0.90	13.7	1081
N5701	0	<	...	...	...	11.40	0.75	14.1	...
N2639	1	7.1	...	...	...	12.65	0.77	13.5	3359
N2775	1	<	...	...	...	11.20	0.78	14.0	965
N2782	1	85.	0.49	0.32	0.14[a]	12.15	0.56	14.6	2529
N3169	1	1.9	3.00	1.6	0.11	11.25	0.71	14.0	1051
N3190	1	<	2.1[c]	...	...	11.95	0.84	14.1	1216
N3227	1	43.	2.0	0.43	0.028	11.55	0.72	14.8	1050
N5377	1	<	4.9[c]	...	...	12.0	0.71	14.6	1950
N5448	1	6.8	1.60	...	...	12.2	...	14.4	2100
N2146	2	52.	0.69	0.33	...	11.20	0.58	14.4	1028
N3504	2	43.	0.94	0.31	...	11.8	0.63	13.6	1479
N5566	2	<	...	...	...	11.35	0.71	14.2	1489
N7217	2	<	4.3[c]	...	0.026	11.10	0.76	13.6	1227
N2613	3	<	...	...	0.017	11.35	0.65	14.2	1444
N2683	3	1.5	1.93	...	0.093	10.55	0.73	13.8	242
N2841	3	<	2.6[c]	...	0.083	10.10	0.73	13.7	700
N3344	3	5.0	0.71	...	0.24	10.50	0.50	14.5	513
N3351	3	17.7	0.45	0.19	...	10.50	0.71	14.3	673
N3627	3	0.5	...	...	0.042	9.70	0.60	13.5	583

TABLE 1 (CONT'D)

NGC/ IC	Type	W_λ(Hα)	[NII]/ Hα	[SII]/ Hα	M(HI)/ L	M_B	B-V	μ_{25}	V_r
(1)	(2)	(3)	(4)	(5)	(6)	(7)	(8)	(9)	(10)
N4995	3	8.8	1.20	...	...	11.90	0.78	14.3	1577
N5746	3	<	...	...	...	11.40	0.75	14.1	1786
N2268	4	13.	0.39	...	...	12.20	0.56	14.2	2466
N2903	4	27.	0.53	0.23	0.17	9.50	0.53	14.1	462
N2964	4	40.	0.64	0.26	...	12.05	0.61	13.6	1261
N3310	4	62.	0.47	0.31	0.21	11.2	0.24	13.6	1063
N3521	4	2.2	...	...	0.30	9.70	0.74	13.7	640
N3646	4	6.6	...	...	...	11.85	0.54	14.2	4194
N5005	4	17.[d]	...	0.36[e]	0.13[b]	10.64	0.71	13.4	1069
N5055[f]	4	3.0	0.80	...	...	9.30	0.64	14.1	587
N5194	4	13.0	1.43	0.39	0.11	8.95	0.52	13.6	565
N5248	4	15.5	0.35	...	0.15[b]	10.80	0.55	14.4	1102
N5371	4	<	5.1[c]	...	0.13	11.40	0.57	14.2	2660
N1637	5	19.	0.85	...	0.31	11.60	0.53	13.9	626
N1961	5	6.8	1.85	...	...	11.9	0.54	14.5	4065
N2276	5	135.	0.37	0.23	...	11.95	0.46	13.8	2579
N2525	5	19.	0.81	...	...	12.20	0.45	14.0	1348
N2776	5	11.	0.36	...	0.45	12.20	0.48	14.3	2643
N2976	5	60.	0.32	...	...	10.85	0.58	13.4	175
N3079	5	8.1	1.08	0.65	0.25	11.20	0.46	13.8	1212
N3198	5	3.2	...	...	0.57	10.94	0.42	14.5	691
N3294	5	28.	0.31	...	...	12.2	0.40	14.0	1507
N3359	5	14.	...	...	0.49	11.00	0.45	14.5	1124
N3726	5	10.	0.50	...	0.52	10.95	0.43	14.4	818
N4605	5	19.	0.25	0.26	...	10.96	...	13.6	286
N5033	5	4.3	1.87	0.98	0.57	10.60	0.44	14.9	961

TABLE 1 (CONT'D)

NGC/ IC	Type	W_λ(Hα)	[NII]/ Hα	[SII]/ Hα	M(HI)/ L	M_B	B-V	μ_{25}	V_r
(1)	(2)	(3)	(4)	(5)	(6)	(7)	(8)	(9)	(10)
N3556	6	35.	0.42	0.35	0.28	10.65	0.46	13.8	772
N6015	6	13.	0.28	...	0.27	11.65	0.43	14.2	1047
N6503	6	8.5	0.48	0.44	0.33	10.90	0.50	13.6	315
I342	6	66.	0.57	0.16	...	9.12	...	15.2	228
N5585	7	15.	0.33	...	0.59	11.4	0.41	14.5	462
N1569	10	124.	0.11	0.14	0.20	11.95	0.46	13.4	87

[a]H I from Heckman et al. (1978).

[b]H I from Lewis and Davies (1973).

[c]Equivalent width [N II].

[d]Equivalent width Hα + [N II].

[e][S II]/Hα + [N II].

[f]Exposure interrupted by earthquake.

TABLE 2

RESULTS OF KENDALL RANK CORRELATION TESTS

	Slit Data			Aperture Date		
Quantities	n	K^*	τ	n	K^*	τ
Hα vs B-V	48	-3.21	-0.32	38	-3.13	-0.35
Hα vs T	51	2.96	0.29	38	2.05	0.23
Hα vs μ_{25}	51	-0.61	-0.06	36	-1.17	-0.14
Hα vs M(H)/L	26	1.87	0.26	...	...	...
Hα vs M_B	43	1.34	0.14	30	0.00	0.00

TABLE 3

ABELL 1367 SPIRALS

Zw (1)	Other (2)	W_λ(Hα) (3)	Type (4)		V_r (5)	M_{pg} (6)
97-26	NGC 6583	52	Sp		6120[a]	13.9
41		6.8	Sp		6632	15.5
62		56	Sp		7680	15.6
64		<	Sp			15.6
68		30	Sp		5898	14.7
72		10	Sp		6240	15.0
73		95	Sp	(Sc)	7239	15.6
76	NGC 6680	<	Sp	Ab		15.5
79		153	Ir	(Ir)	6942	15.7
82	IC 2951	<	Sp	(Ab)	6100	15.0
87	NGC 6697	25	Sp	(Sc)	6571	14.3
91	NGC 3840	16	Sp	(Sb)	7312	15.0
92		45	Sp	(Ab)	6424	15.5
93		44	Sp	(Sb)	4865	15.5
101		<	S0/Sp	(Ab)	6382	15.3
102		2.0	Sp		(6330)[b]	15.1
105		<	S0/Sp	(Ab)	5368	15.4
117	NGC 3857	<	Sp	(Ab)	6183	15.1
120	NGC 3860	18	Sp	(Ab)	5390	14.5
121	NGC 6719	2.5	Sp	(Ab/Sb)	6583	14.6
122	NGC 3859	29	Sp	(Sc)	5432	14.9
129	NGC 3861	2.6	Sp	(Sc)	4956	14.0
130	NGC 3864	<	Sp	(Ab)	6924	15.5
134	NGC 3867	<	S0/Sp	(Ab)	7384	14.6
149		<	Sp			15.6
152		<	S0/Sp			14.1
127-24	NGC 3808	16	Sp		6950[b]	14.1

TABLE 3 (CONT'D)

Zw (1)	Other (2)	W_λ(Hα) (3)	Type (4)	V_r (5)	M_{pg} (6)
28	NGC 3832	8.5	Sp	(7060)[b]	14.0
32	NGC 3821	<	Sp	5731[a]	13.8
45	NGC 6725	7.5	Sp	6841[b]	14.5
52	NGC 3884	4.3	Sp	6937[a]	14.0
54	NGC 3883	<	Sp	7330[a]	14.2
72	NGC 6821	3.0	Sp	(6466)[b]	14.6
82		21	Sp	6485[a]	14.7
95	NGC 3947	12	Sp	6289	14.2
100	NGC 6876	<	Sp		14.9

Notes to Table 3:

[a]Redshift from Dickens and Moss (1976).

[b]Redshift this paper. $V_r = V_\odot - 70$ km s^{-1}.

REFERENCES

Balik, B., Faber, S. M., and Gallagher, J. S. 1976, Ap. J., 209, 710.

Burbidge, E. M., and Burbidge, G. R. 1962, Ap. J., 135, 694.

Burbidge, G. R., and Burbidge, E. M. 1965, Ap. J., 142, 634.

Butcher, H., and Oemler, A. 1978, Ap. J., 226, 559.

Cohen, J. G. 1976, Ap. J., 203, 587.

Cowie, L. L., and McKee, C. F. 1977, Ap. J., 211, 135.

Davies, R. D., and Lewis, B. M. 1973, M.N.R.A.S., 165, 231.

Dickens, R. J., and Moss, C. 1976, M.N.R.A.S., 174, 74.

Dressler, A. 1980, Ap. J., in press.

Gisler, G. R. 1978, M.N.R.A.S., 183, 633.

Gregory, S. A. 1975, Ap. J., 199, 1.

Gudehus, D. H. 1976, Ap. J., 208, 267.

Gunn, J. E., and Gott, J. R. 1972, Ap. J., 176, 1.

Heckman, T. M., Balik, B., and Sullivan, W. T. 1978, Ap. J., 224, 745.

Hollander, M. and Wolfe, D. A. 1973, Nonparametric Statistical Methods (New York: Wiley), p. 185.

Huchtmeier, W. K., Tammann, G., and Wendker, H. J. 1976, Astr. Ap., 46, 381.

Jones, C., Mandel, E., Schwarz, J., Forman, W., Murray, S. S., and Harnden, F. R. 1979, Ap. J. (Letters), submitted.

Kent, S. M. 1979a, Pub. A.S.P., 91, 394.

_____ 1979b, preprint [Chapter II this thesis].

Krumm, N., and Salpeter, E. E. 1979, Ap. J., 227, 776.

Lewis, B. M., and Davies, R. D. 1973, M.N.R.A.S., 165, 213.

Morgan, W. W. 1958, Pub. A.S.P., 70, 364.

Mushotzky, R. F., Serlemitsos, P. J., Smith, B. W., Boldt, E. A., and Holt, S. S. 1978, Ap. J., 225, 21.

Oemler, A. 1974, Ap. J., 194, 1.

Roberts, M. S. 1975, in Galaxies and the Universe, ed. A. Sandage, M. Sandage and J. Kristian (Chicago: University of Chicago Press), ch. 9.

Sandage, A. 1961, Hubble Atlas of Galaxies (Washington: Carnegie Institution of Washington).

Sérsic, J. L., and Pastoriza, M. G. 1967, Pub. A.S.P., 79, 152.

Strom, S. E., and Strom, K. M. 1978, in IAU Symposium No. 77, Structure and Properties of Nearby Galaxies, ed. E. M. Berkhuijsen and R. Wielebinski (Dordrecht: D. Reidel), p. 69.

Sullivan, W. T., and Johnson, P. E. 1978, Ap. J., 225, 751.

Tammann, G. A., Yahil, A., and Sandage, A. 1979, Ap. J., in press.

Tifft, W. G. 1978, Ap. J., 222, 54.

van den Bergh, S. 1976, Ap. J., 206, 883.

de Vaucouleurs, G. 1959, Handbuch der Physik, 53, 286.

de Vaucouleurs, G., de Vaucouleurs, A., and Pence, W. 1974, Ap. J. (Letters), 194, L119.

de Vaucouleurs, G., de Vaucouleurs, A., and Corwin, H. G. 1976, Second Reference Catalog of Bright Galaxies (Austin: University of Texas).

Weedman, D. 1977, Ann. Rev. Astr. Ap., 15, 69.

Zwicky, F., and Herzog, E. 1963, Catalog of Galaxies and and Clusters of Galaxies, Vol III (Pasadena: California Institute of Technology).

FIGURE 1

Distribution of continuum and Hα light along slit for field galaxies. Top: continuum profile. Bottom: Hα profile. Length of each profile is 4!7; west is at left.

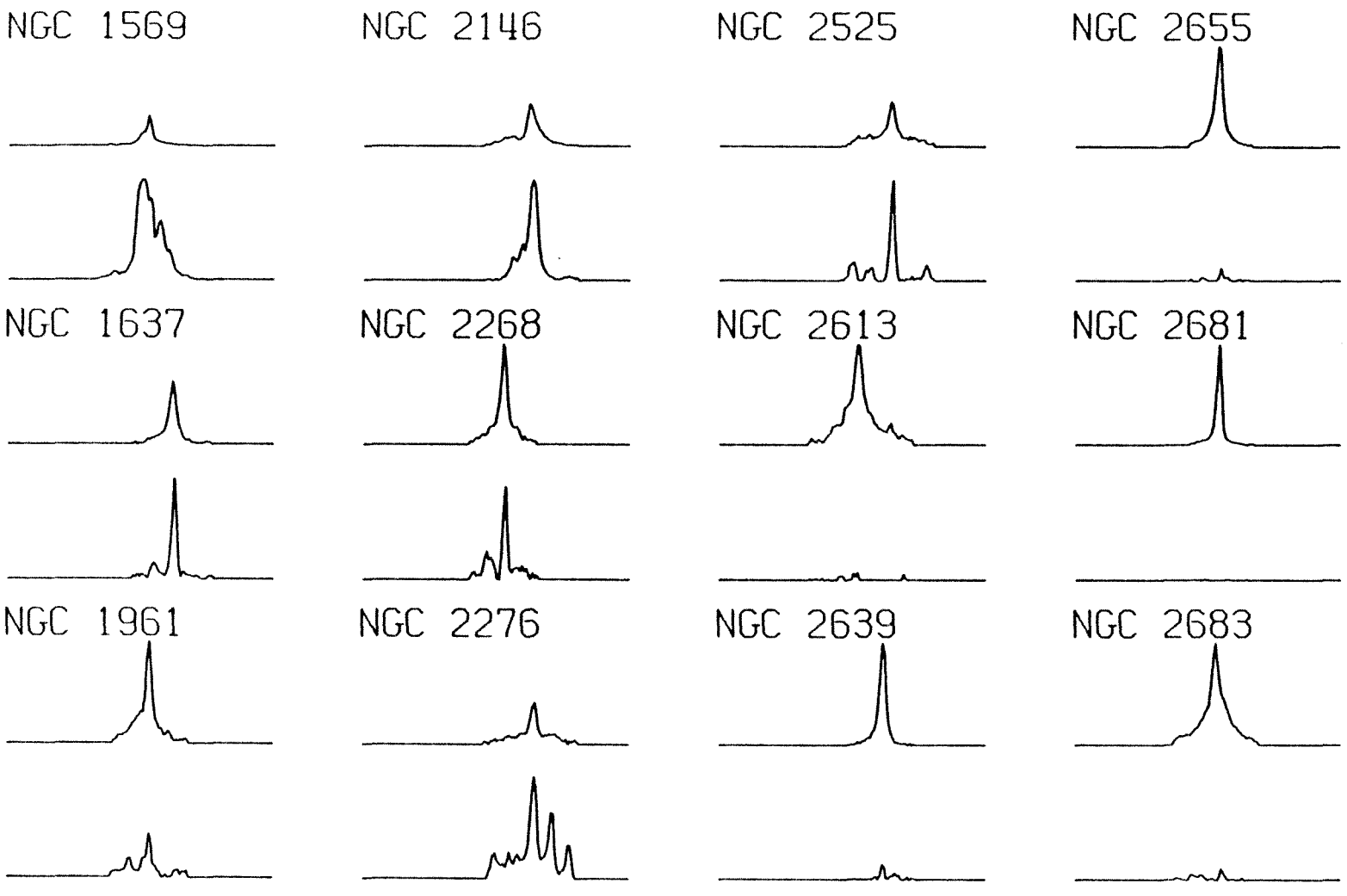
NGC 1569
NGC 2146
NGC 2525
NGC 2655
NGC 1637
NGC 2268
NGC 2613
NGC 2681
NGC 1961
NGC 2276
NGC 2639
NGC 2683

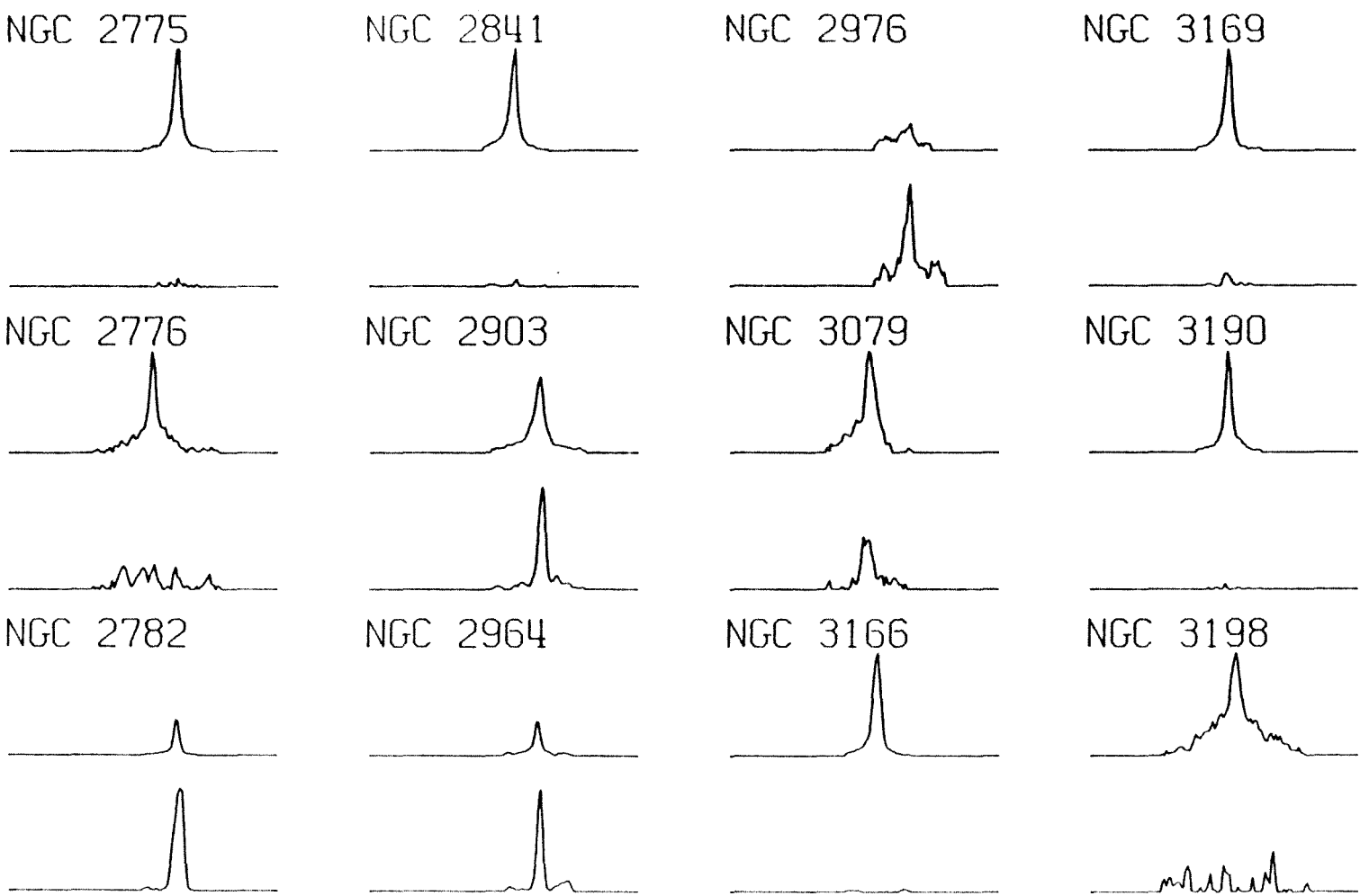
NGC 2775
NGC 2841
NGC 2976
NGC 3169
NGC 2776
NGC 2903
NGC 3079
NGC 3190
NGC 2782
NGC 2964
NGC 3166
NGC 3198

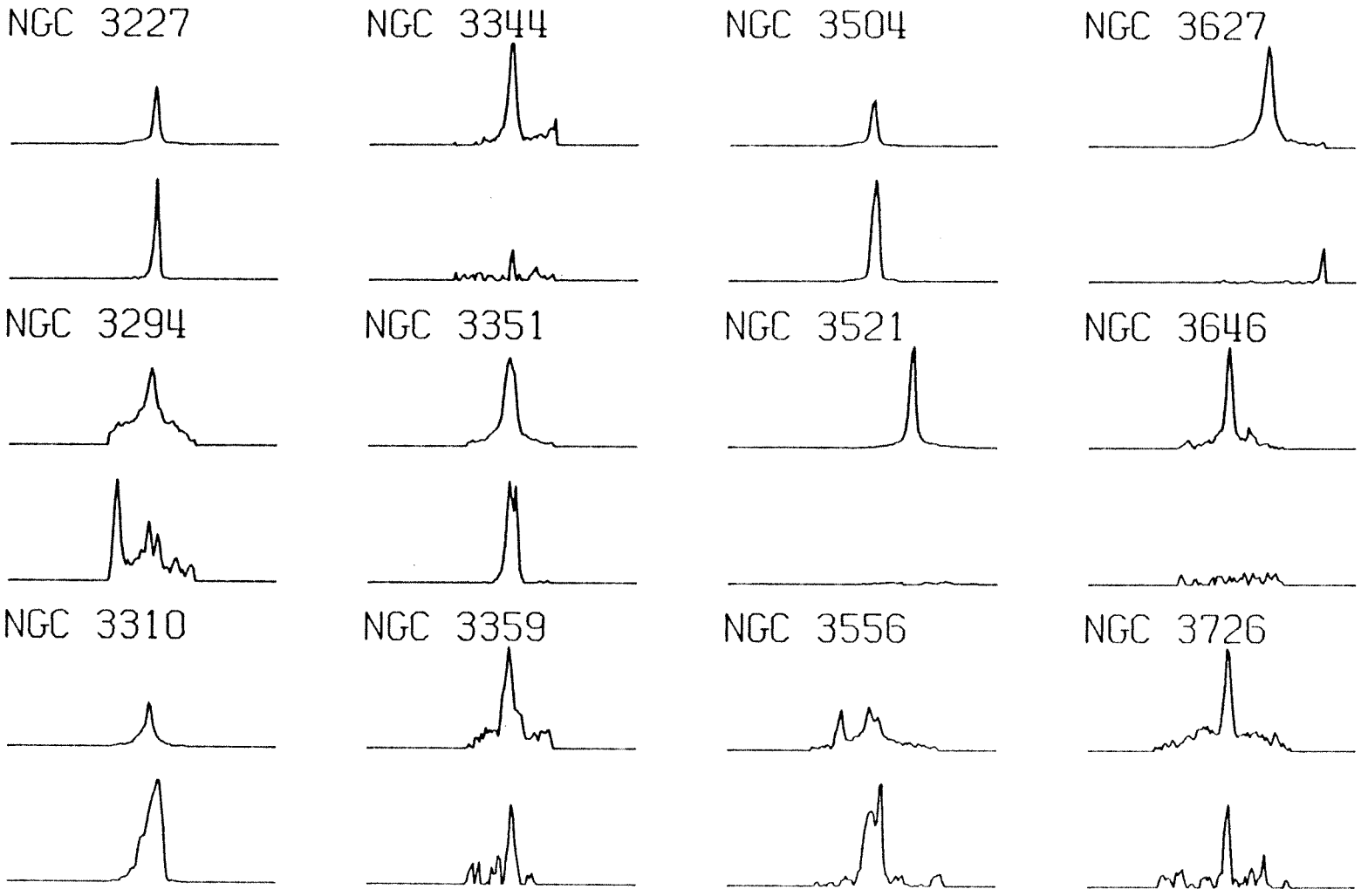
NGC 3227
NGC 3344
NGC 3504
NGC 3627
NGC 3294
NGC 3351
NGC 3521
NGC 3646
NGC 3310
NGC 3359
NGC 3556
NGC 3726

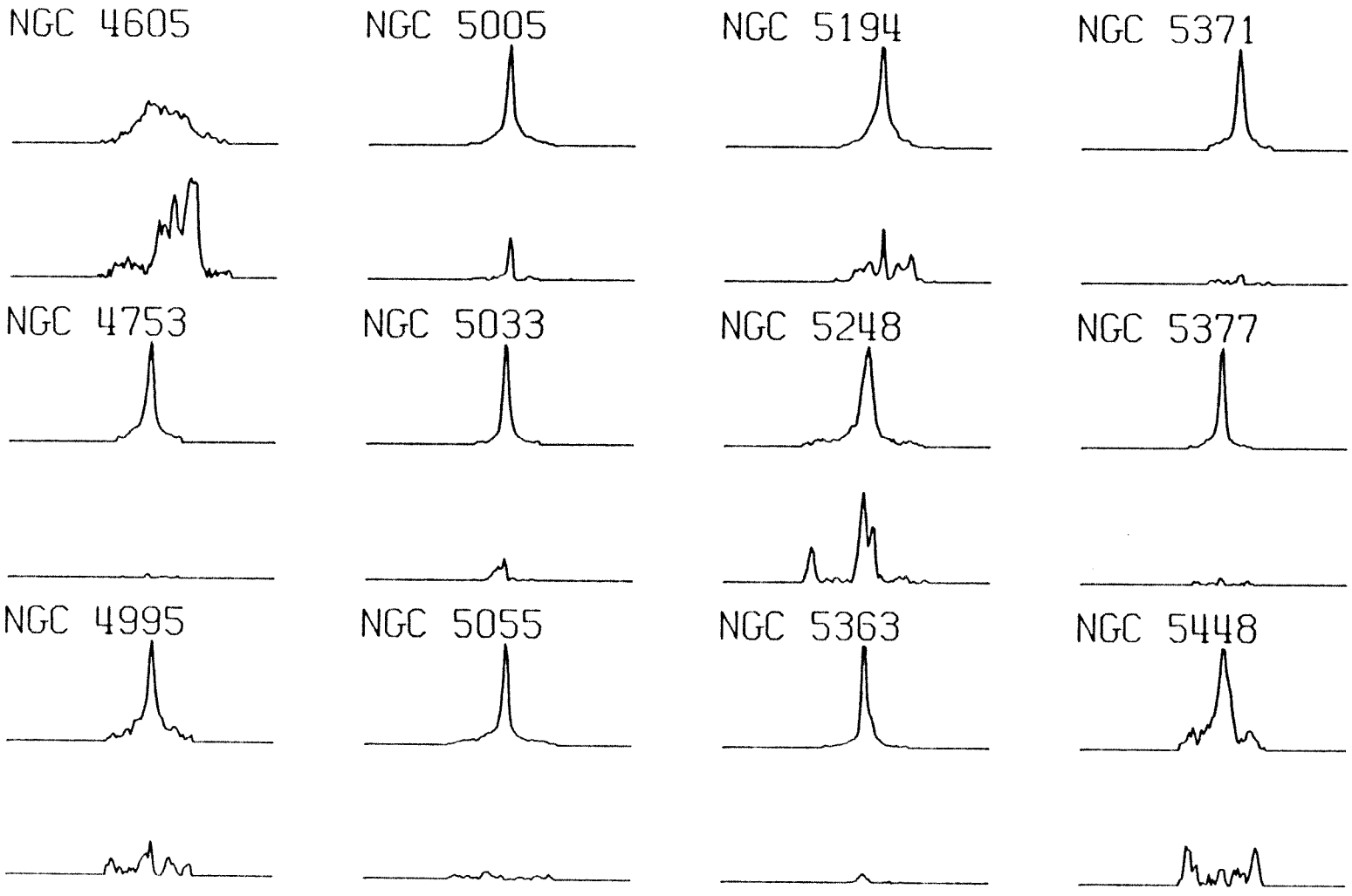
NGC 4605
NGC 5005
NGC 5194
NGC 5371
NGC 4753
NGC 5033
NGC 5248
NGC 5377
NGC 4995
NGC 5055
NGC 5363
NGC 5448

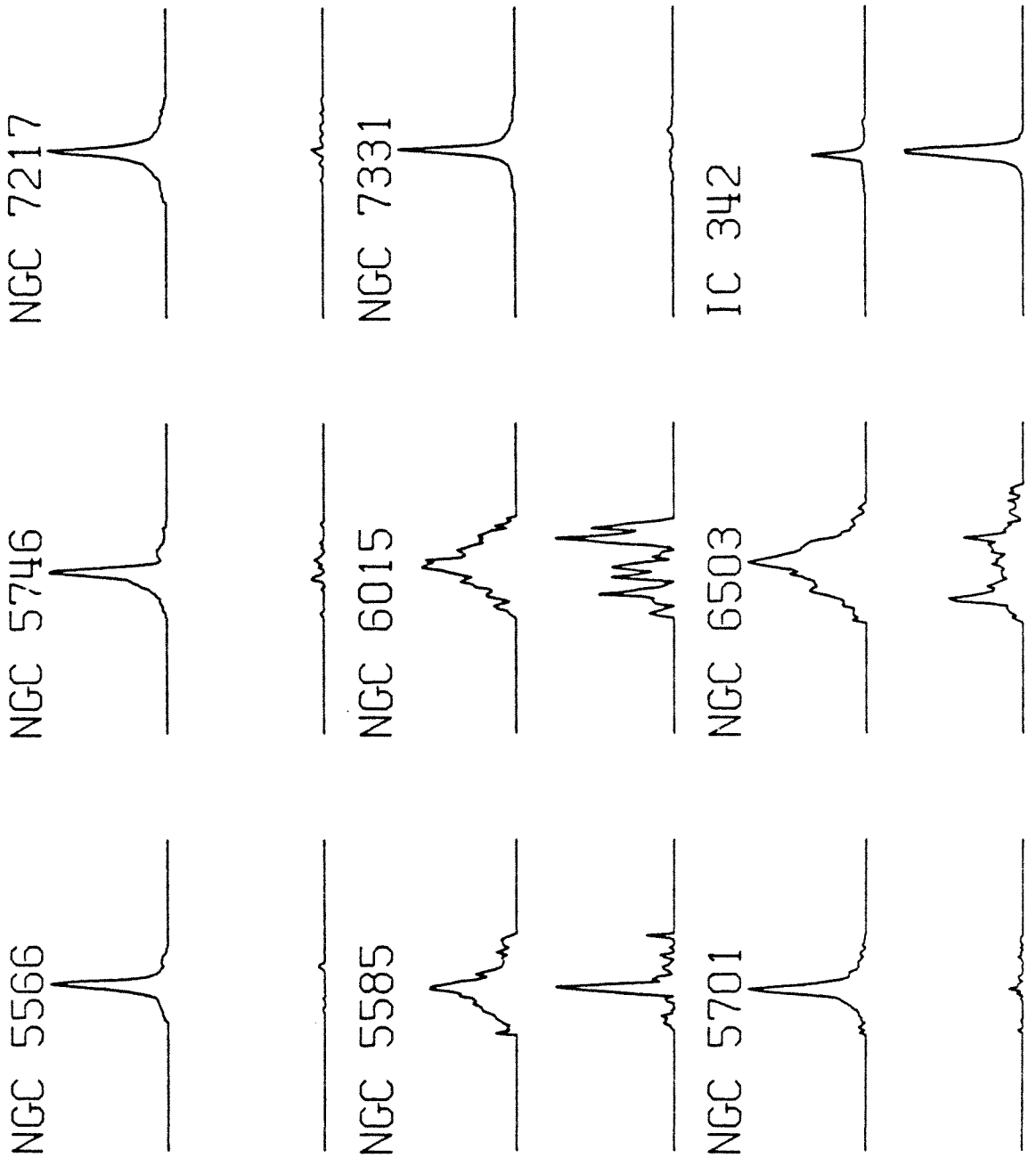
NGC 5566
NGC 5746
NGC 7217
NGC 5585
NGC 6015
NGC 7331
NGC 5701
NGC 6503
IC 342

FIGURE 2

Comparison between slit data (this paper) and aperture data (Cohen 1976) for galaxies observed in common.

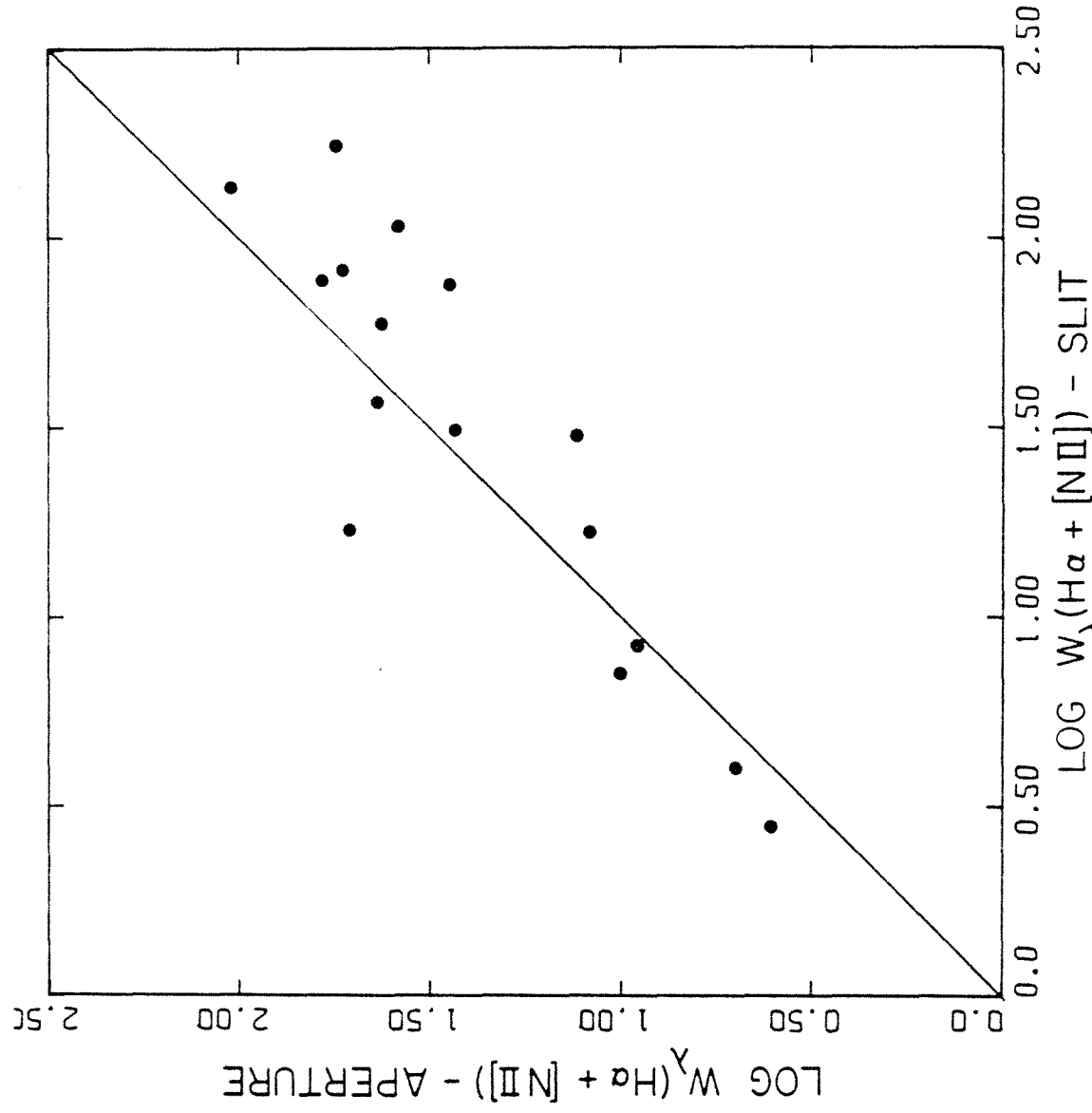
0.0
0.50
1.00
1.50
2.00
2.50
LOG $W_\lambda(H\alpha + [NII])$ - SLIT
LOG $W_\lambda(H\alpha + [NII])$ - APERTURE

FIGURE 3

Correlation between Hα and B-V color. Crosses: data from Cohen (1976). Filled circles: data from this paper.

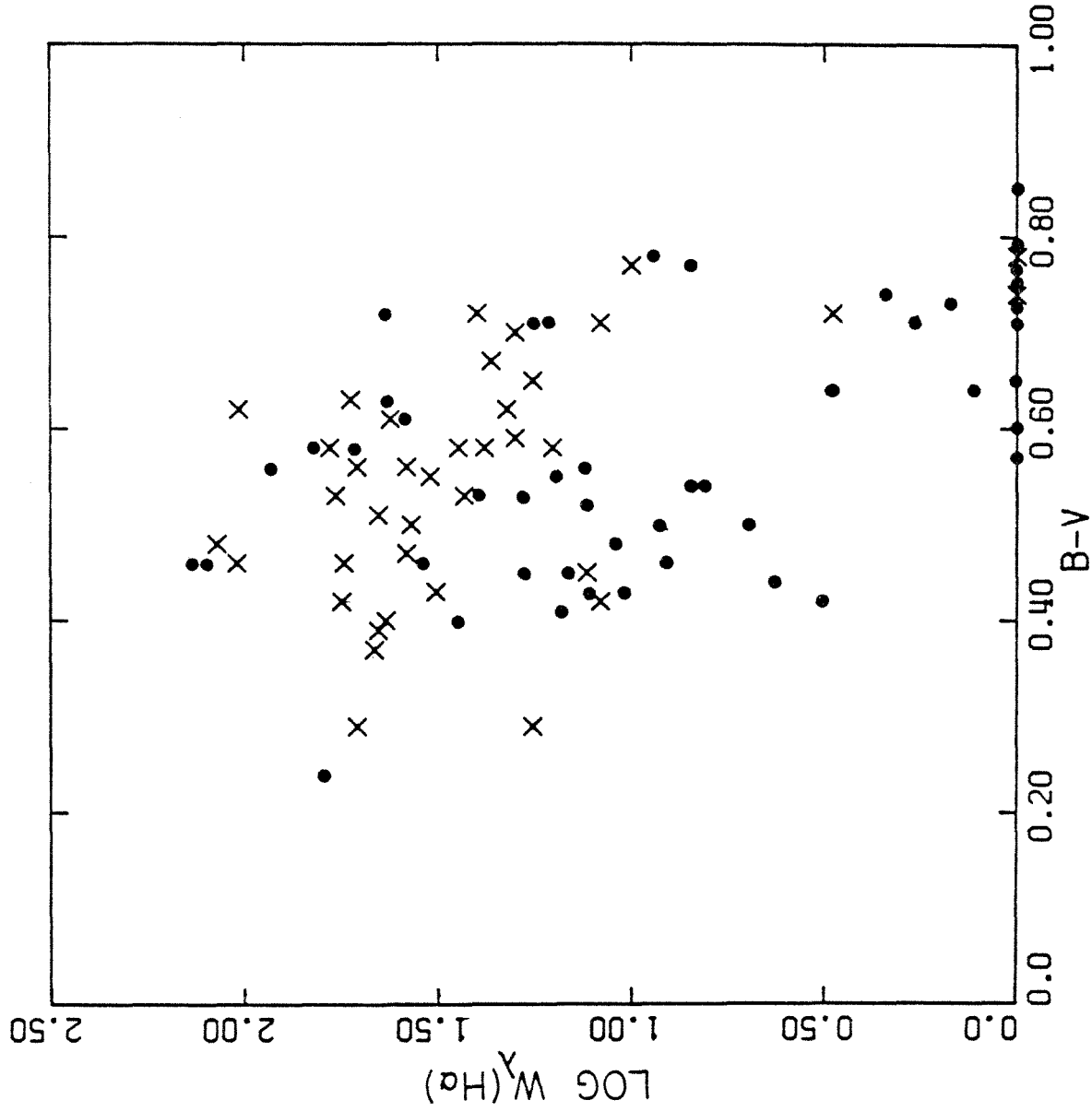
LOG $W_\lambda(H\alpha)$
B-V
0.0
0.50
1.00
1.50
2.00
2.50
0.0
0.20
0.40
0.60
0.80
1.00

FIGURE 4

Same as Fig. 3 but for Hα vs. morphological type.

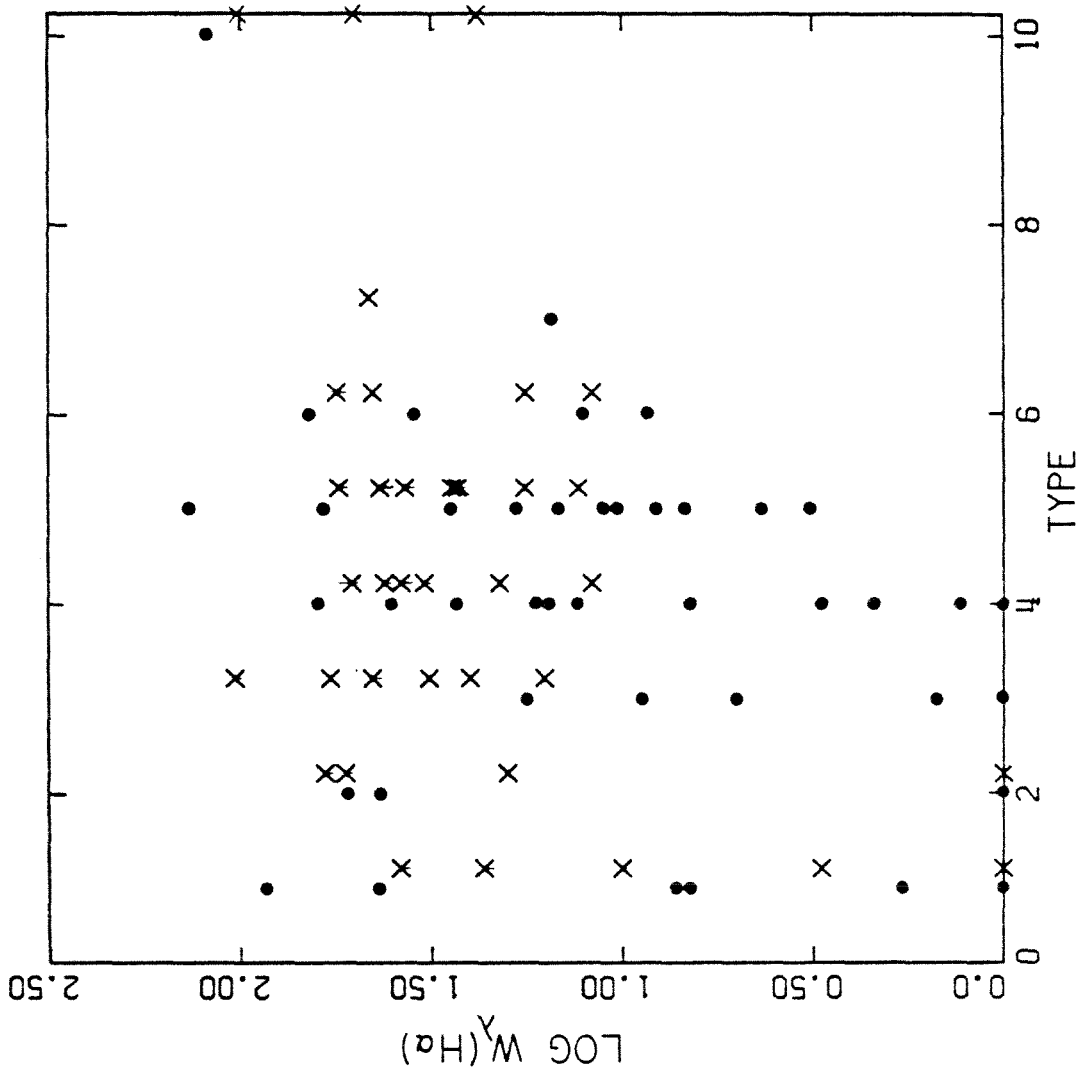
LOG $W_\lambda(H\alpha)$
0.0
0.50
1.00
1.50
2.00
2.50
TYPE
0
2
4
6
8
10

FIGURE 5

Same as Fig. 3 but for Hα vs. surface brightness.

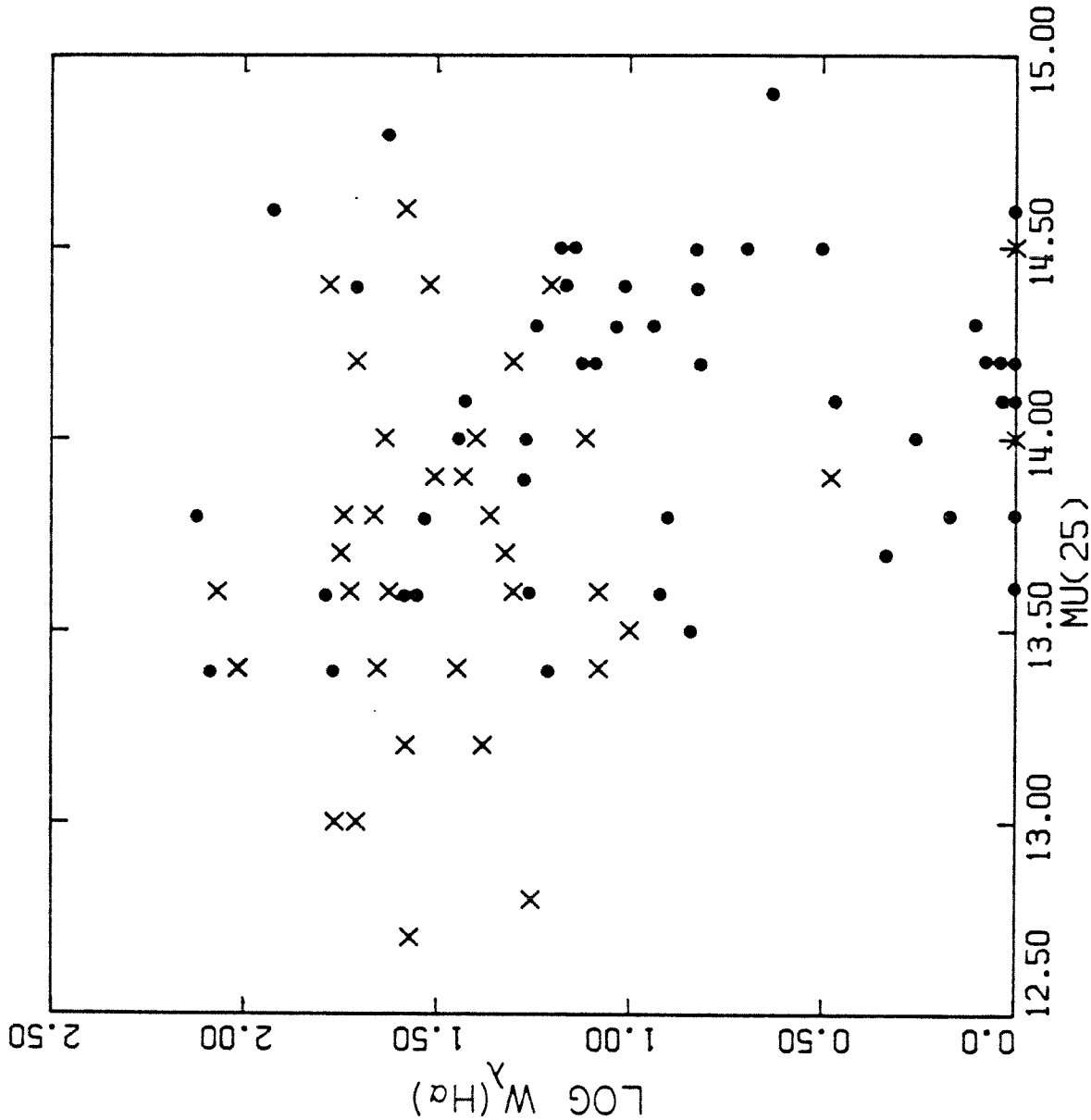
15.00
14.50
14.00
13.50
13.00
12.50
MU(25)
0.0
0.50
1.00
1.50
2.00
2.50
LOG $W_\lambda(H_\alpha)$

FIGURE 6

Same as Fig. 3 but for Hα vs. neutral hydrogen M_H/L.

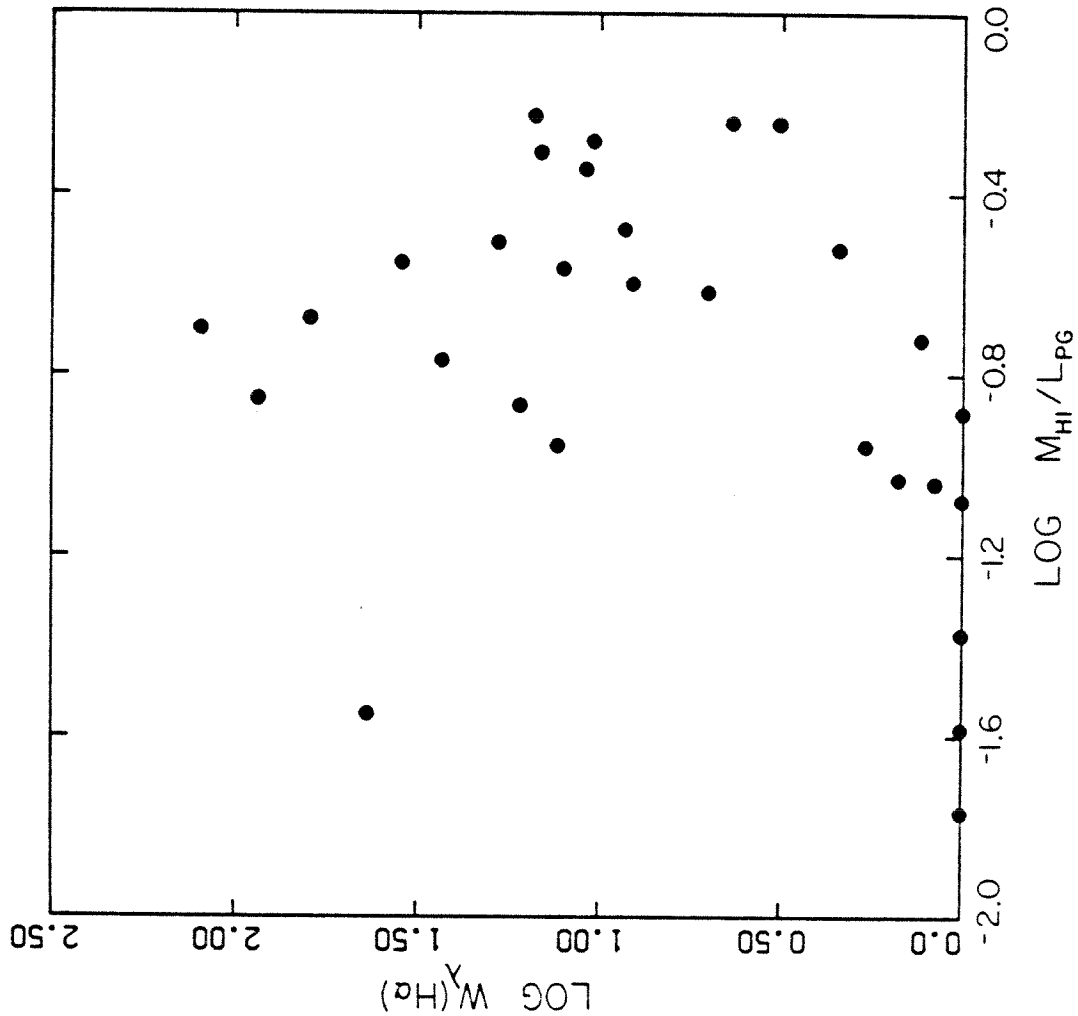
0.0
-0.4
-0.8
-1.2
-1.6
-2.0
LOG M_{HI}/L_{PG}
0.0
0.50
1.00
1.50
2.00
2.50
LOG $W_\lambda(H\alpha)$

FIGURE 7

Same as Fig. 3 but for Hα vs. absolute B magnitude.

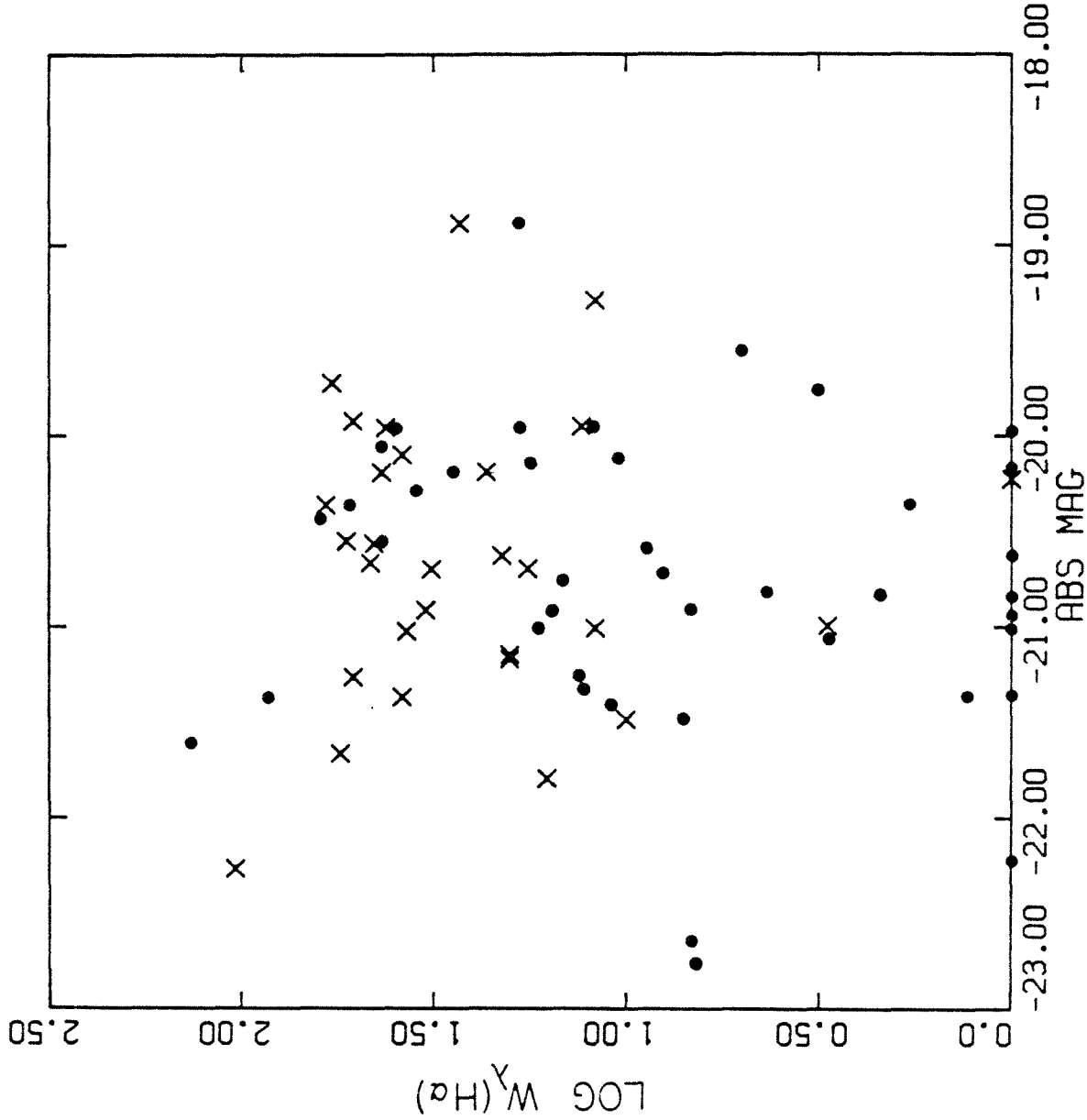
-18.00
-19.00
-20.00
-21.00
-22.00
-23.00
ABS MAG
0.0
0.50
1.00
1.50
2.00
2.50
LOG $W_\lambda(H\alpha)$

FIGURE 8

Distribution of field galaxies as a function of Hα equivalent width. a) Slit data (this paper); b) aperture data (Cohen 1976). Shaded areas represent galaxies with upper limits to Hα.

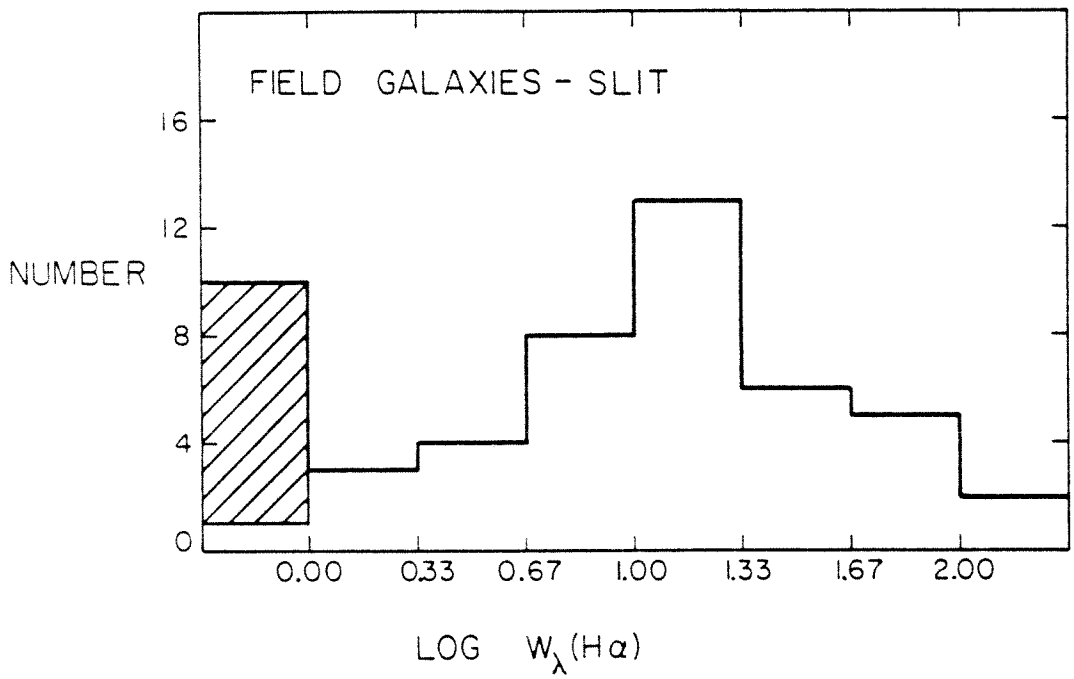
FIELD GALAXIES - SLIT
NUMBER
16
12
8
4
0
0.00
0.33
0.67
1.00
1.33
1.67
2.00
LOG W_λ(Hα)

(a)

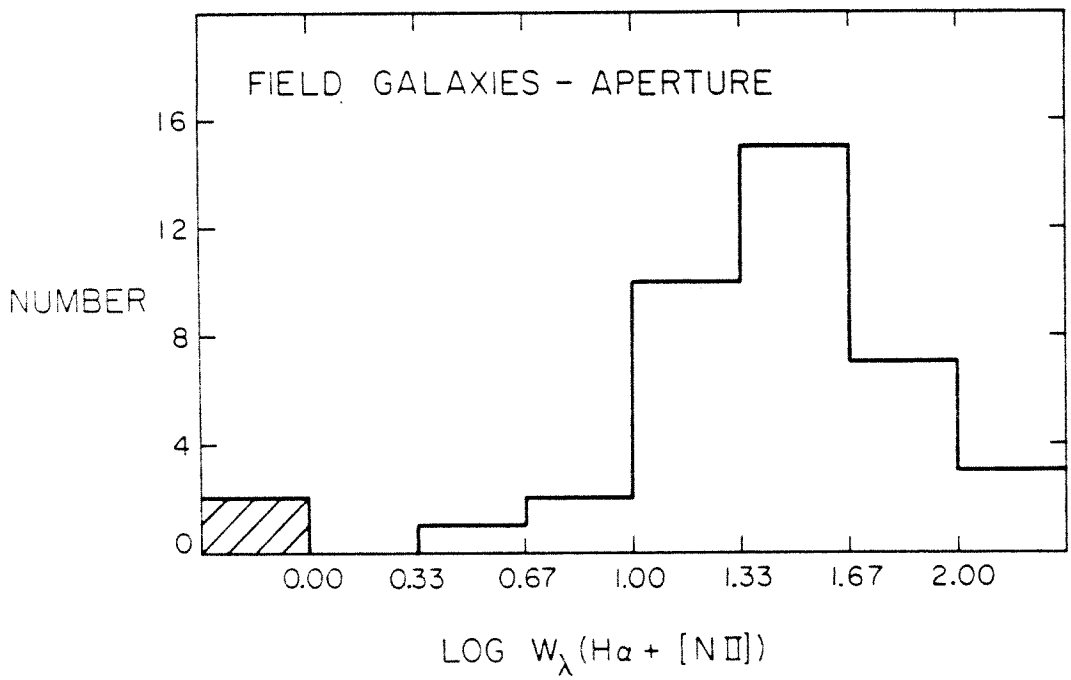
FIELD GALAXIES - APERTURE
NUMBER
16
12
8
4
0
0.00
0.33
0.67
1.00
1.33
1.67
2.00
LOG W_λ(Hα + [N II])

(b)

FIGURE 9

Distribution of A1367 spirals as a function of Hα equivalent width. Galaxies with no detected Hα, indicated by shaded area, are plotted at the values of their upper limits.

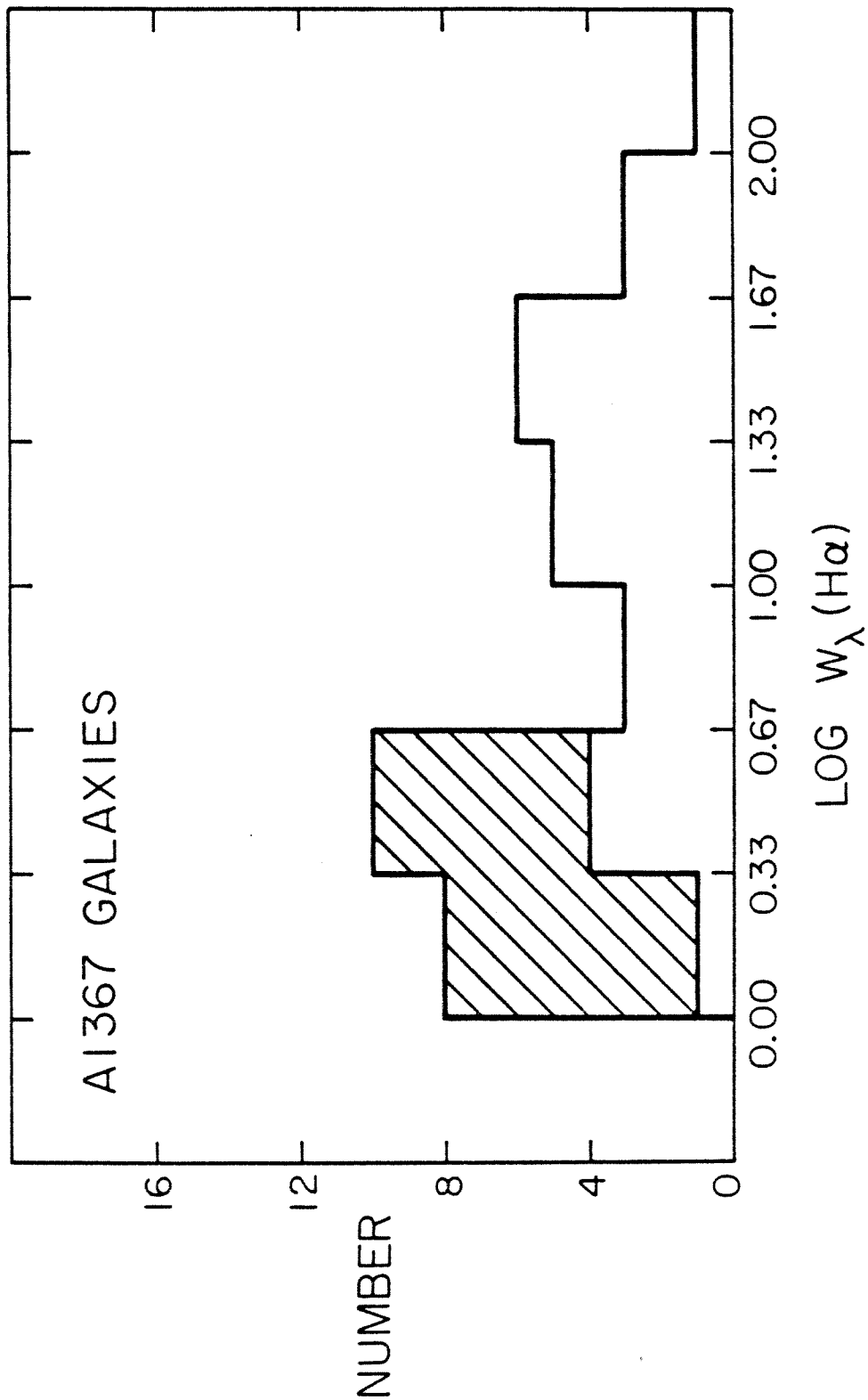
A1367 GALAXIES
NUMBER
0
4
8
12
16
0.00
0.33
0.67
1.00
1.33
1.67
2.00
LOG W_λ (Hα)

FIGURE 10

Plot on sky of all galaxies in A1367 listed in CGCG. North of 21° $30'$ only galaxies for which spectra were obtained are plotted. Filled circle: cluster center. Cross: x-ray centroid from Jones et al. (1979).

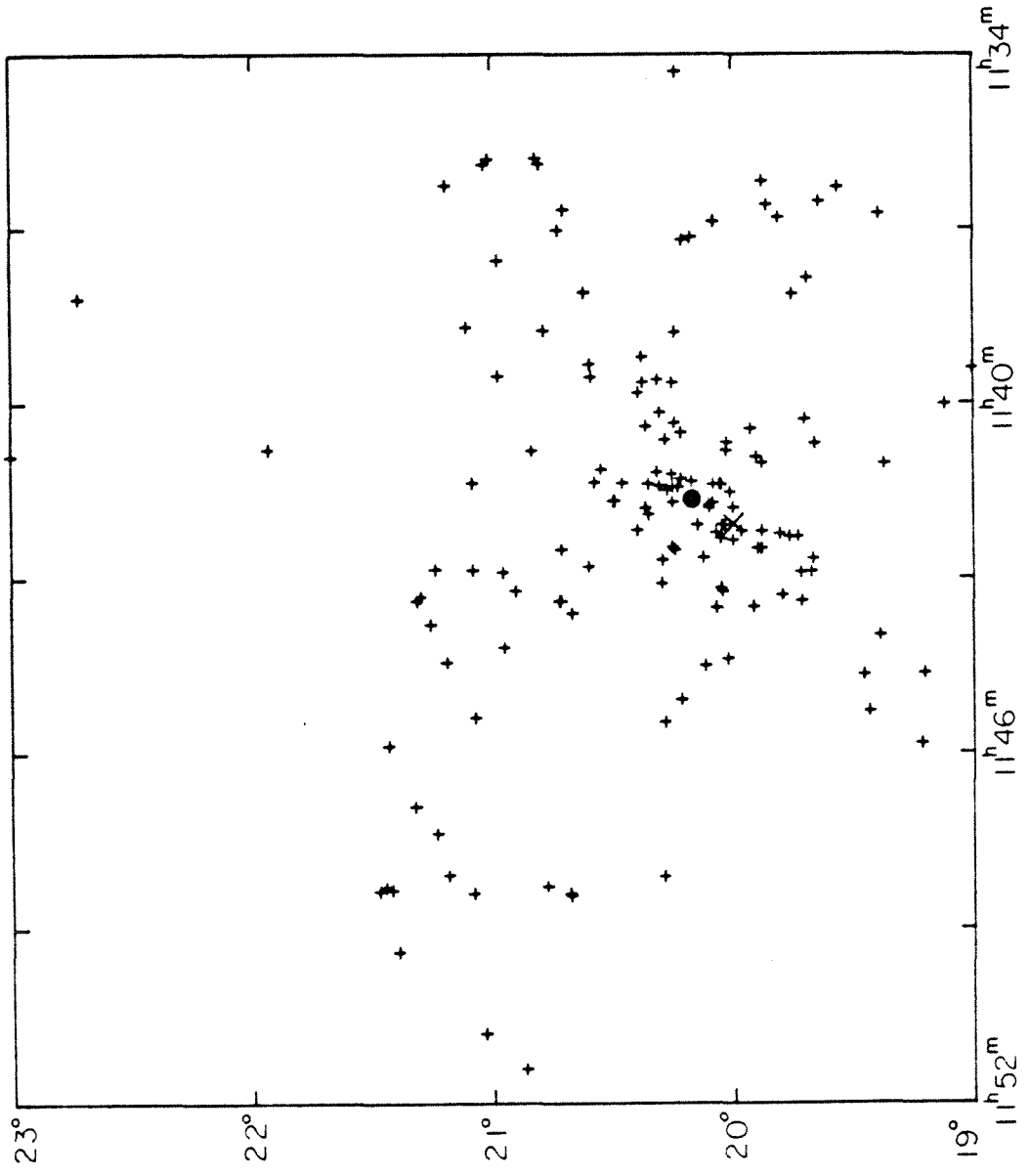
23°
22°
21°
20°
19°
11h34m
11h40m
11h46m
11h52m

FIGURE 11

Same as Figure 10 but only for galaxies listed in Table 3. Filled squares: galaxies with Hα detections; size indicates strength of detection. Open circles: no detections. Note difference in frequency of detection for galaxies northwest and southeast of cluster center.

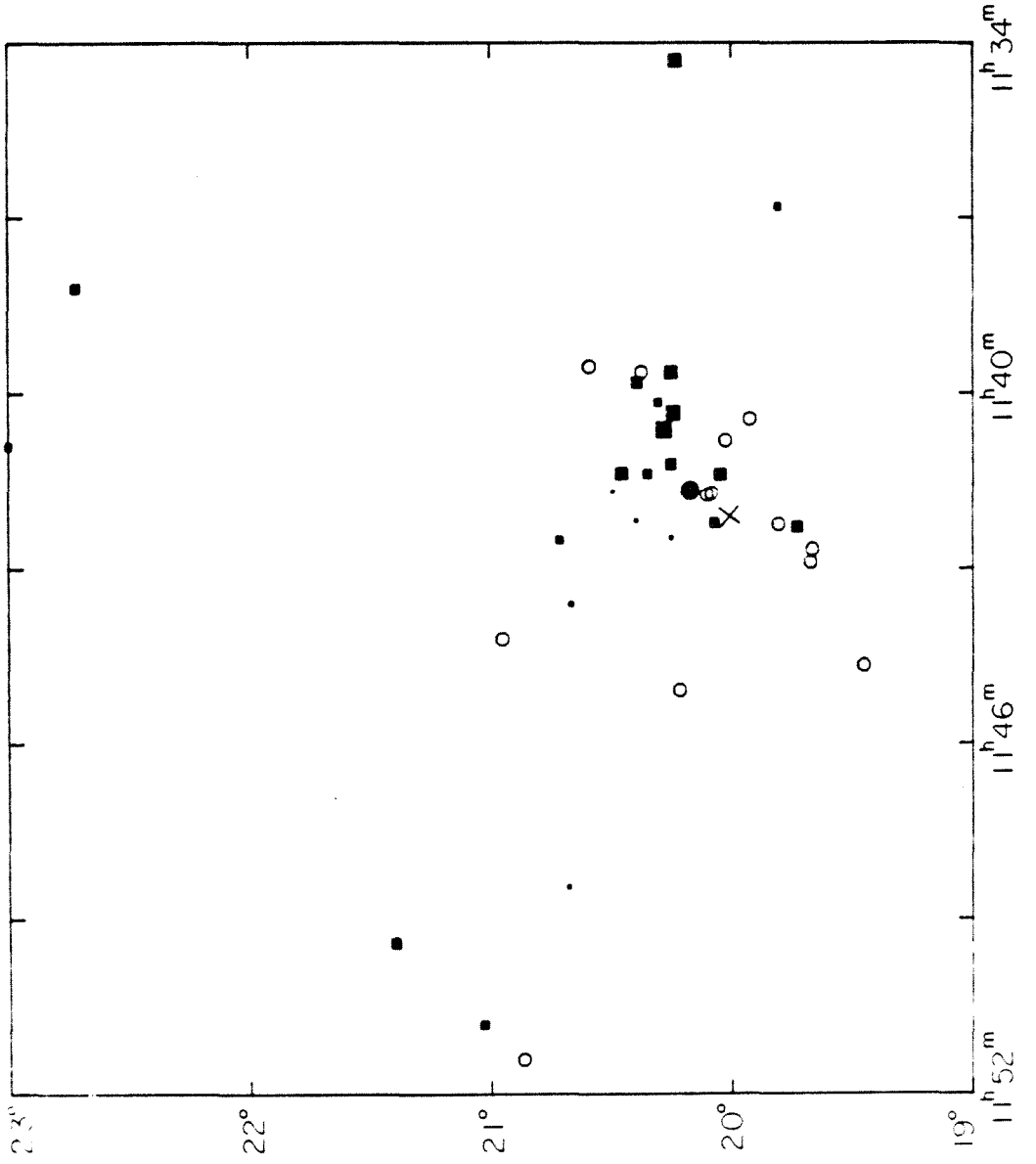
11h34m
11h40m
11h46m
11h52m
22°
21°
20°
19°

CHAPTER IV

ON THE DEMISE OF DISK GALAXIES IN RICH CLUSTERS

I. INTRODUCTION

A long-standing challenge to theories on the formation and evolution of galaxies has been to account for the observation that the morphology of galaxies in rich clusters is systematically different from that of galaxies in the field, in the sense that field galaxies are predominantly spirals, whereas clusters are composed primarily of SO's and ellipticals (e.g., Oemler 1974). A popular explanation for these observations is that clusters originally contained a population of galaxies like that of the field, but that a hot, intra-cluster medium (ICM) has removed the interstellar medium from the spirals, transforming them into SO's. Alternative mechanisms for this interaction include ram-pressure ablation by motion through the ICM (Gunn and Gott 1972) and thermal evaporation (Cowie and Songaila 1977). Numerous investigations of clusters of galaxies, especially those with X-ray emission, have lent qualitative support to these ideas (Bahcall 1977; Melnick and Sargent 1977; Butcher and Oemler 1978; Gisler 1978; Strom and Strom 1978; Tytler and Vidal 1978).

In a recent paper on the properties of galaxies in 55 rich clusters, Dressler (1980) presents evidence which casts serious doubt on the hypothesis that SO's are formed from spirals. In summary, his main arguments are:

1. Significant numbers of SO's are found in low

density regions where stripping or evaporation are presumably unimportant.

2. The population distribution Sp/SO/E is a slow function of the local projected density of galaxies only, and in particular, does not depend on the global properties of a cluster.

3. The bulges and bulge/disk (B/D) ratios are systematically larger for SO's than for spirals, and this differential exists in all density regimes. Furthermore, among the spirals and SO's individually, the bulges and B/D ratios increase with increasing density. If SO's were formed from spirals one would expect these quantities for the two populations to approach each other at high densities.

The purpose of this paper is to present a simple phenomenological explanation for the trends discovered by Dressler. It will be shown that by a combination of a systematic reduction in disk brightness with density of galaxies and a few, well-defined selection effects, all of Dressler's results can be quantitatively reproduced. Further, a quantitative relation between the brightness change and projected density of galaxies will be derived and then used to discuss the physical process by which the disk brightness might be determined.

II. THE SCENARIO

Following Dressler we consider the spirals and SO's to be composed of disks plus bulges, whereas the ellipticals are bulges only. The fundamental process which we shall assume is occurring has already been alluded to by Dressler, although not developed by him in any detail, namely that in regions of high density the disks of galaxies are systematically fainter relative to galaxies in regions of low density. Initially we do not specify how this state of affairs originated, and in fact we shall find below that the exact cause is far from obvious. However, we shall assume that all disks are fainter by equal amounts independent of the other properties of a galaxy.

A second and pivotal assumption is that the division of disk galaxies into spirals and SO's is a function of the B/D ratio only. Furthermore, the division occurs only after the brightness of a disk has been established. This assumption implies that whatever process determines the brightness occurs earlier in the formation of a galaxy than the process which determines whether it becomes a spiral or SO, and that the latter process is unaffected by the former.

We begin with an initial distribution of disk galaxies having properties which correspond to the lowest density region covered by Dressler ($\log \sigma = 0.0$ where σ is the projected surface density in galaxies Mpc^{-2}):

1. The luminosity function is taken to be a simple power law. From Figure 12 of Dressler it is seen to have the form

$$\log n(M) = 0.677\ M + \text{constant} ,$$

where n is the differential number count and M is the absolute magnitude. A magnitude limit at the faint end is imposed, and the turnover in Dressler's sample near this faint end is assumed to be due entirely to incompleteness (although Dressler has informed me that at least part of the turnover is probably intrinsic to the luminosity function).

2. At a given luminosity the disk galaxies will have some distribution in B/D ratio. Following Dressler we shall express this distribution in terms of the parameter $x \equiv m_{bul} - m_{tot}$. While the shape of the distribution can in principle be determined observationally, we shall instead assume it simply to be the sum of two Gaussians (one each for the SO's and spirals):

$$f(x) = A\, e^{-\frac{(x-x_1)^2}{2a_1^2}} + B\, e^{-\frac{(x-x_2)^2}{2a_2^2}} .$$

The initial parameters are taken to be:

SO's: $A = 0.28$ $x_1 = 1.03$ $a_1 = 0.49$,

Sp's: $B = 0.62$ $x_2 = 2.31$ $a_2 = 0.49$.

The SO/Sp ratio then has the convenient form

$$\frac{N(SO)}{N(Sp)} = \frac{A}{B} e^{\frac{x_2^2 - x_1^2}{2a^2}} e^{-\frac{(x_2 - x_1)}{a^2} x} = 37.3e^{-2.61x} . \quad (1)$$

By our second assumption this relation applies at all values of projected density.

3. We start with a population of ellipticals which form 10% of the total initial population. In all that follows the ellipticals and the bulges of the disk galaxies are assumed to remain unaffected.

A final selection effect must be discussed. Galaxies with very small disks may be indistinguishable from ellipticals. We therefore assume that all disk galaxies with x smaller than a minimum x_{min} are counted as ellipticals. x_{min} is taken to be a free parameter (it is, in fact, the only one in the entire calculation).

Our objective is to reproduce the measurements in Figures 4, 13, and 14 of Dressler, which are reproduced here in part in Figures 1-3. The procedure is as follows. We take the initial distribution of galaxies above which is a function of M and x. The disks of all galaxies are reduced by an amount Δm magnitudes. New values of M and x are computed for each galaxy and a new distribution function is derived. Incompleteness limits for faint galaxies are applied.

The distribution is then divided into spirals and SO's according to equation (1). For each group the medium values of x and bulge magnitude m_{bul} are derived and the population fraction is computed. All galaxies with $x < x_{min}$ are counted as ellipticals. The value of Δm is mapped onto log σ by matching the computed spiral fraction to the observationally determined curve of Dressler in Figure 1; the E and SO fractions fractions fall where they may. The median values of x and m_{bul} are then plotted in the appropriate places in Figures 2 and 3. The process is repeated for several values of Δm.

Before discussing the results a few comments are in order. Because we assume that the initial luminosity distribution is a power law and that all processes occur independent of luminosity, the luminosity function at all later stages will be unchanged (except for a constant scaling factor). Such is, in fact, what Dressler observes (see his Fig. 15). This invariance of the luminosity function also implies that changes in $m_{bul} - m_{tot}$ will be exactly correlated with changes in m_{bul}. We note also that any turnover in the initial luminosity function will be shifted to fainter magnitudes, a point which could be checked observationally.

The values for Δm were taken to range from 0 to 1.5 mag in 0.25 mag steps. The value of x_{min} was taken to be 0.13 mag. The results for these calculations are presented

in Figures 1-3, along with the measurements of Dressler. (The values of log σ for each value of Δm are also listed in Table 1 in the column labeled "observed".) In all figures the agreement is quite good, especially considering the crude nature of Dressler's data. First we discuss the nature of the trends in each figure and then comment on the significance of the agreement between observation and prediction.

In Figure 1 the decrease in spiral population which occurs in progressing to higher densities is the result of two factors. First, as the disks become fainter and the B/D ratio becomes larger, more SO's are formed from the available disk galaxies by virtue of the relation in equation (1). Second, and more important, reducing the disk brightness causes the fainter galaxies in the sample to fall below the magnitude limit. These two factors also alter the SO population, except that the first one increases the number of SO's. The fraction of ellipticals increases monotonically, primarily due to the relative decrease in the number of disk galaxies, but also in part due to the misclassification of disk galaxies with large B/D ratios; at the highest density $\sim$ 1/3 of the ellipticals are such galaxies. The apparent increase in absolute bulge magnitude in Figure 2 is due to the fact that galaxies with small bulges fall out of the sample. The decrease in $m_{bul} - m_{tot}$ in Figure 3 is, of

course, a direct consequence of the changes in disk brightness.

Just how fortuitous is the fit in view of the available degrees of freedom? In Figure 1, the predicted spiral fraction is made to match the observed curve by assumption. There is some freedom to adjust the corresponding SO and elliptical fractions by altering x_{min} (within reasonable limits), but the shapes of these curves are not adjustable. In Figure 2 no adjustments are possible. In Figure 3 the individual curves for the spirals and SO's can be shifted vertically by altering x_1 and x_2, but the shapes of the curves again cannot be adjusted. It is apparent then that the good agreement is not due simply to the arbitrary adjustment of the available parameters.

In view of the rather simple-minded nature of this calculation, one may well ask if other equally simple-minded (and possibly more physically motivated) scenarios are possible. We shall consider briefly three possible cases, and find that things are not as easy as they appear.

1. We consider a situation the same as above, but the disks, instead of simply becoming fainter, are processed into the bulges so that the total magnitude of a galaxy remains constant. While we could reproduce the increase in m_{bul} and decrease in $m_{bul} - m_{tot}$, the relative fraction of ellipticals would remain essentially unchanged.

2. We consider the initial SO population to stay constant while a fraction of the spirals (in turn a function of density) are stripped suddenly. The cessation in star formation could cause the disks to fade by perhaps as much as 1 mag in the blue, which is just enough to lower the B/D ratio to values typical for SO's. While this explains the decrease in spiral fraction, the SO/E ratio should increase at higher density, whereas the opposite occurs. Also, the decrease in $m_{bul} - m_{tot}$ for both spirals and SO's is not explained. One might have the spirals stripped and converted to SO's gradually, which would allow for a decrease in the spiral $m_{bul} - m_{tot}$. However, one is still left with the problem of the SO/E ratio and the systematic decrease in $m_{bul} - m_{tot}$ for the SO's.

3. A possible objection to the original scenario is that the SO/Sp ratio is assumed to be the same function of B/D regardless of whatever process determines the disk brightness. As an alternative one might consider the disks becoming fainter as above but treating spirals and SO's separately, i.e., the disk brightness is determined <u>after</u> the division of disk galaxies into spirals and SO's. Calculations show that this quickly leads to trouble, as if the disks change enough to reproduce the population fractions, the value of $m_{bul} - m_{tot}$ for both spirals and SO's decreases much faster than is observed.

III. WHY ARE DISKS FAINTER IN HIGH DENSITY REGIONS?

We are now left with the task of explaining the cause of the systematic change in disk brightness and why it follows a particular relation with density. The situation is rather perplexing, as the effect must be a very slow function of density. As can be seen from Table 1, a change of 2 decades in density requires a change of only 1.5 magnitudes (a factor of 4) in the disk. Also, the effect depends on density only and is independent of the other properties of a galaxy.

It turns out that even without knowing the nature of this process, we can still predict quantitatively how it must work. We proceed in the following, rather abstract manner. Assume that the mass of a disk is distributed with respect to some parameter y according to some function f. That is, we write

$$M(y) = f(y) \ ,$$

where M is the mass $\leq y$. We assume there is an upper cutoff y_{max}. The essential step we take is to assume that the mass distribution is cut off below some value y which depends only on the density of galaxies, i.e., $y = y(\sigma)$. The amount of mass lost is

$$\Delta M = f(y(\sigma)) \ ,$$

and the corresponding magnitude change of the disk becomes

$$\Delta m = -2.5 \log \left[1 - \frac{\Delta M}{M}\right] = -2.5 \log \left[1 - \frac{f(y(\sigma))}{f(y_{max})}\right] \ .$$

The form of the function f must be determined from the measurements in Table 1, and it is found that a logarithmic relation works well. That is,

$$\Delta m = -2.5 \log [1 - D \log \sigma] + C , \qquad (2)$$

where D and C are constants. This equation also implies that the relation between the cutoff value of y and σ is of the form $y \sim \sigma^{\alpha}$ where α is an arbitrary constant. Note that we could also run y in the opposite direction, i.e., have an intrinsic lower cutoff y_{min} to the distribution and then have the density impose an upper cutoff in y, without changing the form of the equation.

In Table 1 we list the predictions of equation (2) for log σ taking D = 0.384 and C = 0. With the possible exception of the entry for $\Delta m = 1.25$ the relation between Δm and log σ is well reproduced. One might wish to try other forms for the function f, but clearly it must be nearly logarithmic over the range of σ considered here.

Equation (2) makes two interesting predictions. First, above log $\sigma = 2.60$ the disk brightness is reduced to 0 and there should be no disk galaxies remaining. Second, the disk magnitude difference between field galaxies (log $\sigma \sim -1$) and the lowest density covered here (log $\sigma \sim 0$) is 0.35 mag. Both these predictions can be checked observationally.

In considering possible models for the brightness changes, one can distinguish between two ways of altering

the properties of disks, namely, an interruption during the formation process or subsequent removal of material after formation. Just what physical property the parameter y corresponds to can be freely specified by each model, but the relation between magnitude change and density in equation (2) places a powerful constraint on a given model.

Ram-pressure stripping is a process involving removal of material after formation. As discussed in Section II, it is probably incapable of producing the large (1.5 - 2.0 mag) magnitude changes required, partly since the gas content of a a spiral is typically only 5 - 10% of the total mass of a galaxy. Also simple stripping theories would predict a much steeper relation between the amount of fading and density than is observed. One might argue that in denser regions stripping has had a longer time to operate and thus been able to affect galaxies at a time when their gas content was much higher. This is possible, but it then becomes very similar to the disruption of the disks during the formation process as discussed below.

Alternatively, dynamic processes such as tidal stripping may be occurring. Richstone (1975, 1976) has argued that in rich clusters such effects could efficiently strip material from galaxies and possibly "fatten up" SO's to make them look like ellipticals. The efficiency of collisional stripping depends very much on the size and mass of

a galaxy, whereas we have shown that it should be independent of either, and it also has the wrong dependence on the density of galaxies. Similarly, we have argued that a scenario involving conversion of disks into bulges is incorrect, and in any case the dependence of fattening on density of galaxies is again of the wrong form. Thus we conclude that dynamical processes are unlikely.

We are therefore left with the idea that the reduction in the brightness of disks actually involves a disruption during their formation. Because disks are believed to have a formation time comparable to the collapse time of clusters such a disruption seems quite possible. Dressler favors this interpretation and we shall not repeat his arguments here. Unfortunately, our gross ignorance of the physical conditions during the formation period precludes much in the way of quantitative analysis. We do note, however, that if virialization of subgroups halts the growth of a disk, then we can understand the relation in equation (2), if it can be shown that the masses of disks grow in time as log t. Then the parameter y corresponds to time and the cutoff time (i.e., the collapse time of the subgroup) is proportional to $\rho^{-\frac{1}{2}}$. A similar picture has recently been proposed by Larson et al. (1979) who consider the changes in brightness to be caused by a combination of the truncation of disk formation during virialization and its subsequent effect on the

luminosity evolution of a galaxy. The magnitude changes predicted by these authors is of the same order as derived in this paper.

Finally, to show that subtleties still lurk in this problem, we close with an interesting calculation. We have been a bit cavalier in talking about the density of galaxies. Dressler derived his relationships in terms of the projected density σ, whereas the physical mechanism above refers more correctly to the spatial density ρ. Suppose all galaxies belong to virialized subgroups, each with a characteristic size r and density ρ. Then $\sigma = \rho r$. It seems reasonable that ρ and r are correlated, so it does not matter whether we refer to ρ or σ. However, Dressler has shown that his relationships hold unchanged for both concentrated and open clusters between which the correlation between ρ and r may not hold very well. Then what physical properties is σ correlated with? If the subgroups are virialized then the velocity dispersion is given by $v^2 \sim \rho r^2$ or $\rho v^2 \sim \rho^2 r^2 = \sigma^2$. That is, Dressler's relationships as functions of σ can be written equivalently as functions of the local ram pressure.

It is a pleasure to thank Alan Dressler for many challenging discussions. I also thank Jim Gunn for several useful comments.

TABLE 1

RELATIONSHIP BETWEEN FADE OF DISK Δm

AND PROJECTED DENSITY σ

Δm	log σ (Observed)	log σ (Predicted)
0.00	0.02	0.00
0.25	0.50	0.53
0.50	0.93	0.96
0.75	1.32	1.30
1.00	1.60	1.56
1.25	1.85	1.78
1.50	1.95	1.95

REFERENCES

Bahcall, N. A. 1977, Ap. J. (Letters), 218, L93.

Butcher, H. R., and Oemler, A. 1978, Ap. J., 226, 559.

Cowie, L. L., and Songaila, A. 1977, Nature, 266, 501.

Dressler, A. 1980, Ap. J., in press.

Gisler, G. R. 1978, M.N.R.A.S., 183, 633.

Gunn, J. E., and Gott, J. R. 1972, Ap. J., 176, 1.

Larson, R. B., Tinsley, B. M., and Caldwell, C. N. 1979, preprint.

Melnick, J., and Sargent, W. L. W. 1977, Ap. J., 215, 401.

Oemler, A. 1974, Ap. J., 194, 1.

Richstone, D. O. 1975, Ap. J., 200, 535.

_____ 1976, Ap. J., 204, 642.

Strom, S. E., and Strom, K. E. 1978, in IAU Symposium No. 77, Structure and Properties of Nearby Galaxies, ed. E. M. Berkhuijsen and R. Wielebinski (Dordrecht: D. Reidel), p. 69.

Tytler, D., and Vidal, N. 1978, M.N.R.A.S., 182, 33P.

FIGURE 1

The fraction of E, S0, and Sp galaxies as a function of the local projected density, in galaxies Mpc^{-2}. The solid lines are the mean relations observed by Dressler (1980); the points are computed in this paper.

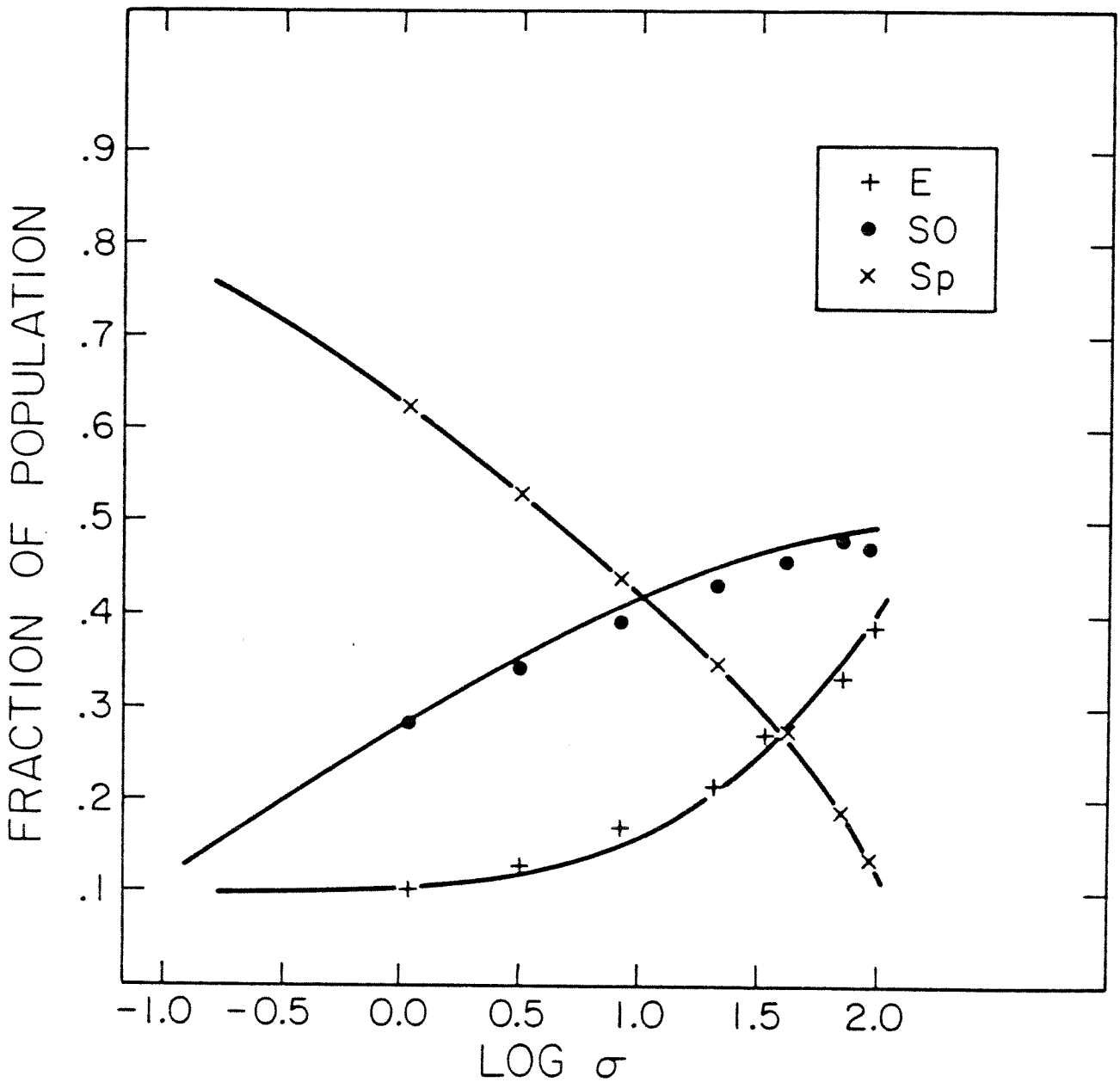
FRACTION OF POPULATION
.9
.8
.7
.6
.5
.4
.3
.2
.1
+ E
• SO
× Sp
-1.0
-0.5
0.0
0.5
1.0
1.5
2.0
LOG σ

FIGURE 2

The median bulge magnitude as a function of the local projected density (see Fig. 1). The error bar represents typical values for the quartile points on the observed distribution.

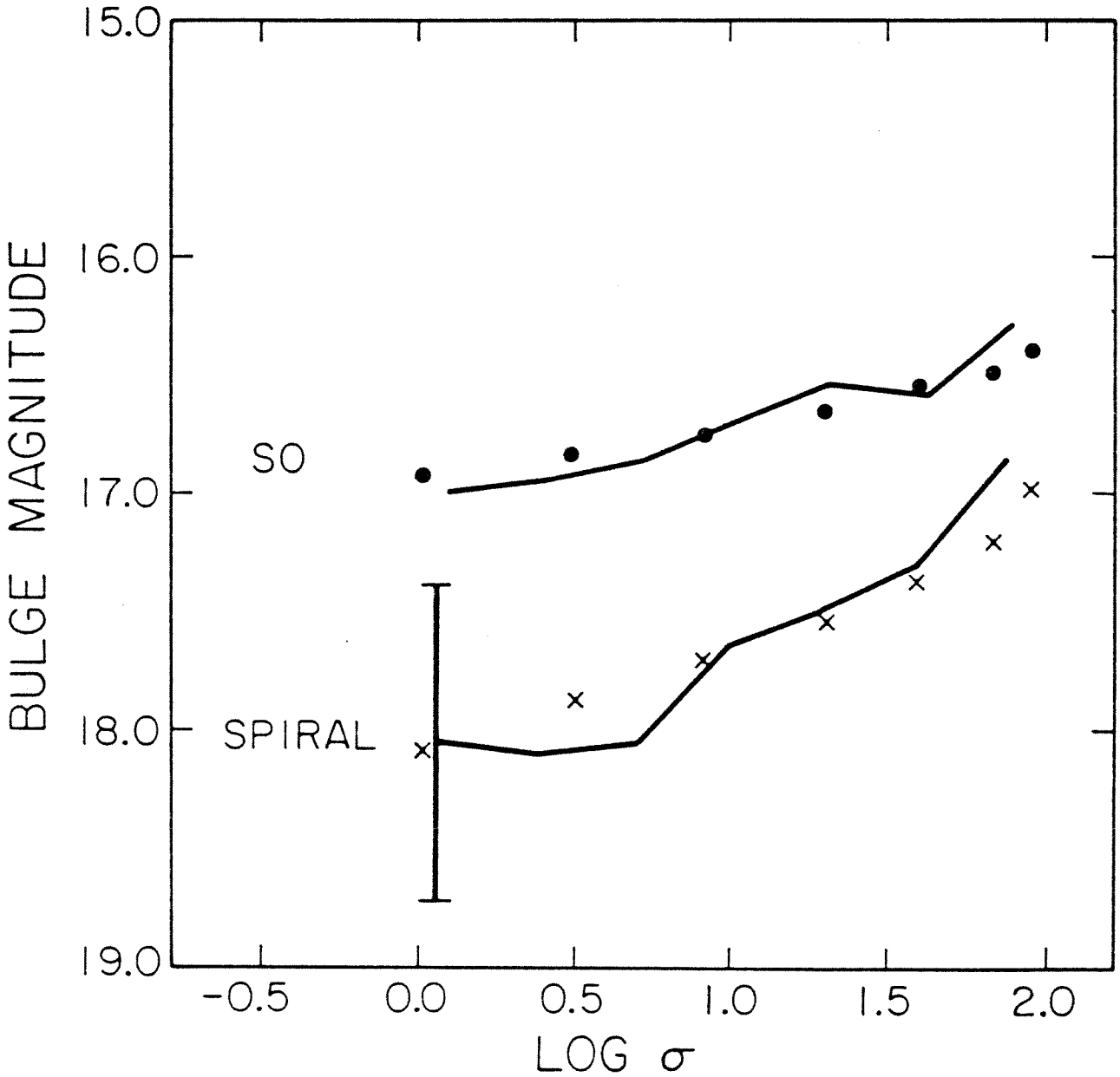
15.0
16.0
17.0
18.0
19.0
BULGE MAGNITUDE
S0
SPIRAL
-0.5
0.0
0.5
1.0
1.5
2.0
LOG σ

FIGURE 3

The quantity $m_{bul} - m_{tot}$ as a function of the local projected density (see Figs. 1 and 2).

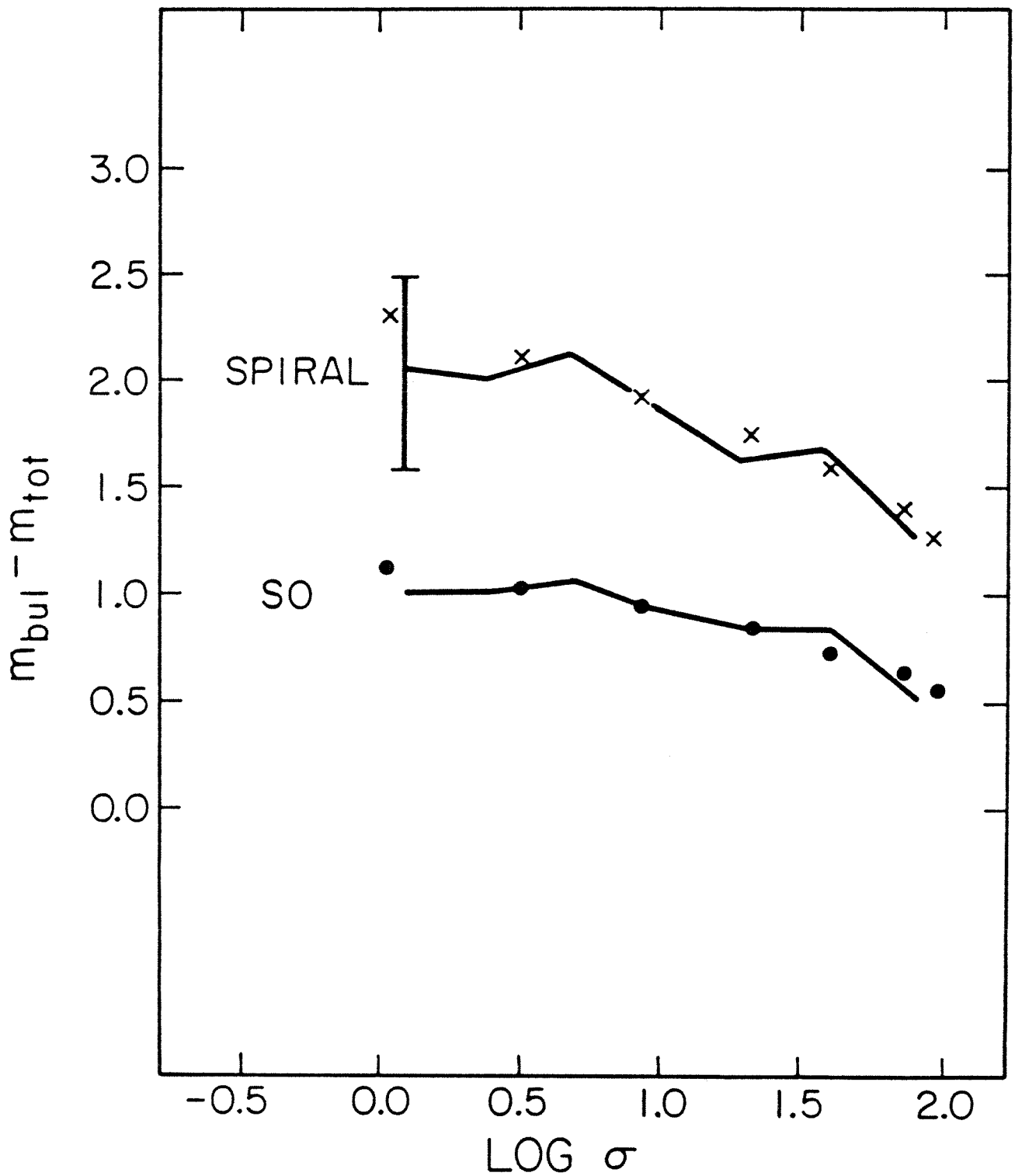
3.0
2.5
2.0
1.5
1.0
0.5
0.0
$m_{bul} - m_{tot}$
SPIRAL
SO
-0.5
0.0
0.5
1.0
1.5
2.0
LOG σ